UNIVERSITY OF SOUTHERN CALIFORNIA

DEPARTMENT OF CIVIL ENGINEERING

DISPLACEMENTS NEAR A THREE-DIMENSIONAL HEMISPHERICAL CANYON SUBJECTED TO INCIDENT PLANE WAVES

by

Vincent W. Lee

Report No. CE 78-16

A Report on Research Conducted Under Contracts from the
U.S. Geological Survey and the U.S. Nuclear Regulatory Commission

Los Angeles, California

December, 1978

TABLE OF CONTENTS

Abstract

The three-dimensional scattering and diffraction of plane waves by a hemispherical canyon in the homogeneous elastic half-space has been analyzed. Using the series solution for a general angle of wave incidence, ground motion near the canyon has been studied. The nature of ground motion has been found to depend on three key parameters:

(1) γ, the angle of incidence,

(2) η, a dimensionless frequency of wave number proportional to the ratio of the diameter of the canyon to wavelength of the incident P-wave, and

(3) κ, The ratio of longitudinal to transverse wave speeds.

The displacement amplitudes and phases on nearby ground surface show significant departure from the uniform half-space motions. The angle of incidence γ determines the overall trends of motion amplitudes. For oblique incidence, for example, considerable amplification is observed in front of the canyon, and a prominent shadow zone is realized behind the canyon.

Introduction

In this analysis, the problem of scattering and diffraction of a plane wave by a three-dimensional hemispherical canyon has been studied. The purpose of this study is to add the exact series solution to the limited collection of exact or approximate solutions describing the effects of surface topography on wave propagation in an elastic half-space. It should also be useful for the approximate evaluation of the amplification effects near topographic features that can be approximated by a hemispherical canyon. Furthermore, the results presented here may also be of value for different approximate techniques based on finite element or integral equation schemes, since the model studied here can be used for comparison with results obtained by approximate methods.

The Wave Equation in Spherical Coordinates

The geometry of the model to be presented here is best described by the spherical co-ordinates (r,θ,ϕ) (Figure 1). Given a function $F(\underset{\sim}{r},t)$ of space and time, the wave equation in spherical coordinates

$$c^2\nabla^2 F - \partial^2 F/\partial t^2 = 0 \tag{1}$$

is given by

$$\frac{1}{r^2}\frac{\partial}{\partial r}\left(r^2\frac{\partial F}{\partial r}\right) + \frac{1}{r^2\sin\theta}\frac{\partial}{\partial\theta}\left(\sin\theta\frac{\partial F}{\partial\theta}\right) + \frac{1}{r^2\sin^2\theta}\frac{\partial^2 F}{\partial\phi^2} - \frac{1}{c^2}\frac{\partial^2 F}{\partial t^2} = 0 \tag{2}$$

Since an arbitrary time variation of the function can be represented by Fourier analysis in terms of harmonic components, there is no essential loss of generality in studying only the harmonic solution of the form

$$F(r,\theta,\phi,t) = f(r,\theta,\phi)e^{-i\omega t} \tag{3}$$

where $i = \sqrt{-1}$, ω is the harmonic frequency and f satisfies Helmoltz equation

$$\nabla^2 f + k^2 f = 0\ , \tag{4}$$

with $k = \omega/c$ being the wave number.

Equation (4) is separable into the form

$$f(r,\theta,\phi) = f_1(r)f_2(\theta)f_3(\phi) \tag{5}$$

with the factors satisfying

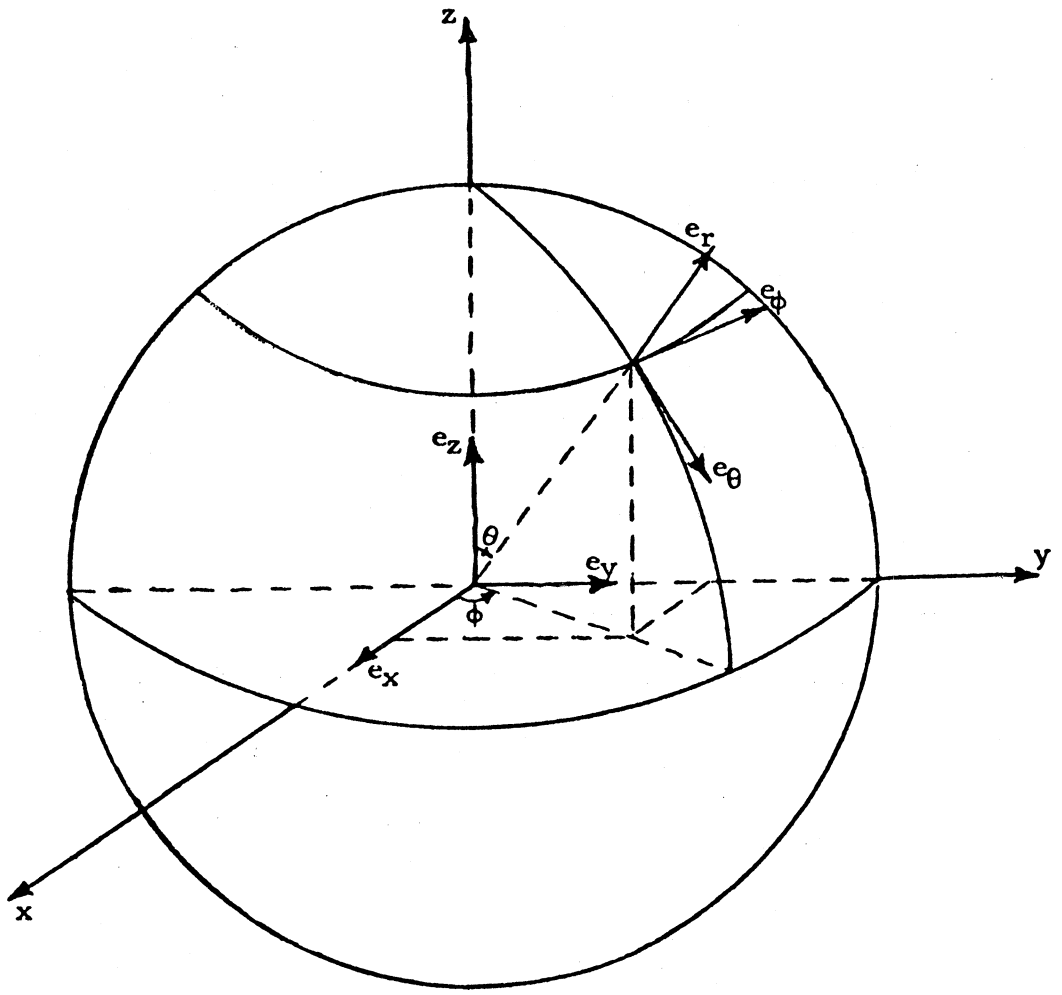

Figure 1

Spherical Coordinates

$$\frac{d}{dr}\,(r^2\,df_1/dr) + (k^2r^2 - p^2)f_1 = 0 \tag{6}$$

$$\frac{1}{\sin\theta}\frac{d}{d\theta}\left(\sin\theta\,\frac{df_2}{d\theta}\right) + \left(p^2 - \frac{q^2}{\sin^2\theta}\right) f_2 = 0 \tag{7}$$

and

$$\frac{d^2f_3}{d\phi^2} + q^2 f_3 = 0\ , \tag{8}$$

with p and q as separation constants.

It is necessary that $f_3(\phi)$ be a periodic function of period 2π, so $q = m$ is an integer. Setting $p^2 = \nu(\nu+1)$, $\mu = \cos\theta$, (7) becomes

$$(1-\mu^2)\,\frac{d^2f_2}{d\mu^2} - 2\mu\,\frac{df_2}{d\mu} + \left[\nu(\nu+1) - \frac{m^2}{1-\mu^2}\right] f_2 = 0 \tag{9}$$

which is the associated Legendre equation with solutions $P_\nu^m(\mu)$, $Q_\nu^m(\mu)$.

For regularity of the function at $\mu = \pm 1$ ($\theta = 0,\pi$), we must have $\nu = n$, an integer. $Q_n^m(\mu)$ is singular at $\mu = \pm 1$, and is thus excluded from spherical problems which require finiteness at $\mu = 1$ and/or $\mu = -1$.

Equation (6) then becomes

$$r^2\,\frac{d^2f_1}{dr^2} + 2r\,\frac{df_1}{dr} + [k^2r^2 - n(n+1)]f_1 = 0 \tag{10}$$

which has solutions $z_n^{(i)}(kr)$, $i = 1,2,3,4$, the spherical Bessel and Hankel functions:

$$z_n^{(1)} \equiv j_n(kr) = \left(\frac{\pi}{2kr}\right)^{\frac{1}{2}} J_{n+\frac{1}{2}}(kr)$$

$$z_n^{(2)} \equiv y_n(kr) = \left(\frac{\pi}{2kr}\right)^{\frac{1}{2}} Y_{n+\frac{1}{2}}(kr)$$

$$z_n^{(3)} \equiv h_n^{(1)}(kr) = j_n(kr) + i\,y_n(kr) = \left(\frac{\pi}{2kr}\right)^{\frac{1}{2}} H_{n+\frac{1}{2}}^{(1)}(kr)$$

$$z_n^{(4)} \equiv h_n^{(2)} = j_n(kr) - i\, y_n(kr) = \left(\frac{\pi}{2kr}\right)^{\frac{1}{2}} H_{n+\frac{1}{2}}^{(2)}(kr) \qquad (11)$$

$J_{n+\frac{1}{2}}$, $Y_{n+\frac{1}{2}}$, $H_{n+\frac{1}{2}}^{(1)}$, $H_{n+\frac{1}{2}}^{(2)}$ are the cylindrical Bessel and Hankel functions.

In summary, a general harmonic solution of (1) is then a linear combination of any two of the four basic solutions of the form

$$z_n^{(i)}(kr) P_n^m(\mu) \begin{matrix}\cos \\ \sin\end{matrix} m\phi \exp(-i\omega t) \qquad (12)$$

with $i = 1,2,3,4$, $m,n = 0,1,2, \ldots$ and $m \leq n$.

The three-dimensional model studied in this paper is shown in Figure 2. It represents a half-space ($z < 0$) from which a hemisphere of radius a is removed to form a canyon. The half-space is assumed to be elastic, isotropic and homogeneous. Its material properties are given by the Lamé constants λ, μ and mass density ρ, for which we have

$$\text{longitudinal wave velocity, } \alpha = \sqrt{\frac{\lambda+2\mu}{\rho}} \quad , \text{ and}$$

$$\text{transverse wave velocity, } \beta = \sqrt{\frac{\mu}{\rho}} \quad . \qquad (13)$$

Two coordinate systems are employed. The rectangular coordinate system has its origin at the center of the hemisphere with the x and y axis on the surface of the half-space and the z axis perpendicular to it. The spherical coordinate system (r,θ,ϕ) has a common origin with the rectangular system.

All the basic equations of linear elasticity are applicable to the model and will be used in the analysis that follows.

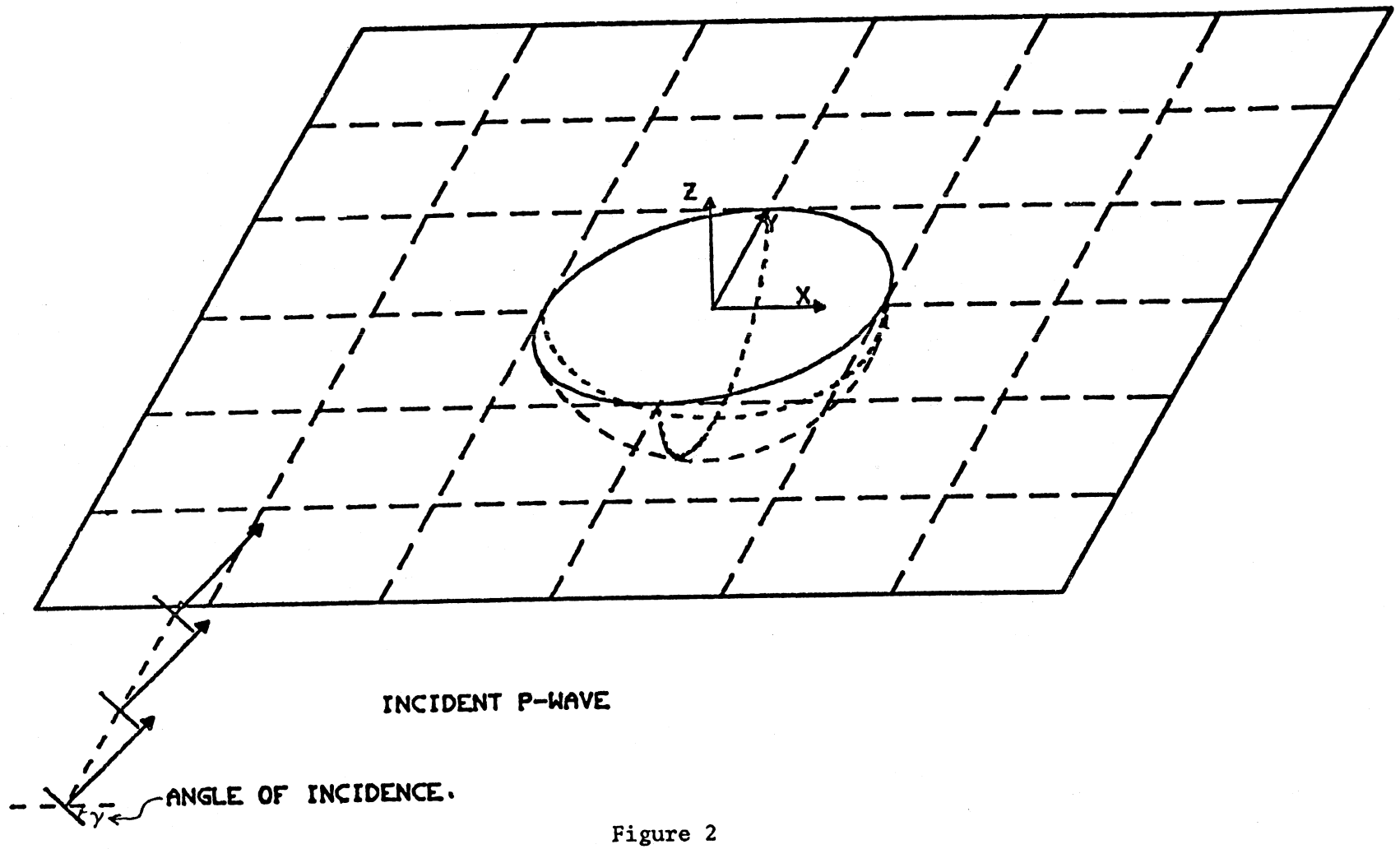

Figure 2

The Model

Excitation: Incident P-Wave

The excitation of the half-space consists of a plane longitudinal (P) wave whose displacement and propagation vector is situated in the x-z plane with angle of incidence γ. It has circular frequency ω and can be represented by the potential

$$\Phi^{(i)} = \exp[i\, k_\alpha(x \sin\gamma + z \cos\gamma) - i\omega t] \tag{1.1}$$

of wavelength $\lambda_\alpha = 2\pi/k_\alpha$, where $k_\alpha = \omega/\alpha$ is the longitudinal wave number. From this point on the time factor $\exp(-i\omega t)$ will be understood and omitted from all expressions.

The corresponding displacement vector is given by

$$\underset{\sim}{u}^{(i)} = ik_\alpha(\sin\gamma\, \underset{\sim}{e}_x + \cos\gamma\, \underset{\sim}{e}_z)\exp ik_\alpha(x \sin\gamma + z \cos\gamma) \tag{1.2}$$

where $\underset{\sim}{e}_x$, $\underset{\sim}{e}_z$ are unit vectors in the x and z direction, respectively. The magnitude of the displacement vector, $|\underset{\sim}{u}^{(i)}|$, is k_α.

In the presence of only the free half-space boundary, the incident wave is reflected from the plane free surface ($z = 0$), generating, in general, both plane reflected longitudinal (P) and transverse (SV) waves, with displacement vectors respectively given by

$$\text{(P):}\quad \underset{\sim}{u}_1^{(r)} = iK_1k_\alpha(\sin\gamma\, \underset{\sim}{e}_x - \cos\gamma\, \underset{\sim}{e}_z)\exp ik_\alpha(x \sin\gamma - z \cos\gamma) \tag{1.3}$$

$$\text{(SV):}\quad \underset{\sim}{u}_2^{(r)} = iK_2k_\beta(\cos\delta\, \underset{\sim}{e}_x + \sin\delta\, \underset{\sim}{e}_z)\exp ik_\beta(x \sin\delta - z \cos\delta) \tag{1.4}$$

where $k_\beta = \omega/\beta$ is the transverse wave number, δ is the angle of reflection of the transverse wave, and K_1 and K_2 are reflection coefficients given by

$$K_1 = \frac{\sin 2\gamma \sin 2\delta - (\alpha/\beta)^2 \cos^2 2\delta}{\sin 2\gamma \sin 2\delta + (\alpha/\beta)^2 \cos^2 2\delta}$$

$$K_2 = \frac{2 \sin 2\gamma \cos 2\delta}{\sin 2\gamma \sin 2\delta + (\alpha/\beta)^2 \cos^2 2\delta} \tag{1.5}$$

The resulting displacement vector

$$\underset{\sim}{u}^{(i+r)} = \underset{\sim}{u}^{(i)} + \underset{\sim 1}{u}^{(r)} + \underset{\sim 2}{u}^{(r)} \tag{1.6}$$

satisfies the stress-free boundary conditions

$$\sigma_{zz} = \sigma_{zx} = \sigma_{zy} = 0 \qquad \text{at } z = 0 , \tag{1.7}$$

and each component of it satisfies the corresponding scalar wave equation.

In terms of displacement spherical potentials, $\underset{\sim}{u}^{(i)}$, $\underset{\sim 1}{u}^{(r)}$ correspond to $\Phi^{(i)}$ and $\Phi^{(r)}$, respectively while $\underset{\sim 2}{u}^{(r)}$ corresponds to $\Psi^{(r)}$ and $\chi^{(r)}$. These potentials have the spherical wave expansions of the form

$$\Phi^{(i)} = \sum_{m,n} A_{mn}^{(i)} \, j_n(k_\alpha \gamma) P_n^m(\mu) \cos m\phi$$

$$\Psi^{(i)} = \chi^{(i)} = 0$$

$$\Phi^{(r)} = \sum_{m,n} A_{mn}^{(r)} \, j_n(k_\alpha \gamma) P_n^m(\mu) \cos m\phi$$

$$\Psi^{(r)} = \sum_{m,n} k_\beta B_{mn}^{(r)} \, j_n(k_\beta \gamma) P_n^m(\mu) \sin m\phi$$

$$\chi^{(r)} = \sum_{m,n} C_{mn}^{(r)} \, j_n(k_\beta \gamma) P_n^m(\mu) \cos m\phi \tag{1.8}$$

where the summation is for $m,n = 0,1,2,\ldots$ and $m \leq n$. The expansion is carried out in Appendix I.

Reflected and Scattered Spherical Waves

In the presence of the canyon, two types of outgoing spherical waves (longitudinal and transverse) are reflected back into the medium. These waves can be represented by the potentials

$$\Phi^{(s)} = \sum_{m,n} A_{mn}^{(3)} \, z_n^{(3)}(k_\alpha \gamma) P_n^m(\mu) \cos m\phi$$

$$\Psi^{(s)} = \sum_{m,n} k_\beta B_{nm}^{(3)} \, z_n^{(3)}(k_\beta \gamma) P_n^m(\mu) \sin m\phi$$

$$\chi^{(s)} = \sum_{m,n} C_{mn}^{(3)} \, z_n^{(3)}(k_\beta \gamma) P_n^m(\mu) \cos m\phi \quad , \qquad (2.1)$$

where the summation is for $m,n = 0,1,2, \ldots$ and $m \leq n$. The spherical Hankel function $z_n^{(3)} \equiv h_n^{(1)}$ is used because the product $h_n^{(1)}(r)\exp(-i\omega t)$ represents an outward propagating wave. $A_{mn}^{(3)}$, $B_{mn}^{(3)}(=0)$ and $C_{mn}^{(3)}$ are expansion coefficients corresponding to potentials satisfying the boundary conditions of a spherical cavity in an infinite medium and subjected to an incident P-wave. The expansion is carried out in Appendix II.

In the presence of both the plane free boundary ($z = 0$) and the hemispherical canyon ($r = a$, $z < 0$), the reflected plane P- and SV-waves will be scattered from and diffracted around the canyon, and the scattered spherical waves from the canyon will be reflected back into the medium from the plane free surface. These waves can be represented in the most general form by potentials

$$\Phi^{(R)} = \sum_{j,m,n} A_{mn}^{(j)} \, z_n^{(j)}(k_\alpha \gamma) P_n^m(\mu) \cos m\phi$$

$$\Psi^{(R)} = \sum_{j,m,n} k_\beta B_{mn}^{(j)} \, z_n^{(j)}(k_\beta \gamma) P_n^m(\mu) \sin m\phi$$

$$\chi^{(R)} = \sum_{j,m,n} C_{mn}^{(j)} \, z_n^{(j)}(k_\beta \gamma) P_n^m(\mu) \cos m\phi \quad , \qquad (2.2)$$

where $j = 1,2$, $m,n = 0,1,2, \ldots$ with $m \leq n$, and $z_n^{(1)}$, $z_n^{(2)}$ are given in equation (11).

The potentials $\Phi^{(R)}$, $\Psi^{(R)}$ and $\chi^{(R)}$ satisfy their associated scalar wave equations and the six sets of unknowns

$$\left\{A_{mn}^{(j)}, B_{mn}^{(j)}, C_{mn}^{(j)}\right\} \quad j = 1,2 \; ; \; m,n = 0,1,2, \ldots \text{ with } m \leq n$$

will be determined from the boundary conditions.

Boundary Conditions

The resulting potentials at any point are then given by the sum of the preceding potentials

$$\Phi = \Phi^{(i)} + \Phi^{(r)} + \Phi^{(s)} + \Phi^{(R)}$$

$$\Psi = \Psi^{(r)} + \Psi^{(s)} + \Psi^{(R)}$$

$$\chi = \chi^{(r)} + \chi^{(s)} + \chi^{(R)} \qquad (3.1)$$

Similarly, the displacement vector at any point is

$$\underset{\sim}{u} = \underset{\sim}{u}^{(i)} + \underset{\sim}{u}^{(r)} + \underset{\sim}{u}^{(s)} + \underset{\sim}{u}^{(R)} \quad , \qquad (3.2)$$

and the stress matrix is given by

$$[\sigma] = [\sigma^{(i)}] + [\sigma^{(r)}] + [\sigma^{(s)}] + [\sigma^{(R)}] \quad . \qquad (3.3)$$

Each term of the resulting potentials satisfies the associated wave equations. They must together satisfy the boundary conditions. At $r = a$, $0 \le \phi \le 2\pi$, $\pi/2 \le \theta \le \pi$

$$\sigma_{rr} = \sigma_{r\theta} = \sigma_{r\phi} = 0 \quad , \qquad (3.4)$$

and at $z = 0$, all x,y s.t. $x^2 + y^2 \ge a^2$

$$\sigma_{zz} = \sigma_{zx} = \sigma_{zy} = 0 \quad . \qquad (3.5)$$

In spherical co-ordinates, (3.5) is equivalent to:

$$\sigma_{\theta\theta} = \sigma_{\theta r} = \sigma_{\theta\phi} = 0$$

at $\theta = \pi/2$, $0 \le \phi \le 2\pi$, $r \ge a$ (3.6)

From Appendix II, at $r = a$ there follows:

$$\sigma_{rr}^{(i)} + \sigma_{rr}^{(s)} = 0$$

$$\sigma_{r\theta}^{(i)} + \sigma_{r\theta}^{(s)} = 0$$

$$\sigma_{r\phi}^{(i)} + \sigma_{r\phi}^{(s)} = 0 \quad . \tag{3.7}$$

Therefore, at $r = a$, $0 \leq \phi \leq 2\pi$, $\pi/2 \leq \theta \leq \pi$

$$\sigma_{rr}^{(r)} + \sigma_{rr}^{(R)} = 0$$

$$\sigma_{r\theta}^{(r)} + \sigma_{r\theta}^{(R)} = 0$$

$$\sigma_{r\phi}^{(r)} + \sigma_{r\phi}^{(R)} = 0 \tag{3.8}$$

From equation (1.7), at $z = 0$ there follows:

$$\sigma_{zz}^{(i)} + \sigma_{zz}^{(r)} = 0$$

$$\sigma_{zx}^{(i)} + \sigma_{zx}^{(r)} = 0$$

$$\sigma_{zy}^{(i)} + \sigma_{zy}^{(r)} = 0 \tag{3.9}$$

Therefore, at $z = 0$, all x,y such that $x^2 + y^2 \geq a^2$

$$\sigma_{zz}^{(s)} + \sigma_{zz}^{(R)} = 0$$

$$\sigma_{zx}^{(s)} + \sigma_{zx}^{(R)} = 0$$

$$\sigma_{zy}^{(s)} + \sigma_{zy}^{(R)} = 0 \tag{3.10}$$

Equations (3.8) and (3.10) will be the boundary conditions to be applied to calculate the coefficients appearing in $\Phi^{(R)}$, $\Psi^{(R)}$ and $\chi^{(R)}$.

Solution of the Problem

Following the analysis in Appendix II, applying (3.8) to each "(m,n) component," we get, for each $m,n = 0,1,2,\ldots,\ m \le n$,

$$\sigma_{rr}: \quad A_{mn}^{(r)}E_{11}^{(1)} + C_{mn}^{(r)}E_{13}^{(1)} + \sum_j A_{mn}^{(j)}E_{11}^{(j)} + C_{mn}^{(j)}E_{13}^{(j)} = 0$$

$$A_{mn}^{(r)}E_{41}^{(1)} + C_{mn}^{(r)}E_{43}^{(1)} + \sum_j A_{mn}^{(j)}E_{41}^{(j)} + C_{mn}^{(j)}E_{43}^{(j)} = 0$$

$$\sigma_{r\theta},\sigma_{r\phi}: \quad B_{mn}^{(r)}E_{42}^{(1)} + \sum_j B_{mn}^{(j)}E_{42}^{(j)} = 0 \qquad (4.1)$$

with $j = 1,2$ in the summation.

The terms $E_{ik}^{(j)} = E_{ik}^{(j)}(m,n)$ are given in Appendix III.

Equation (4.1) gives a set of three equations for the unknowns $A_{mn}^{(1)}$, $A_{mn}^{(2)}$, $B_{mn}^{(1)}$, $B_{mn}^{(2)}$, $C_{mn}^{(1)}$ and $C_{mn}^{(2)}$. To complete the analysis, equation (3.10) is applied. In spherical co-ordinates, (3.10) is equivalent to (at $\theta = \pi/2$, $0 \le \phi \le 2\pi$, $r \ge a$):

$$\sigma_{\theta\theta}^{(s+R)} = \sigma_{\theta\theta}^{(s)} + \sigma_{\theta\theta}^{(R)} = 0 \qquad (4.2)$$

$$\sigma_{\theta r}^{(s+R)} = \sigma_{\theta r}^{(s)} + \sigma_{\theta r}^{(R)} = 0 \qquad (4.3)$$

$$\sigma_{\theta\phi}^{(s+R)} = \sigma_{\theta\phi}^{(s)} + \sigma_{\theta\phi}^{(R)} = 0 \quad . \qquad (4.4)$$

The form of equation (4.2) is first to be analyzed. Writing

$$\sigma_{\theta\theta}^{(s)} = \frac{2\mu}{r^2}\sum_m \mathscr{E}_2^{(3)}(m,r)\ \cos m\phi$$

$$\sigma_{\theta\theta}^{(R)} = \frac{2\mu}{r^2}\sum_m \left[\mathscr{E}_2^{(1)}(m,r) + \mathscr{E}_2^{(2)}(m,r)\right]\cos m\phi\ , \qquad (4.5)$$

where for $j = 1,2,3$, $m = 0,1,2,\ldots$

$$\mathscr{E}_2^{(j)}(m,r) = \sum_{n=m}^{\infty} A_{mn}^{(j)} \mathscr{E}_{21}^{(j)} + k_\beta r B_{mn}^{(j)} \mathscr{E}_{22}^{(j)} + C_{mn}^{(j)} \mathscr{E}_{23}^{(j)} , \tag{4.6}$$

with $\mathscr{E}_{2k}^{(j)} = \mathscr{E}_{2k}^{(j)}(m,n,r)$, $k = 1,2,3$ given in Appendix III.

For equation (4.2) to hold for all ϕ, one needs for all m, all $r \geq a$

$$\mathscr{E}_2^{(1)}(m,r) + \mathscr{E}_2^{(2)}(m,r) + \mathscr{E}_2^{(3)}(m,r) = 0 \tag{4.7}$$

These terms involve spherical Bessel functions of order $n=0,1,2,\ldots$ and of the form $j_n(k_\alpha r)$, $y_n(k_\alpha r)$, $j_n(k_\beta r)$, $y_n(k_\beta r)$. Since $k_\alpha \neq k_\beta$, they are not orthogonal to each other. Hence, they are replaced by their series representations in r, and the orthogonality condition is then applied to

$$\{r^n \mid n=0,\pm 1,\pm 2, \ldots\} \quad . \tag{4.8}$$

Using their series expansion in r given in Appendix IV, it is possible to expand $\mathscr{E}_{2j}^{(1)}$, $\mathscr{E}_{2j}^{(2)}$ in series of r. For all $m,n=0,1,2,\ldots, m \leq n$, $j=1$ and 3, we write

$$\mathscr{E}_{2j}^{(1)}(m,n,r) = \sum_k e_{2j}^{(1)}(m,n,k)(r/2)^{n+2k}$$

$$\mathscr{E}_{2j}^{(2)}(m,n,r) = \sum_k e_{2j}^{(2)}(m,n,k)(r/2)^{-n-1+2k} \tag{4.9}$$

and for $j = 2$, we write

$$k_\beta r\, \mathscr{E}_{22}^{(1)}(m,n,r) = \sum_k e_{22}^{(1)}(m,n,k)(r/2)^{n+2k+1}$$

$$k_\beta r\, \mathscr{E}_{22}^{(2)}(m,n,r) = \sum_k e_{22}^{(2)}(m,n,k)(r/2)^{-n+2k} \tag{4.10}$$

with $k = 0,1,2,\ldots$ in the summation. The $e_{2j}^{(1)}$, $e_{2j}^{(2)}$ terms are given in Appendix V.

Each $e_{2j}^{(1)}$, $e_{2j}^{(2)}$, $j = 1,2,3$ involves a factor $P_n^m(\cos\theta)$ and/or its derivative evaluated at $\theta = \pi/2$, and for $m,\ell = 0,1,2, \ldots$

$$P^m_{m+2\ell+1}(0) = 0 \tag{4.11}$$

so that depending on m, either the odd or even terms remain. From (4.6), $\mathscr{E}_2^{(1)}(m,r)$ then becomes

$$\mathscr{E}_2^{(1)}(m,r) = \sum_{\ell,k} \left[A_{m,m+2\ell}^{(1)} e_{21}^{(1)} + B_{m,m+2\ell-1}^{(1)} e_{22}^{(1)} + C_{m,m+2\ell}^{(1)} e_{23}^{(1)} \right] (r/2)^{m+2\ell+2k} \tag{4.12}$$

with $\ell,k = 0,1,2, \ldots$ in the summation, and

$$e_{21}^{(1)} = e_{21}^{(1)}(m,m+2\ell,k)$$

$$e_{22}^{(1)} = e_{22}^{(1)}(m,m+2\ell-1,k)$$

$$e_{23}^{(1)} = e_{23}^{(1)}(m,m+2\ell,k) \qquad k,\ell = 0,1,2, \ldots \tag{4.13}$$

Substituting $n = \ell+k$ in (4.12), $k = n-\ell$ in (4.13), (4.12) can be rewritten as

$$\mathscr{E}_2^{(1)}(m,r) = \sum_n \left[\sum_{\ell=0}^{n} A_{m,m+2\ell}^{(1)} e_{21}^{(1)} + B_{m,m+2\ell-1}^{(1)} e_{22}^{(1)} + C_{m,m+2\ell}^{(1)} e_{23}^{(1)} \right] (r/2)^{m+2n} \tag{4.14}$$

with $n = 0,1,2, \ldots$ in the summation.

Similarly, $\mathscr{E}_2^{(2)}(m,r)$ can be expanded as

$$\mathscr{E}_2^{(2)}(m,r) = \sum_n \left[\sum_\ell A_{m,m+2\ell}^{(2)} e_{21}^{(2)} + B_{m,m+2\ell+1}^{(2)} e_{22}^{(2)} + C_{m,m+2\ell}^{(2)} e_{23}^{(2)} \right] (r/2)^{-m-1+2n}$$

with $n = -\infty$ to ∞ in the summation, and for $n < 0$, $\ell = 0$ to ∞ and for $n \geq 0$, $\ell = n$ to ∞, and

$$e_{21}^{(2)} = e_{21}^{(2)}(m,m+2\ell,\ell-n)$$

$$e_{22}^{(2)} = e_{22}^{(2)}(m,m+2\ell+1,\ell-n)$$

$$e_{23}^{(2)} = e_{23}^{(2)}(m,m+2\ell,\ell-n) \quad . \tag{4.15}$$

Similar expansion can be carried out for $\mathscr{E}_2^{(3)}(m,r)$, where $z_n^{(3)} \equiv h_n^{(1)}$ is expressed as $j_n + iy_n$. Again, the series expansion of j_n and y_n are used, thus obtaining a series expansion for $\mathscr{E}_2^{(3)}(m,r)$.

From the series expansion of $\mathscr{E}_2^{(1)} + \mathscr{E}_2^{(2)} + \mathscr{E}_2^{(3)} = 0$, and the requirement that the coefficients of each power of r be equated to zero, the following set of equations for $m = 0,1,2, \ldots$, is obtained

$$(r/2)^{m+2n}: \sum_{\substack{\ell=0 \\ j=1,3}}^{n} A_{m,m+2\ell}^{(j)} e_{21}^{(1)} + B_{m,m+2\ell-1}^{(j)} e_{22}^{(1)} + C_{m,m+2\ell}^{(j)} e_{23}^{(1)} = 0 \quad . \qquad n = 0,1,2, \ldots$$

$$(r/2)^{-m-1-2n}: \sum_{\ell=\max(0,n)}^{\infty} \begin{pmatrix} A_{m,m+2\ell}^{(2)} \\ + \\ iA_{m,m+2\ell}^{(3)} \end{pmatrix} e_{21}^{(2)} + \begin{pmatrix} B_{m,m+2\ell+1}^{(2)} \\ + \\ iB_{m,m+2\ell+1}^{(3)} \end{pmatrix} e_{22}^{(2)} + \begin{pmatrix} C_{m,m+2\ell}^{(2)} \\ + \\ iC_{m,m+2\ell}^{(3)} \end{pmatrix} e_{23}^{(2)} = 0 \,,$$

$$n = 0, \pm 1, \pm 2, \ldots \tag{4.16}$$

where $i = \sqrt{-1}$.

Similarly, for each $m = 0,1,2, \ldots$, the boundary conditions

$$\sigma_{\theta r}^{(R)} + \sigma_{\theta r}^{(s)} = 0 \tag{4.17}$$

$$\sigma_{\theta\phi}^{(R)} + \sigma_{\theta\phi}^{(s)} = 0 \tag{4.18}$$

and use of (4.17) gives, for $n = 0,1,2, \ldots$

$$(r/2)^{m+2n+1}: \sum_{\substack{\ell=0 \\ j=1,3}}^{n} A_{m,m+2\ell+1}^{(j)} e_{41}^{(1)} + B_{m,m+2\ell}^{(j)} e_{42}^{(1)} + C_{m,m+2\ell+1}^{(j)} e_{43}^{(1)} = 0$$

and

$$(r/2)^{-m-2n}: \sum_{\ell=\max(0,n)}^{\infty} \begin{pmatrix} + A_{m,m+2\ell-1}^{(2)} \\ iA_{m,m+2\ell-1}^{(3)} \end{pmatrix} e_{41}^{(2)} + \begin{pmatrix} + B_{m,m+2\ell}^{(2)} \\ iB_{m,m+2\ell}^{(3)} \end{pmatrix} e_{42}^{(2)} + \begin{pmatrix} + C_{m,m+2\ell-1}^{(2)} \\ iC_{m,m+2\ell-1}^{(3)} \end{pmatrix} e_{43}^{(2)} = 0 \tag{4.19}$$

where

$$e_{41}^{(1)} = e_{41}^{(1)}(m,m+2\ell+1,n-\ell)$$

$$e_{42}^{(1)} = e_{42}^{(1)}(m,m+2\ell,n-\ell)$$

$$e_{43}^{(1)} = e_{43}^{(1)}(m,m+2\ell+1,n-\ell)$$

$$e_{41}^{(2)} = e_{41}^{(2)}(m,m+2\ell-1,\ell-n)$$

$$e_{42}^{(2)} = e_{42}^{(2)}(m,m+2\ell,\ell-n)$$

$$e_{43}^{(2)} = e_{43}^{(2)}(m,m+2\ell-1,\ell-n) \tag{4.20}$$

An identical set of equations with $e_{4k}^{(j)}$ replaced by $e_{6k}^{(j)}$ follows on applying (4.18), the last boundary condition:

$$(r/2)^{m+2n+1}: \sum_{\substack{\ell=0 \\ j=1,3}}^{n} A_{m,m+2\ell+1}^{(j)} e_{61}^{(1)} + B_{m,m+2\ell}^{(j)} e_{62}^{(1)} + C_{m,m+2\ell+1}^{(j)} e_{63}^{(1)} = 0 . \quad n = 0,1,2, \ldots$$

$$(r/2)^{-m-2n}: \sum_{\ell=\max(0,n)}^{\infty} \begin{pmatrix} A_{m,m+2\ell-1}^{(2)} \\ + \\ iA_{m,m+2\ell-1}^{(3)} \end{pmatrix} e_{61}^{(2)} + \begin{pmatrix} B_{m,m+2\ell}^{(2)} \\ + \\ iB_{m,m+2\ell}^{(3)} \end{pmatrix} e_{62}^{(2)} + \begin{pmatrix} C_{m,m+2\ell-1}^{(2)} \\ + \\ iC_{m,m+2\ell-1}^{(3)} \end{pmatrix} e_{63}^{(2)} = 0 .$$

$$n = 0, \pm 1, \pm 2, \ldots \qquad (4.21)$$

Numerical Calculation

For each m, equations (4.1), (4.16), (4.19) and (4.21) constitute a system of homogeneous linear equations in the unknowns $A_{mn}^{(1)}$, $A_{mn}^{(2)}$, $B_{mn}^{(1)}$, $B_{mn}^{(2)}$, $C_{mn}^{(1)}$, $C_{mn}^{(2)}$, $n = 0,1,2, \ldots$ Symbolically, the system of equations can be represented by

$$\sum_{j=0}^{\infty} \mathcal{M}_{ij} x_j = n_i \qquad i = 0,1,2, \ldots , \qquad (5.1)$$

with

$\{\mathcal{M}_{ij}\}$ the known coefficients of an infinite matrix,

$\{x_j\}$ the unknown infinite sequence, and

$\{n_i\}$ a known infinite sequence.

Both the array $\{\mathcal{M}_{ij}\}$ and the sequence $\{n_i\}$ can be evaluated numerically. A standard way to solve for the unknown x_j's is to truncate the matrix into a finite size array and then invert the finite matrix. This procedure gives well convergent results when the matrix is "essentially banded," with terms close to the diagonal large in magnitude compared with the off-diagonal terms. This is achieved in the following two steps.

First, there are two particular types of terms in the matrix. One type is associated with the series expansion of j_n and the other type with that of y_n. They have differences in magnitude of large order. The first step is to "average out" the two types of terms by performing elementary operations of scaling and additions of rows of the

matrix. Let the resulting new matrix equation be denoted by

$$[\mathcal{M}_1]\{x\} = \{\mathcal{N}_1\} \tag{5.2}$$

The next step is to consider, instead, the matrix equation

$$[\mathcal{M}_1]^T[\mathcal{M}_1]\{x\} = [\mathcal{M}_1]^T\{\mathcal{N}_1\} \quad , \tag{5.3}$$

which is satisfied by the same set of x_j's. The new infinite matrix $[\mathcal{M}_1]^T[\mathcal{M}_1]$ has the advantage of being "essentially banded." By truncating (5.3) to a finite size array, the resulting finite matrix is ready for inversion. A sufficiently large number of terms are calculated so that last few terms will contribute less than the rounded-off errors.

Surface Displacements

From the strong-motion seismological and earthquake engineering points of view, an important aspect of the above analysis is the description of the displacement amplitudes and relative phases at various points along the surface of the half-space close to the hemispherical canyon. The precise description of the amplitudes and phases of surface ground motion will give the space-dependent transfer function of the hemispherical canyon and its dependence on incidence angle γ and the position of observation point. This information then helps to understand and interpret the effects of topographic features similar to the model studied here.

The amplitudes and phases of the displacement vector (u_r, u_θ, u_ϕ) are readily available from equations (1.2), (1.3), (1.4), (2.1) and (2.2), using equation (A3.2) given in Appendix III. These components are related to the rectangular components (u_x, u_y, u_z) by the relation

$$\begin{Bmatrix} u_x \\ u_y \\ u_z \end{Bmatrix} = \begin{bmatrix} \sin\theta\cos\phi & \cos\theta\cos\phi & -\sin\phi \\ \sin\theta\sin\phi & \cos\theta\sin\phi & \cos\phi \\ \cos\theta & -\sin\theta & 0 \end{bmatrix} \begin{Bmatrix} u_r \\ u_\theta \\ u_\phi \end{Bmatrix} \qquad (6.1)$$

For each of the complex components of $\underset{\sim}{u}$, we call its modulus along the plane stress-free surface (Figure 2) the 'displacement amplitude' of that component, given by

Displacement amplitudes:

$$|u_x| = \left[\mathrm{Re}^2(u_x) + \mathrm{Im}^2(u_x)\right]^{\frac{1}{2}}$$

$$|u_y| = \left[\mathrm{Re}^2(u_y) + \mathrm{Im}^2(u_y)\right]^{\frac{1}{2}}$$

$$|u_z| = \left[\mathrm{Re}^2(u_z) + \mathrm{Im}^2(u_z)\right]^{\frac{1}{2}} , \qquad (6.2)$$

and the corresponding phases in the x- and z-direction:

$$\phi_x = \tan^{-1}(\mathrm{Im}(u_x)/\mathrm{Re}(u_x))$$

$$\phi_z = \tan^{-1}(\mathrm{Im}(u_z)/\mathrm{Re}(u_z)) \quad , \tag{6.3}$$

with Re(•) and Im(•) denoting the real and imaginary parts of a complex number, respectively. Only the x- and z-components' phases are considered because the propagation vector $\underset{\sim}{k}$ of the incident P-wave is only in the x-z plane.

Both the amplitude and the phase of each component depend on: (i) the angle of incidence of the plane P-waves, (ii) their frequency ω, (iii) the radius of the hemispherical canyon, a, and (iv) $\kappa = \alpha/\beta$, the ratio of longitudinal to transverse wave speeds in the half-space.

In the absence of the hemispherical canyon, the surface displacement amplitude of each component in the uniform half-space is no more than 2, for incident P-wave of unit amplitude. The z-component amplitude is 2 for the case of a vertically incident plane P-wave ($\gamma = 0$). Also, for $\gamma < 90°$ the phase angles ϕ_x, ϕ_z are both given by

$$\phi_x = \phi_z = k_\alpha \sin\gamma \; x \quad , \tag{6.4}$$

which is a linear function of x. In the presence of the hemispherical canyon, the incident and plane reflected waves scatter and diffract around the canyon. The scattered and diffracted waves, $\underset{\sim}{u}^{(s)}$, $\underset{\sim}{u}^{(R)}$ interfere with the plane incident and reflected waves, $\underset{\sim}{u}^{(i)}$, $\underset{\sim}{u}^{(r)}$. Amplitudes and phases of the resulting motion near the canyon may then significantly depart from that of the far-field motion.

Following reference 8, the following dimensionless parameter is

introduced to simplify the description of the problem,

$$\eta^{*} = 2a/\lambda_{\beta} = k_{\beta}a/\pi = \omega a/\pi\beta \quad . \tag{6.5}$$

η is the ratio of the diameter of the hemispherical canyon to wavelength of the transverse waves present in the half-space. From equation (6.5), it can also be considered as a dimensionless wave number ($=k_{\beta}a/\pi$), or dimensionless frequency ($=\omega a/\pi\beta$).

The wave speed α differs from β for all real solids and their ratio, $\kappa = \alpha/\beta$, is a function of Poisson's ratio ν,

$$\kappa = \alpha/\beta = \left(\frac{2-2\nu}{1-2\nu}\right)^{\frac{1}{2}} \tag{6.6}$$

The typical value of $\nu = 0.25$, or $\kappa^2 = 3$ is chosen for the following presentation.

Figures 3 to 21 present typical characteristics of amplitudes and phases of surface displacements at dimensionless points (x/a, y/a) near the canyon for angles of incidence $\gamma = 0°$, $30°$, $60°$, and $85°$. The value of dimensionless frequency, η, is 0.5 and Poisson's ratio, ν, is 0.25, ($\kappa = \sqrt{3}$). Lower values of η have been found to show less departure from uniform half-space motions. This is because small η corresponds to waves with wavelengths long compared to the radius of the canyon, and long waves do not "see" short topographic irregularities. Higher values of η than 0.5 in the present model will require more detailed numerical analysis and use of a higher-order matrix for convergence.

In Figures 3 to 21, the incident P-waves have their propagation vectors in the x-z plane ($y = 0$), the resulting motions are thus symmetric about $y = 0$, and so only the amplitudes on the positive y/a-axis

*Designated by ETA in the figures.

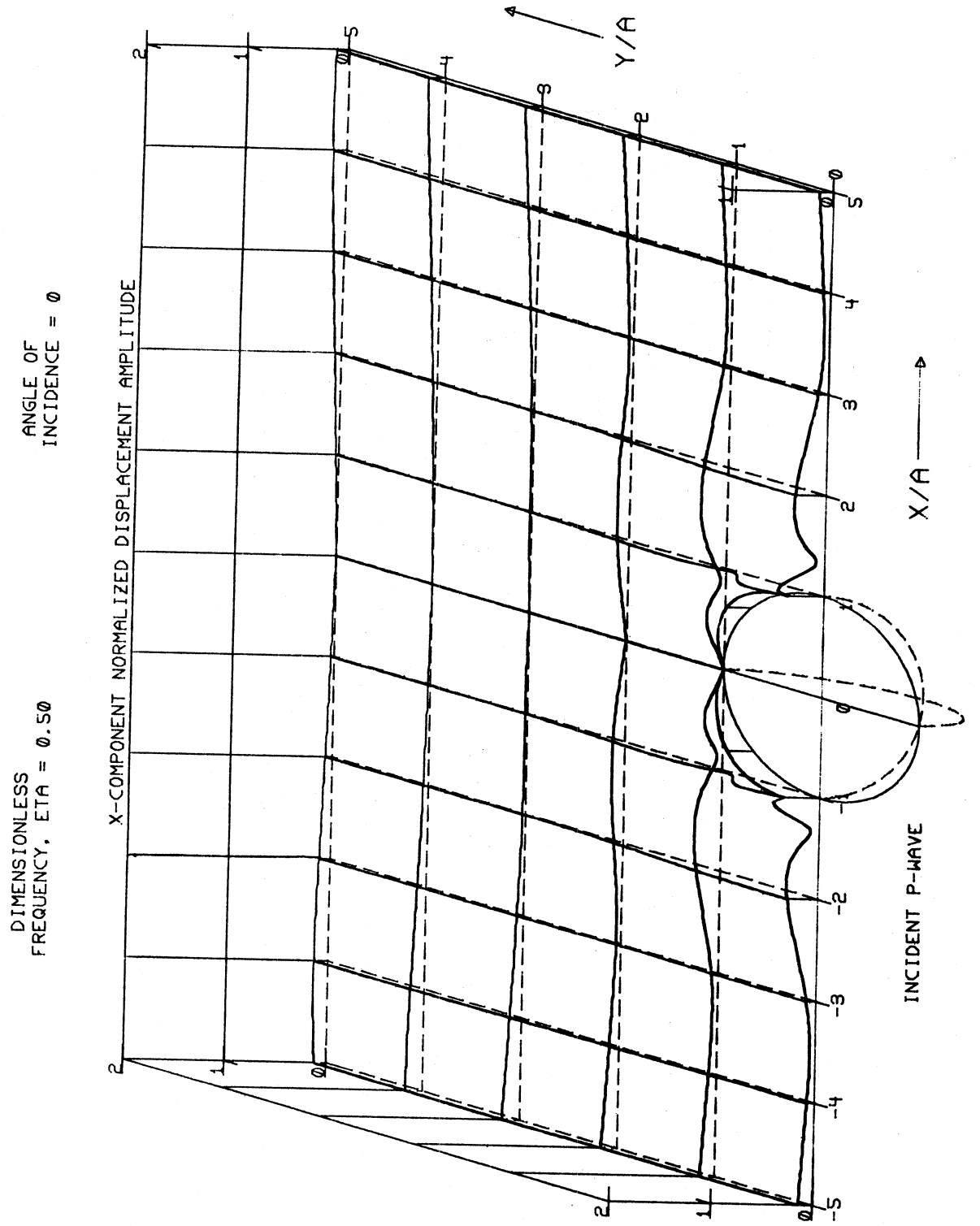

Figure 3

Free-Field Amplitude, $|u_x| = 0$

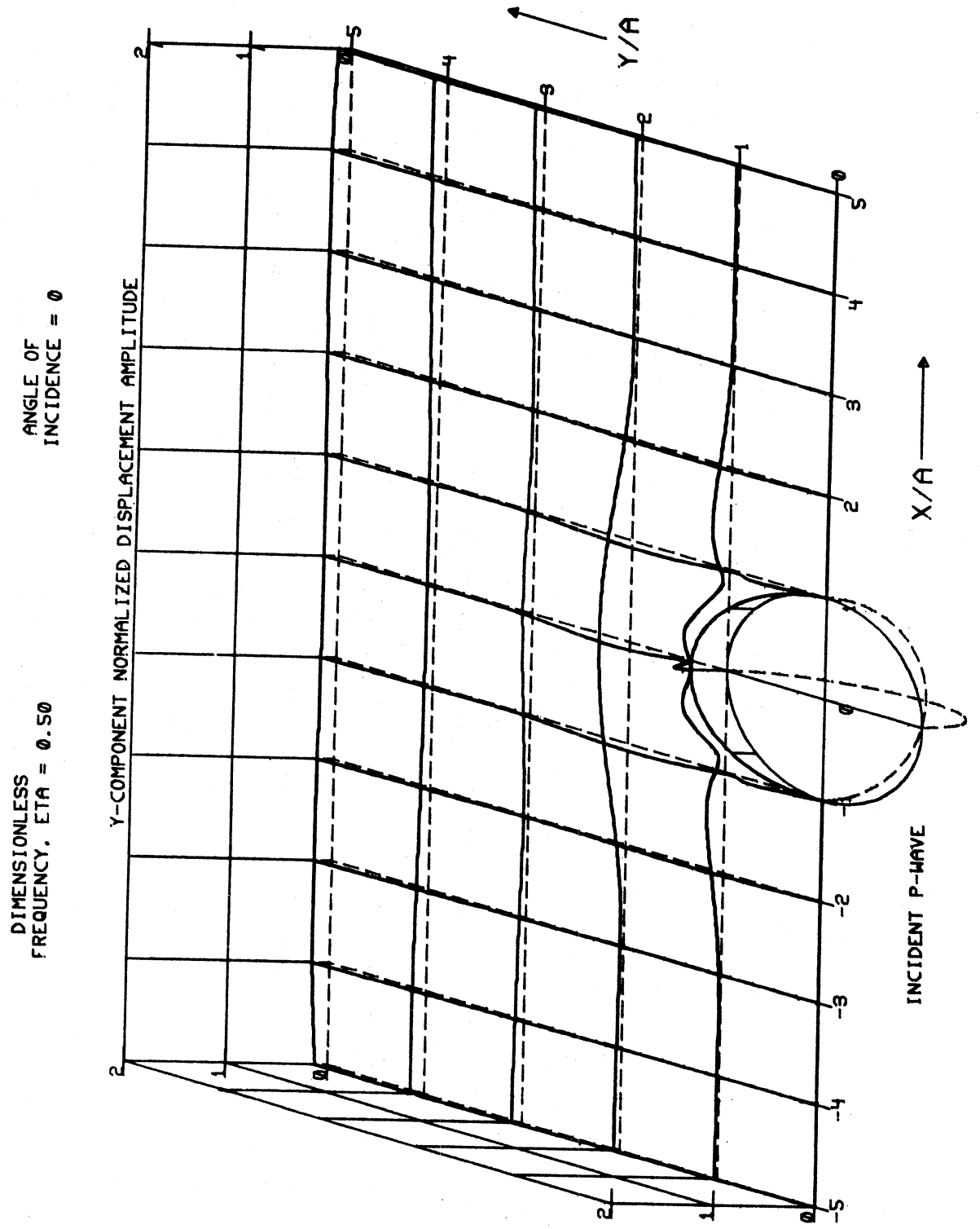

Figure 4

Free-Field Amplitude = $|u_y| = 0$

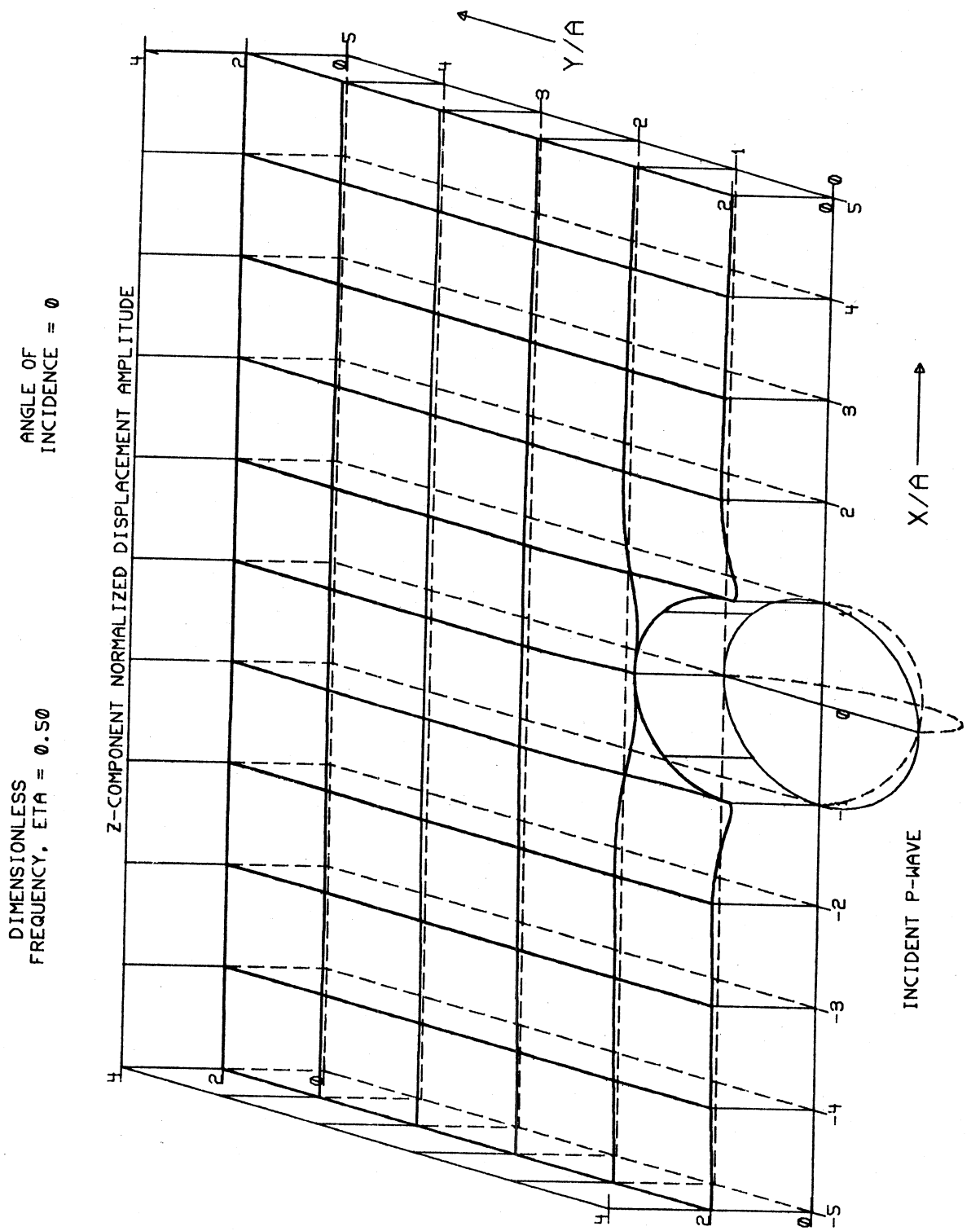

Figure 5

Free-Field Amplitude, $|u_z| = 2$

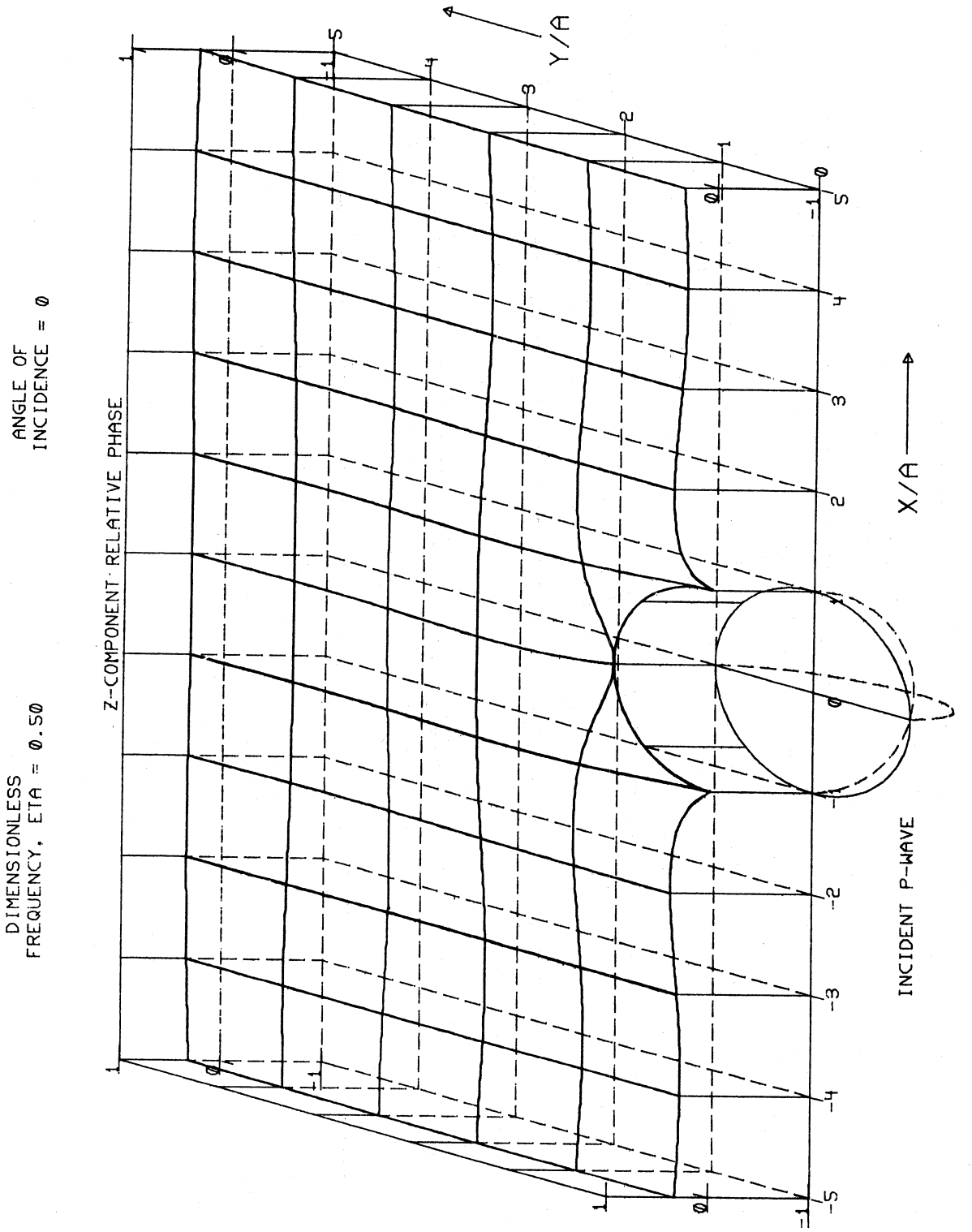

Figure 6

Phase/π

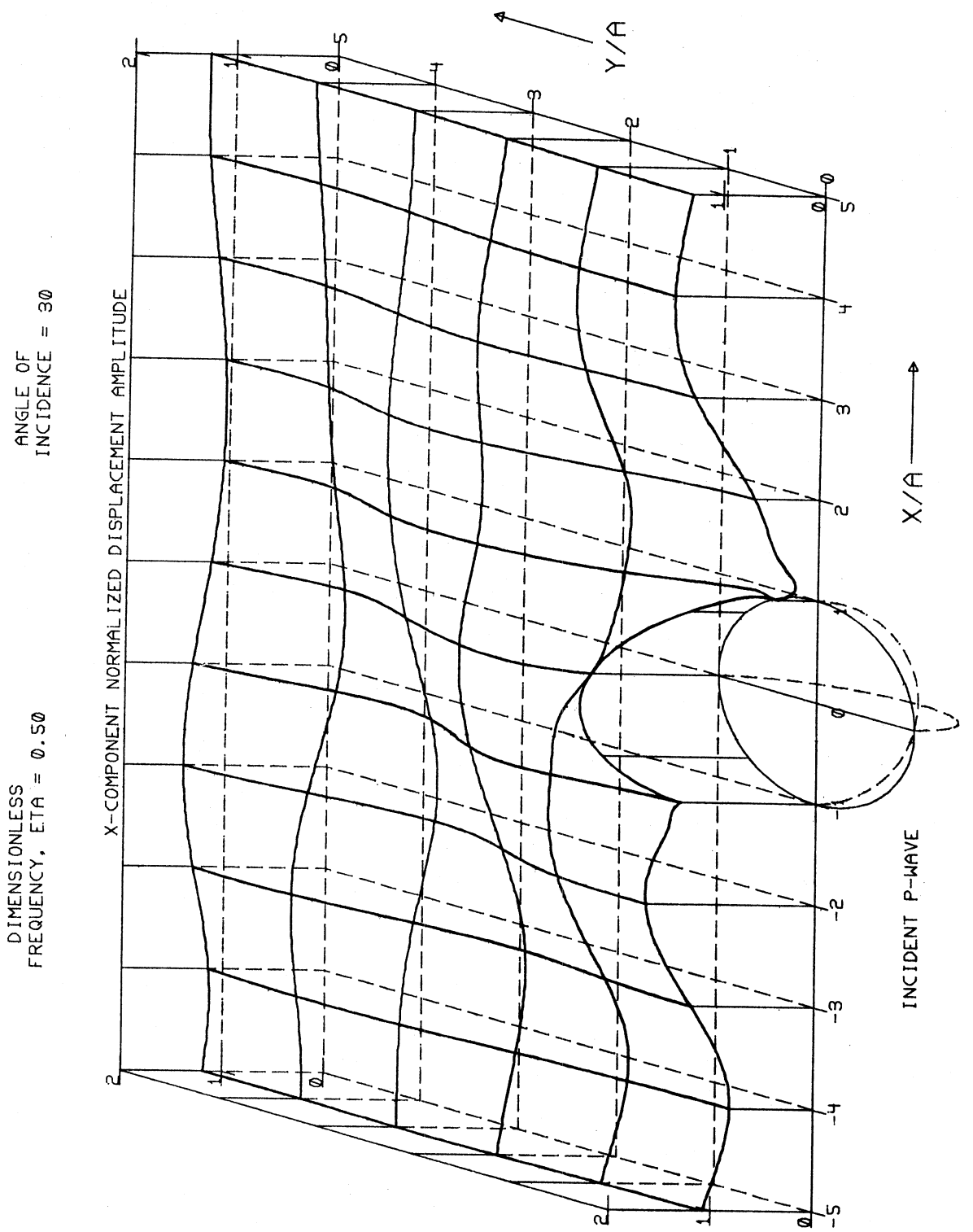

Figure 7

Free-Field Amplitude, $|u_x| = 1.121$

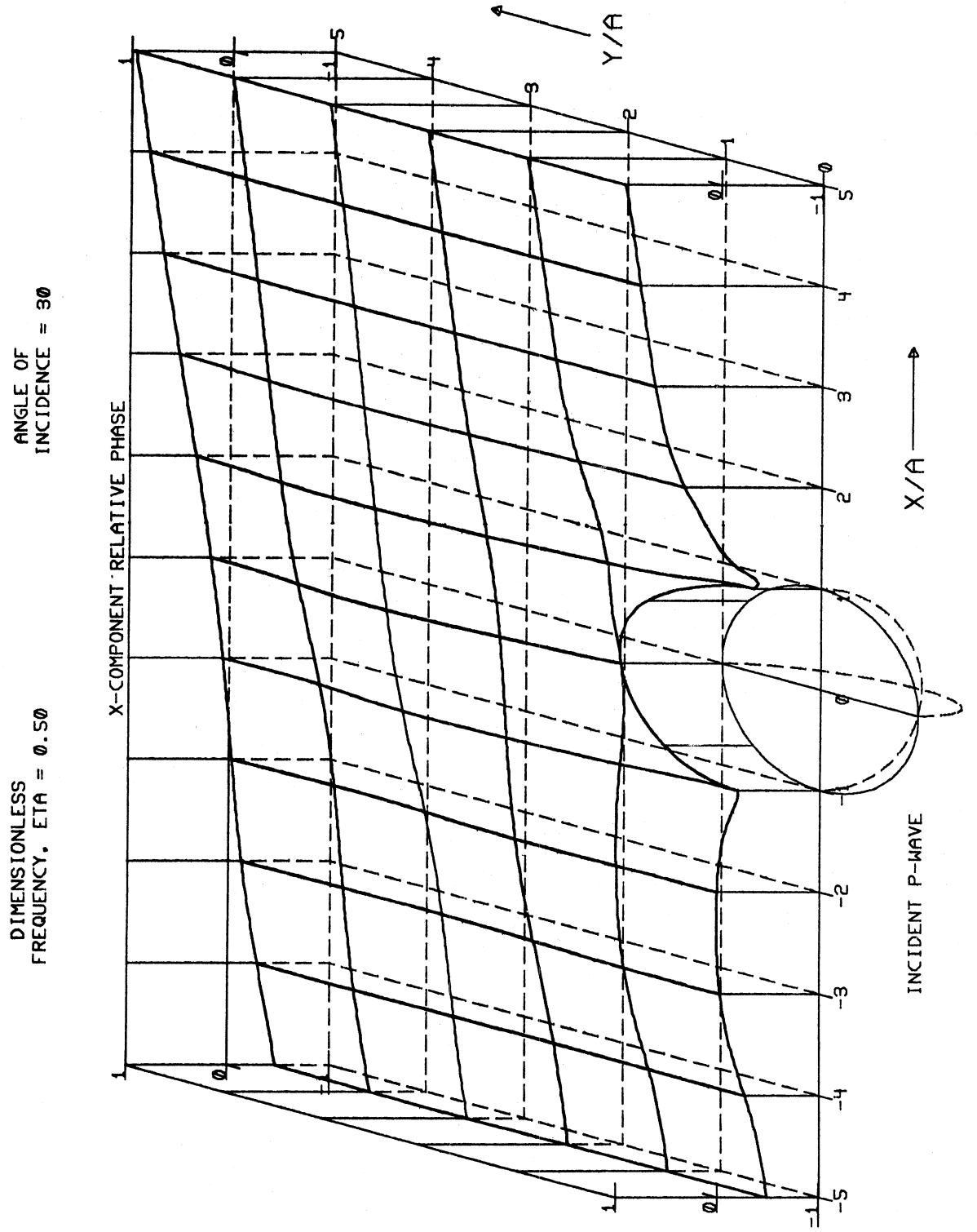

Figure 8

Phase/π

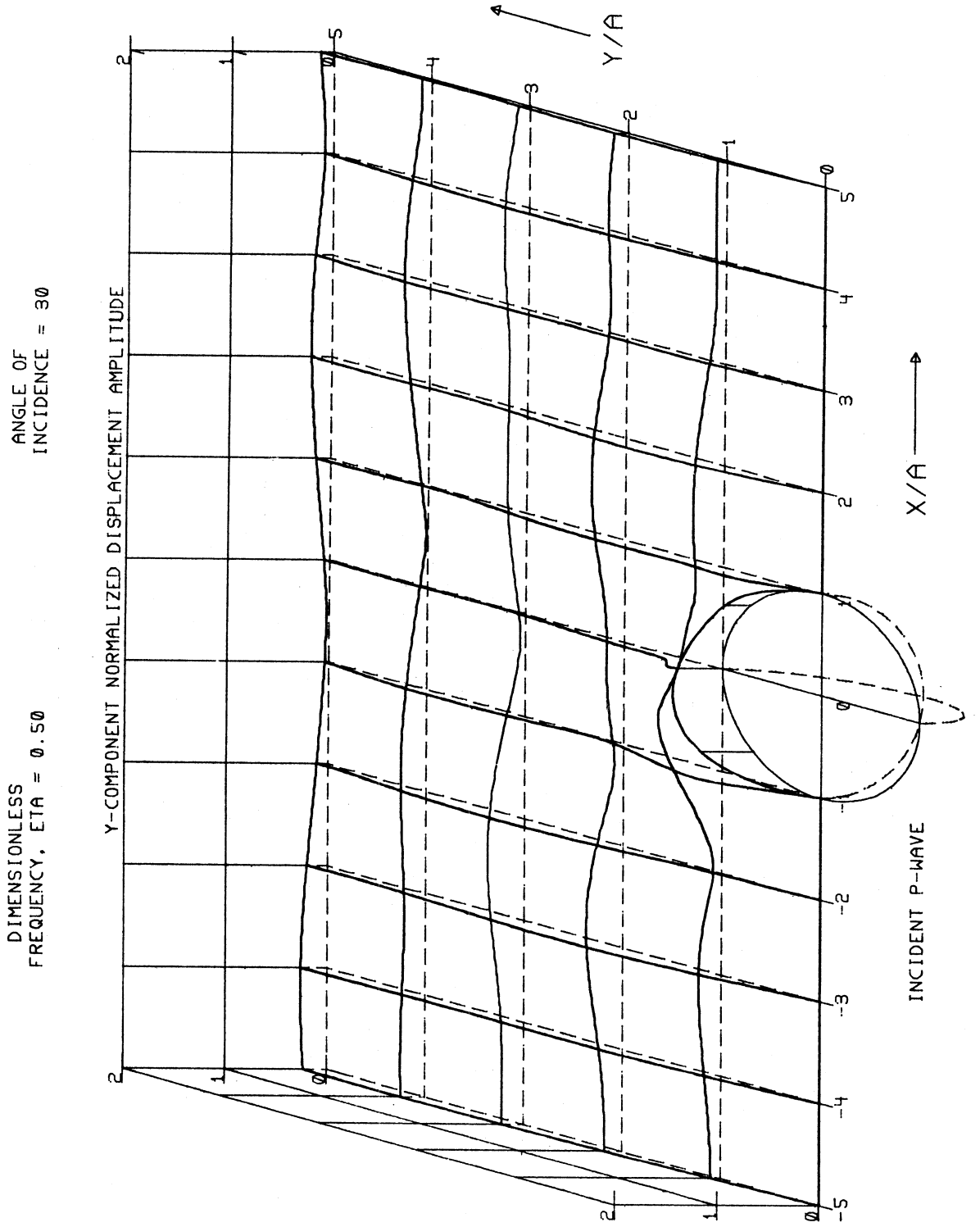

Figure 9

Free-Field Amplitude, $|u_y| = 0$

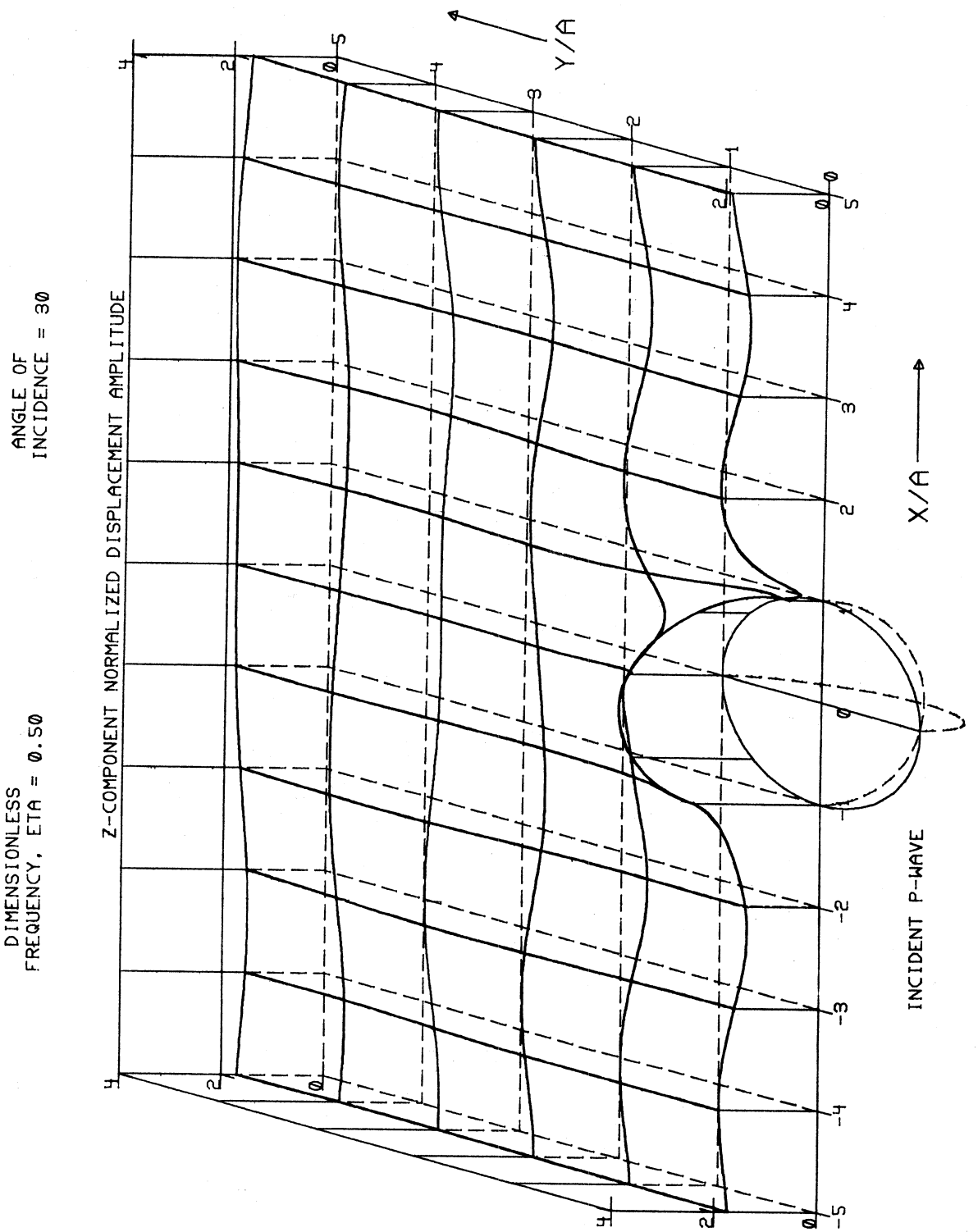

Figure 10

Free-Field Amplitude, $|u_z| = 1.690$

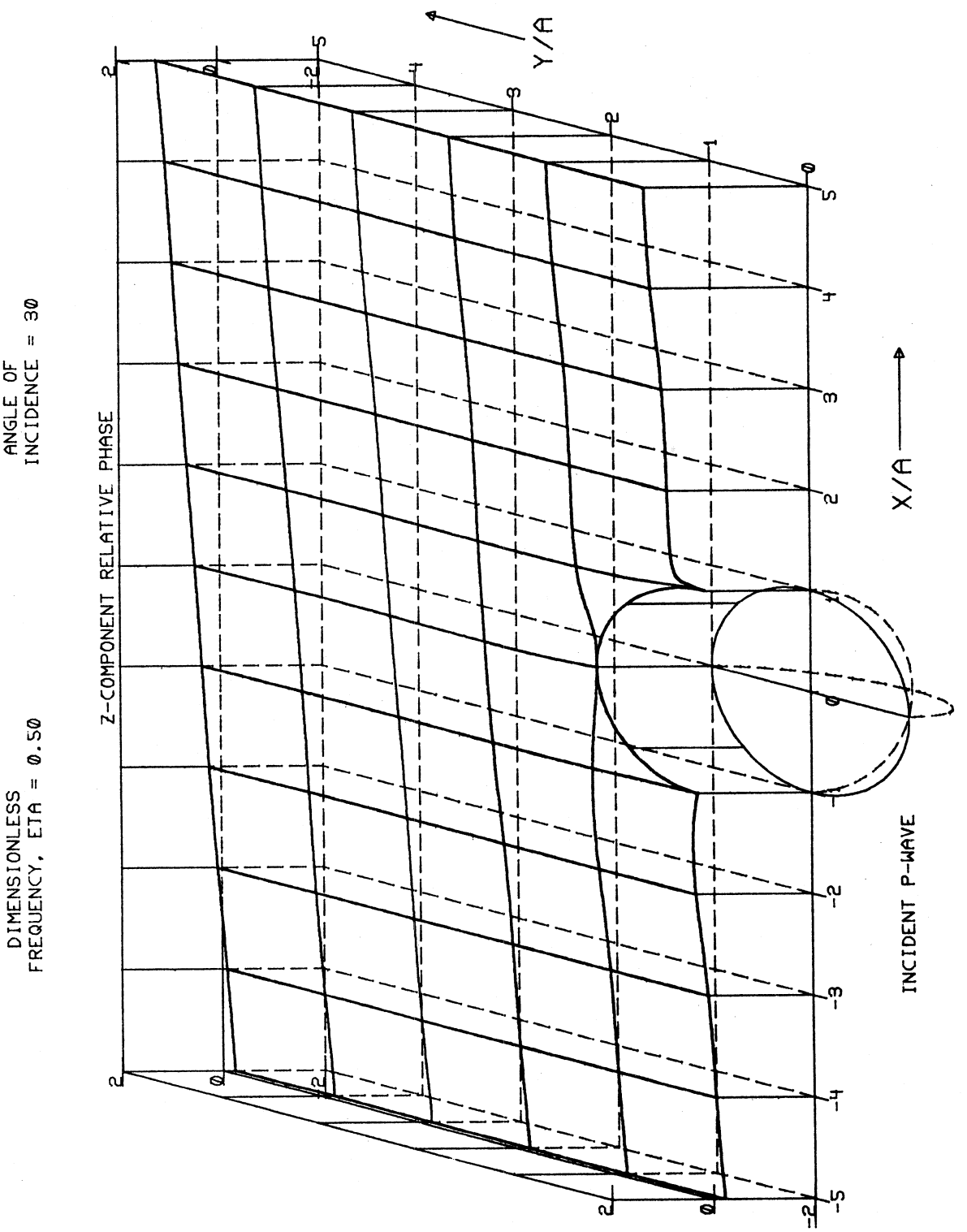

Figure 11

Phase/π

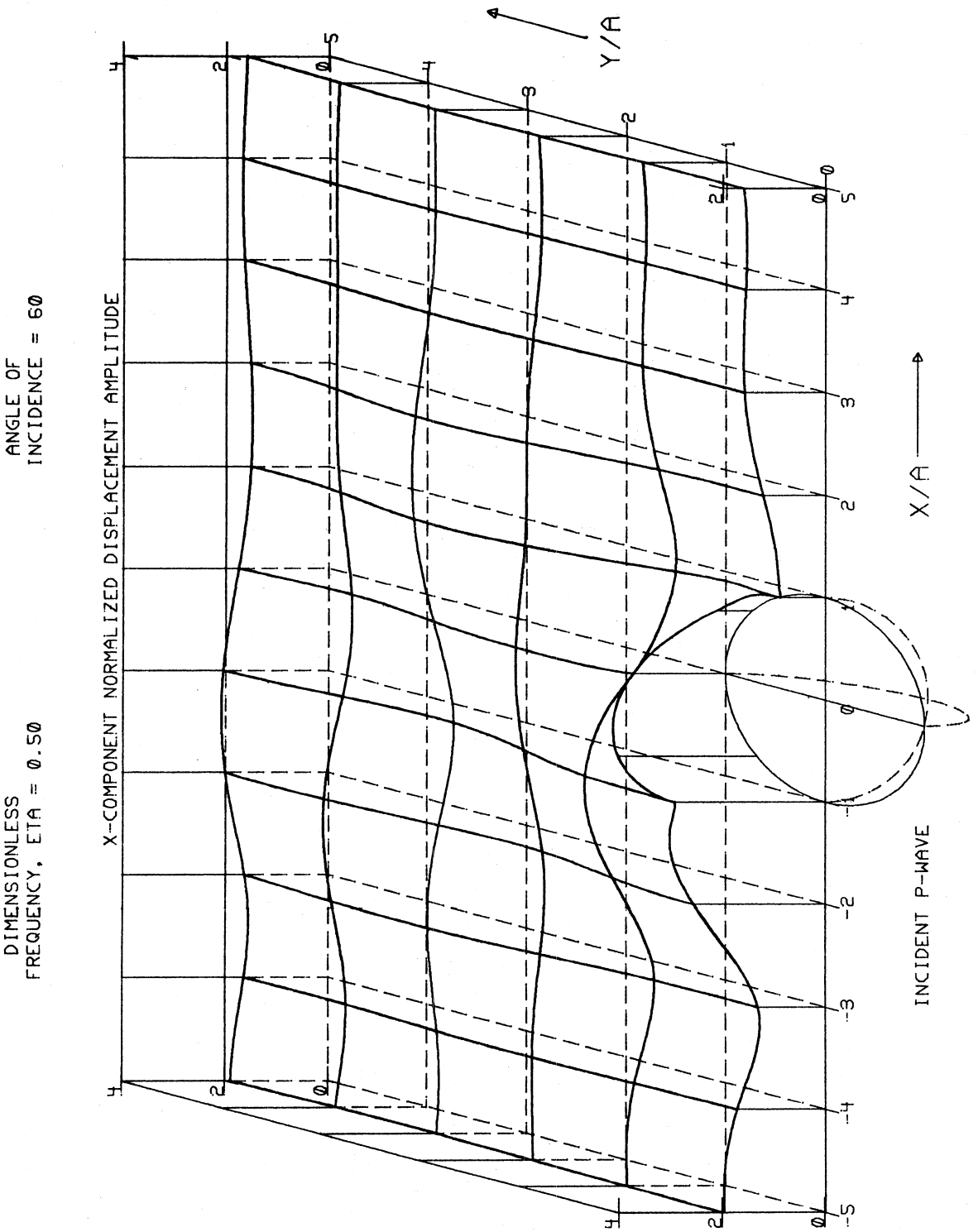

Figure 12

Free-Field Amplitude, $|u_x| = 1.732$

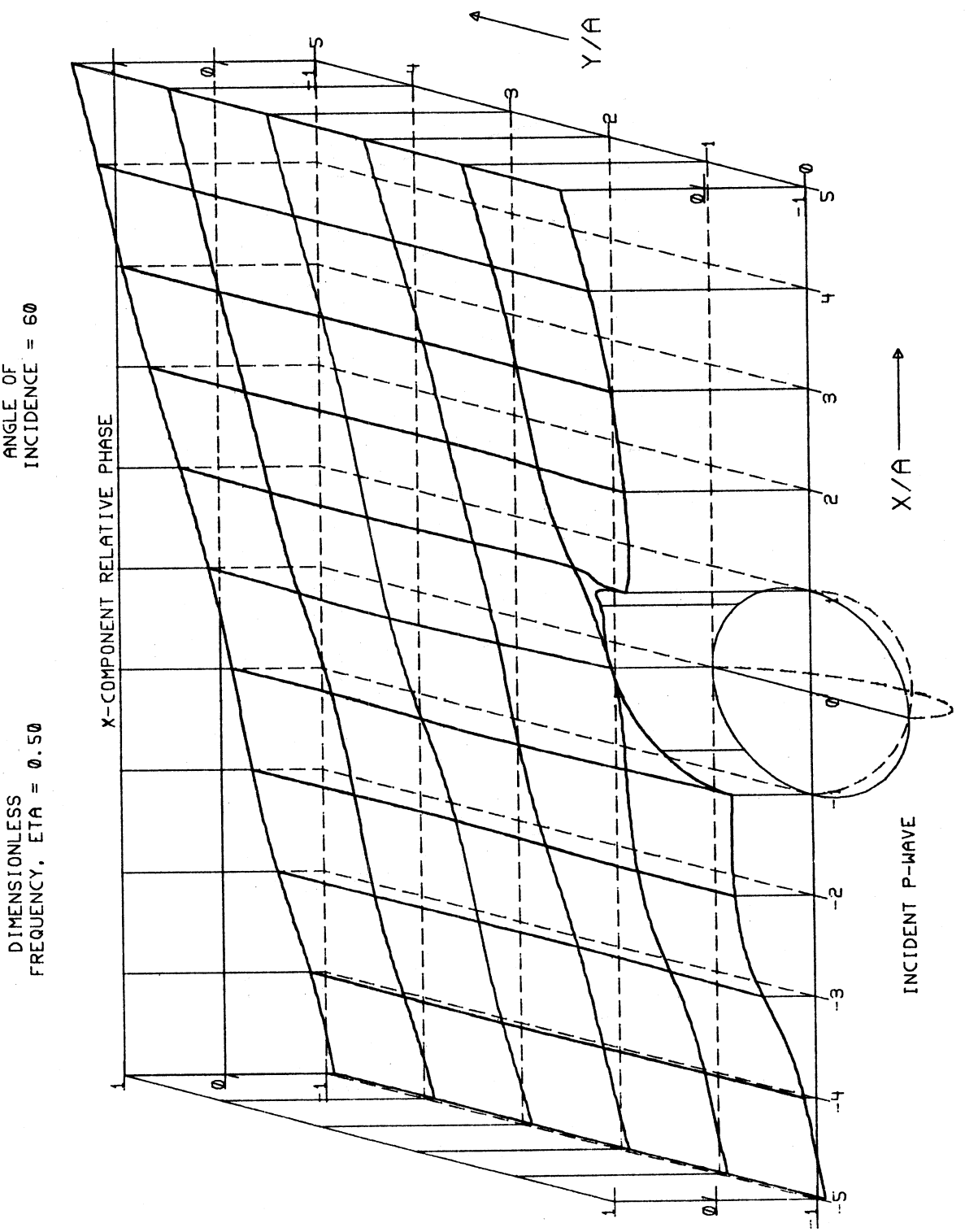
ANGLE OF
INCIDENCE = 60
DIMENSIONLESS
FREQUENCY, ETA = 0.50
X-COMPONENT RELATIVE PHASE
Y/A
X/A
INCIDENT P-WAVE
Phase/π

Figure 13

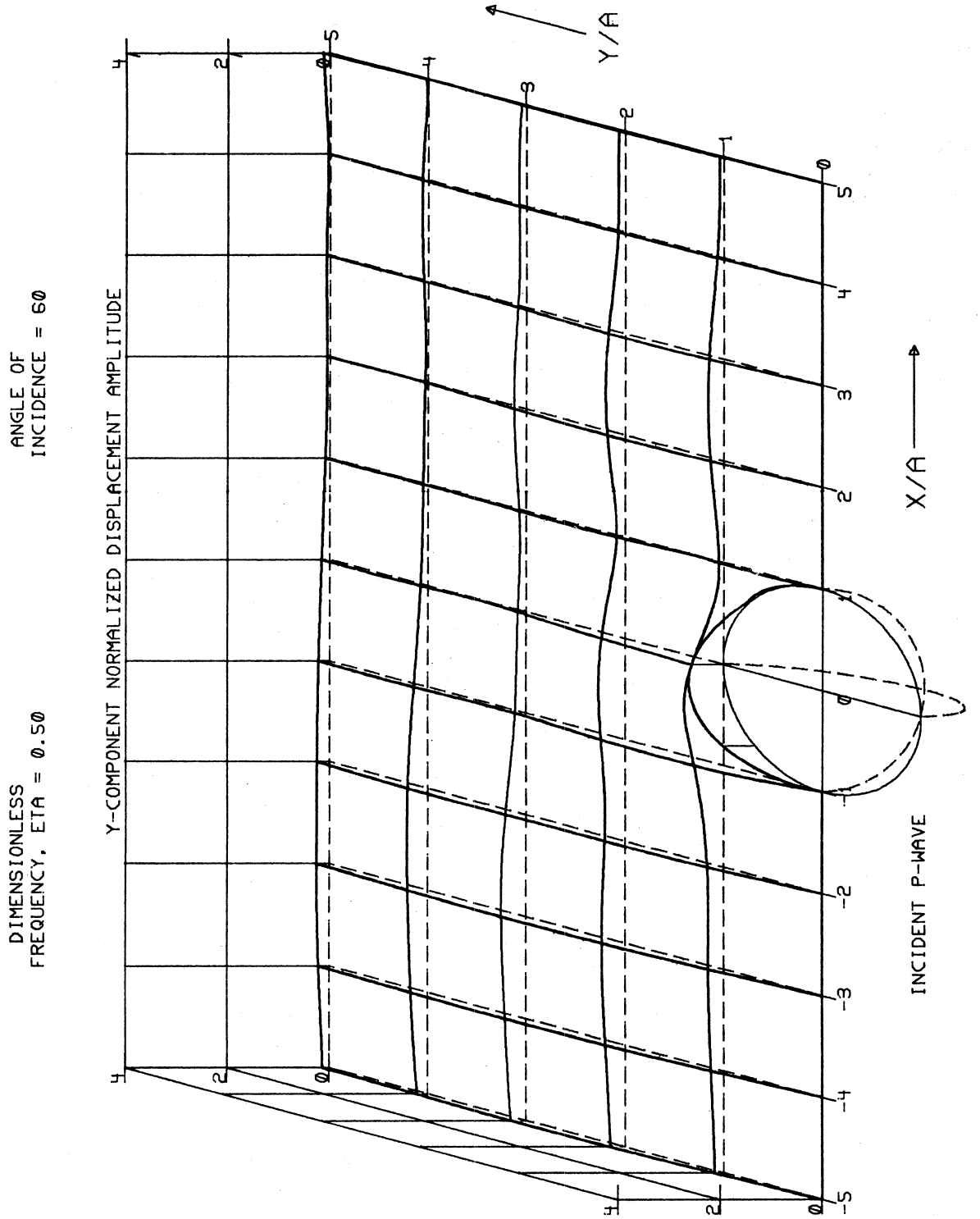

Figure 14

Free-Field Amplitude, $|u_y| = 0$

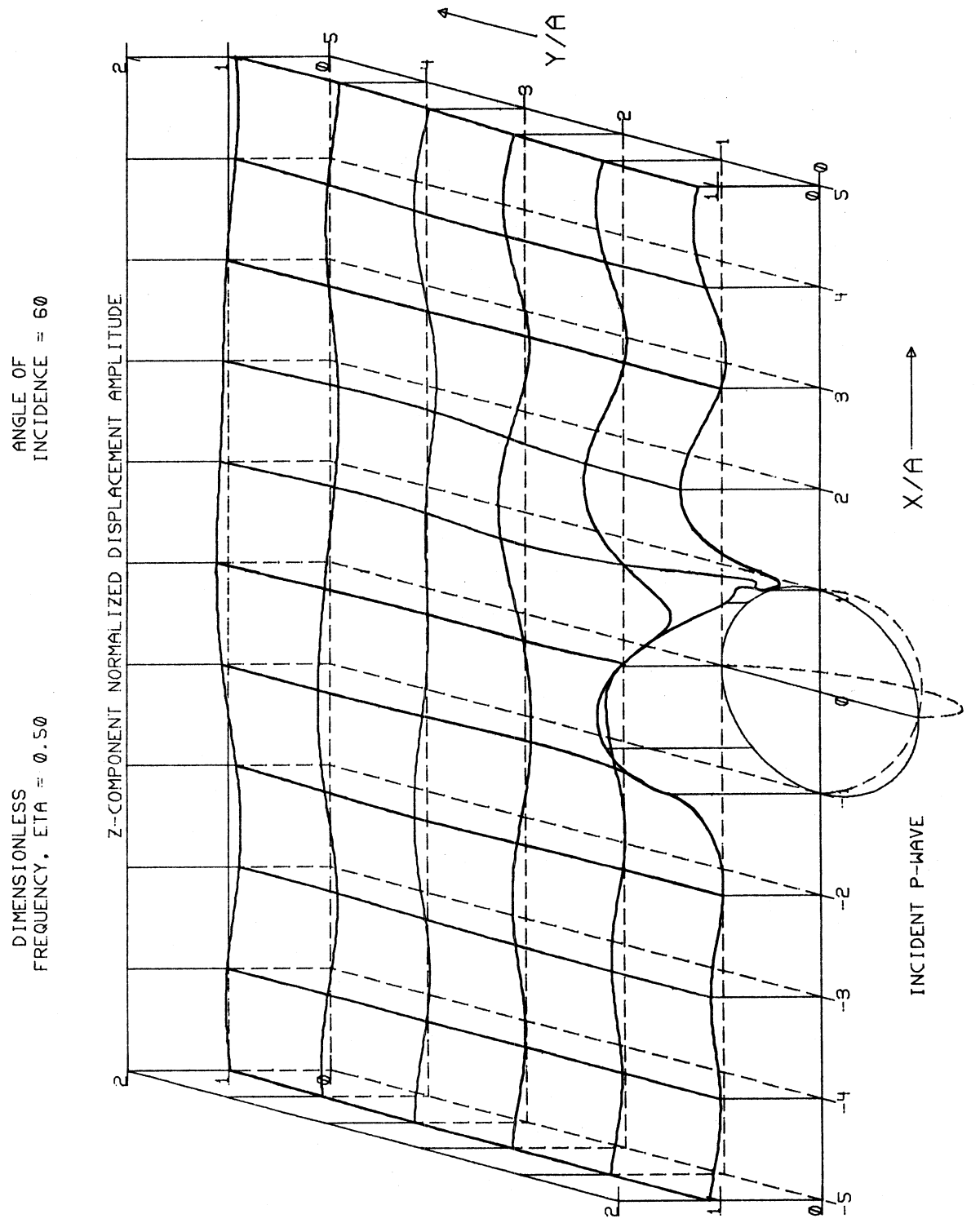

Figure 15

Free-Field Amplitude, $|u_z| = 1.00$

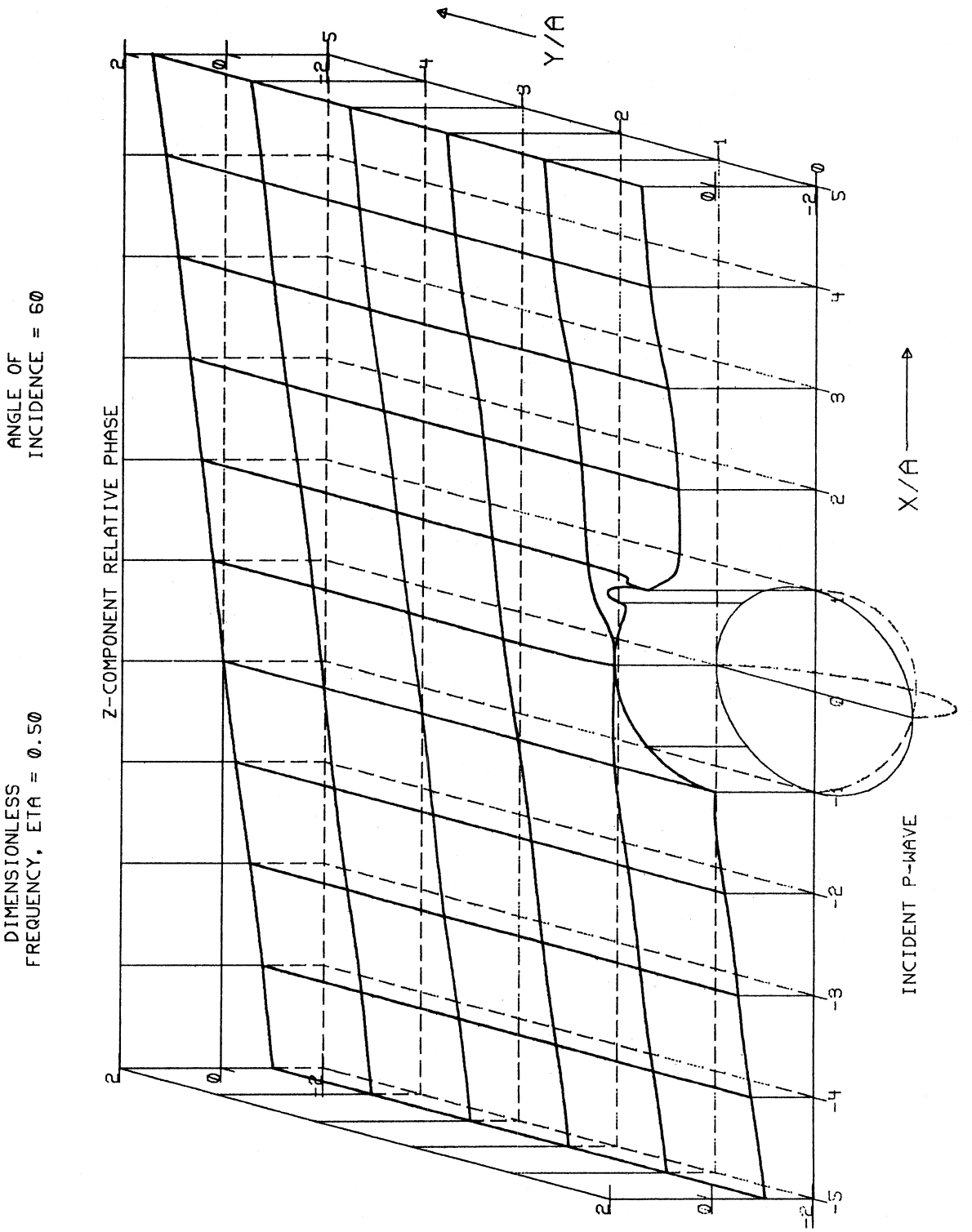

Figure 16

Phase/π

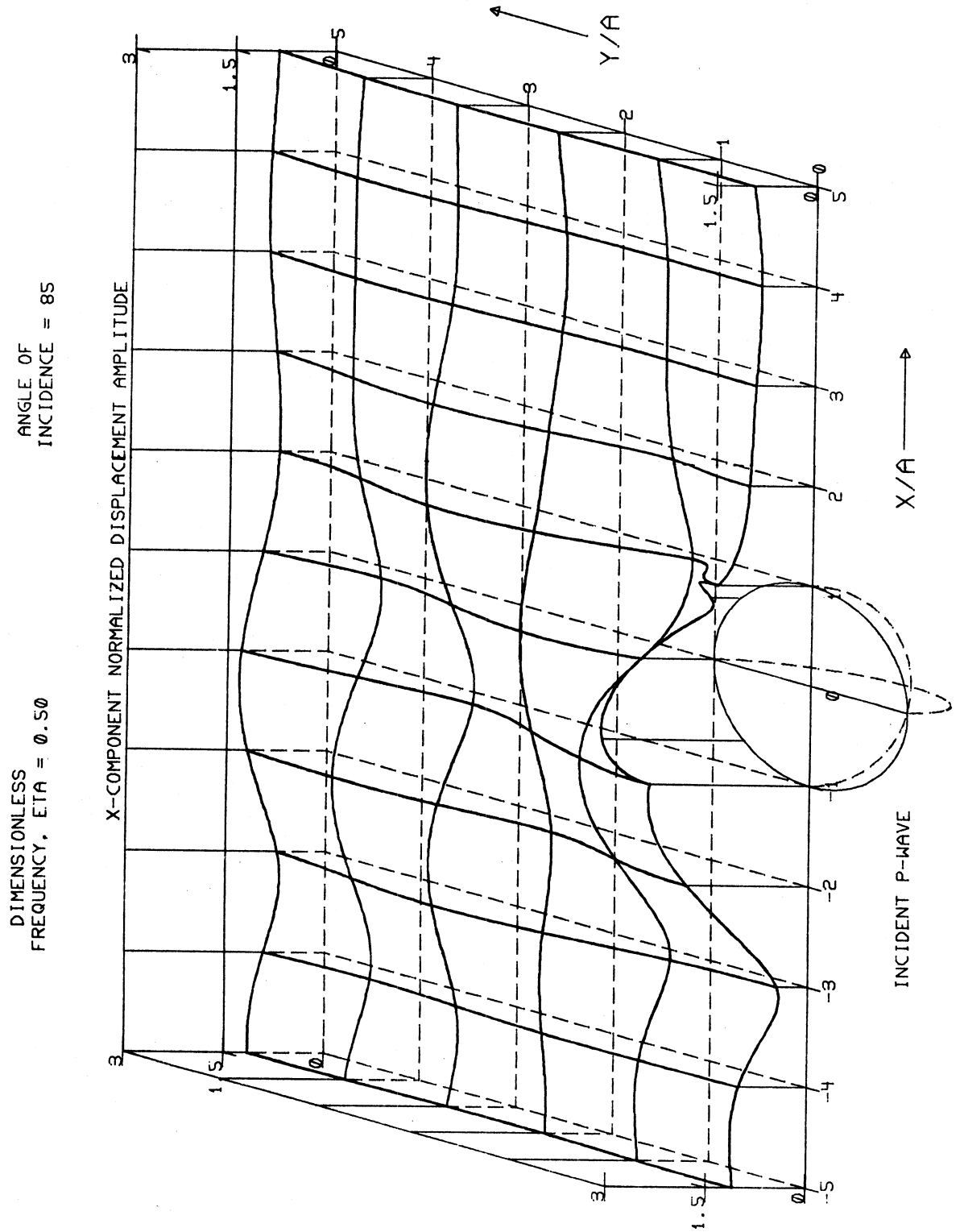

Figure 17

Free-Field Amplitude, $|u_x| = 0.971$

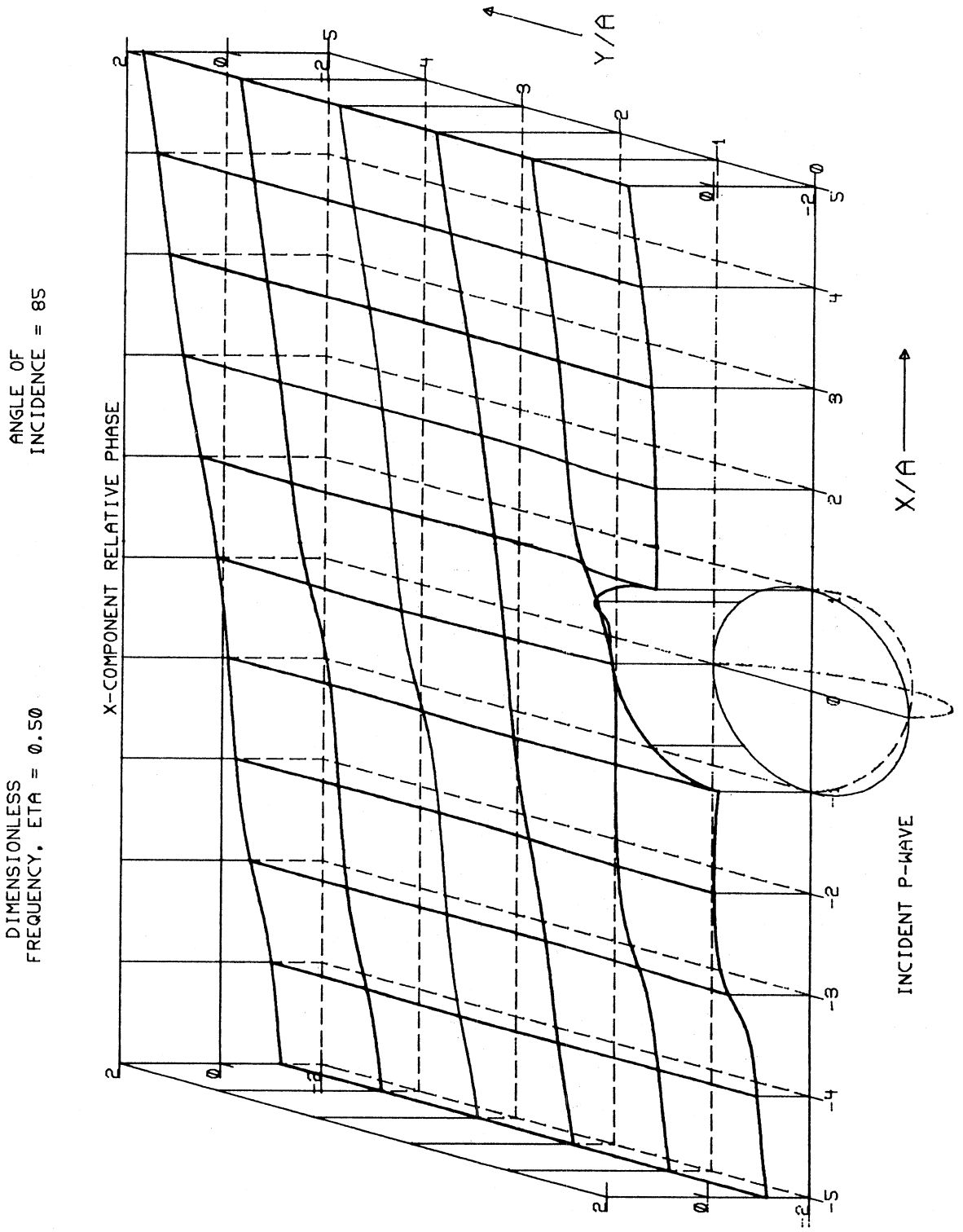

Figure 18

Phase/π

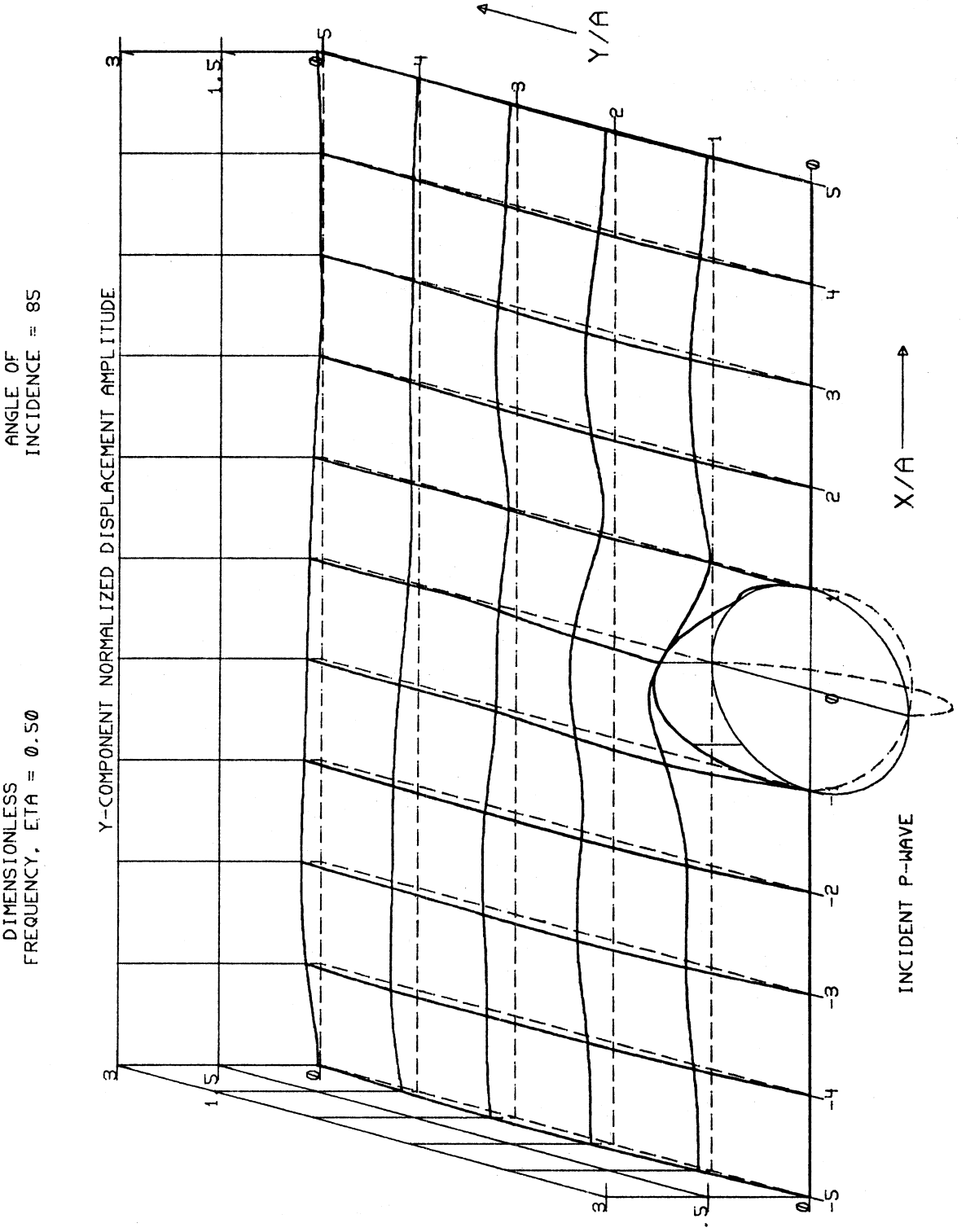

Figure 19

Free-Field Amplitude, $|u_y| = 0$

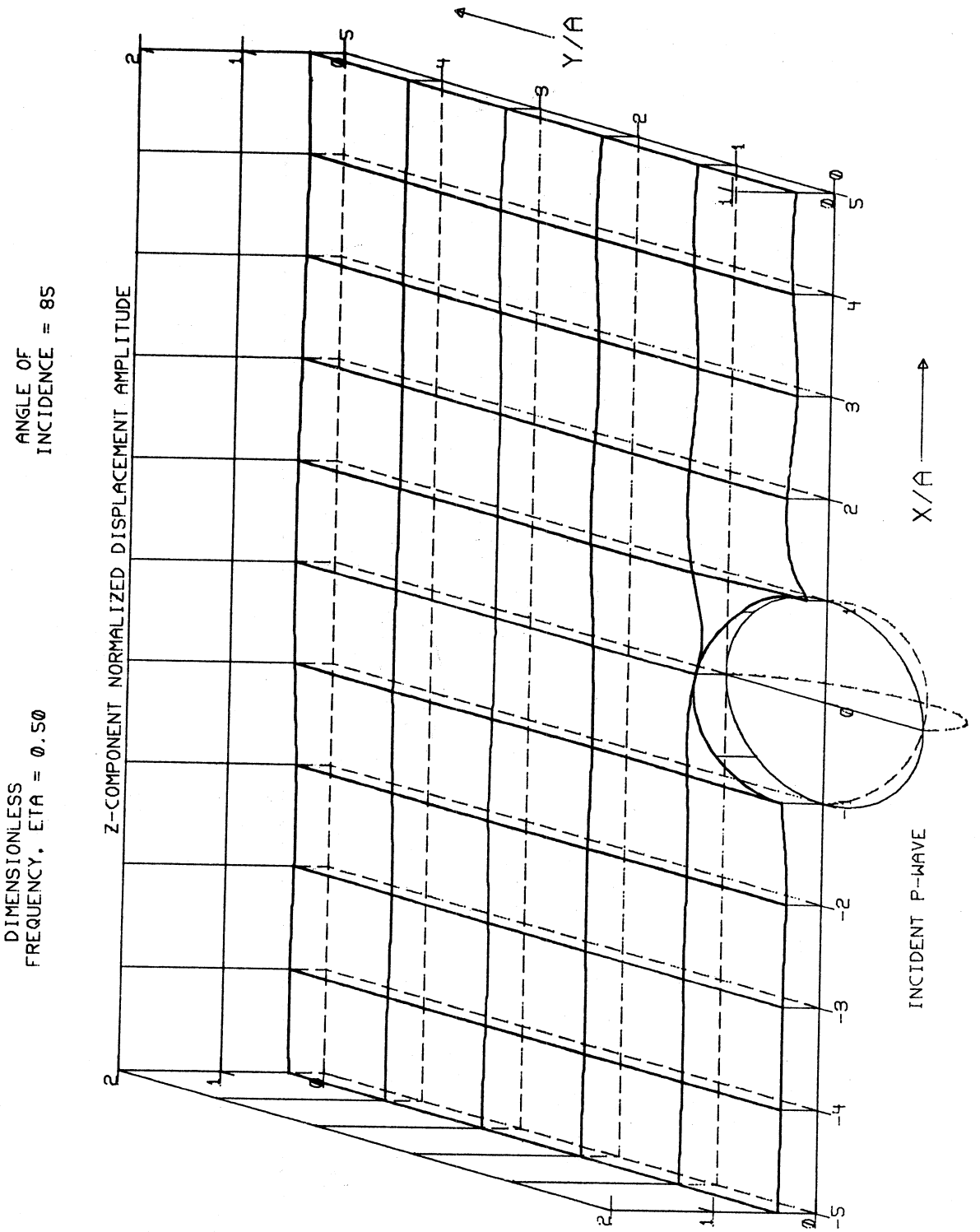

Figure 20

Free-Field Amplitude, $|u_z| = 0.349$

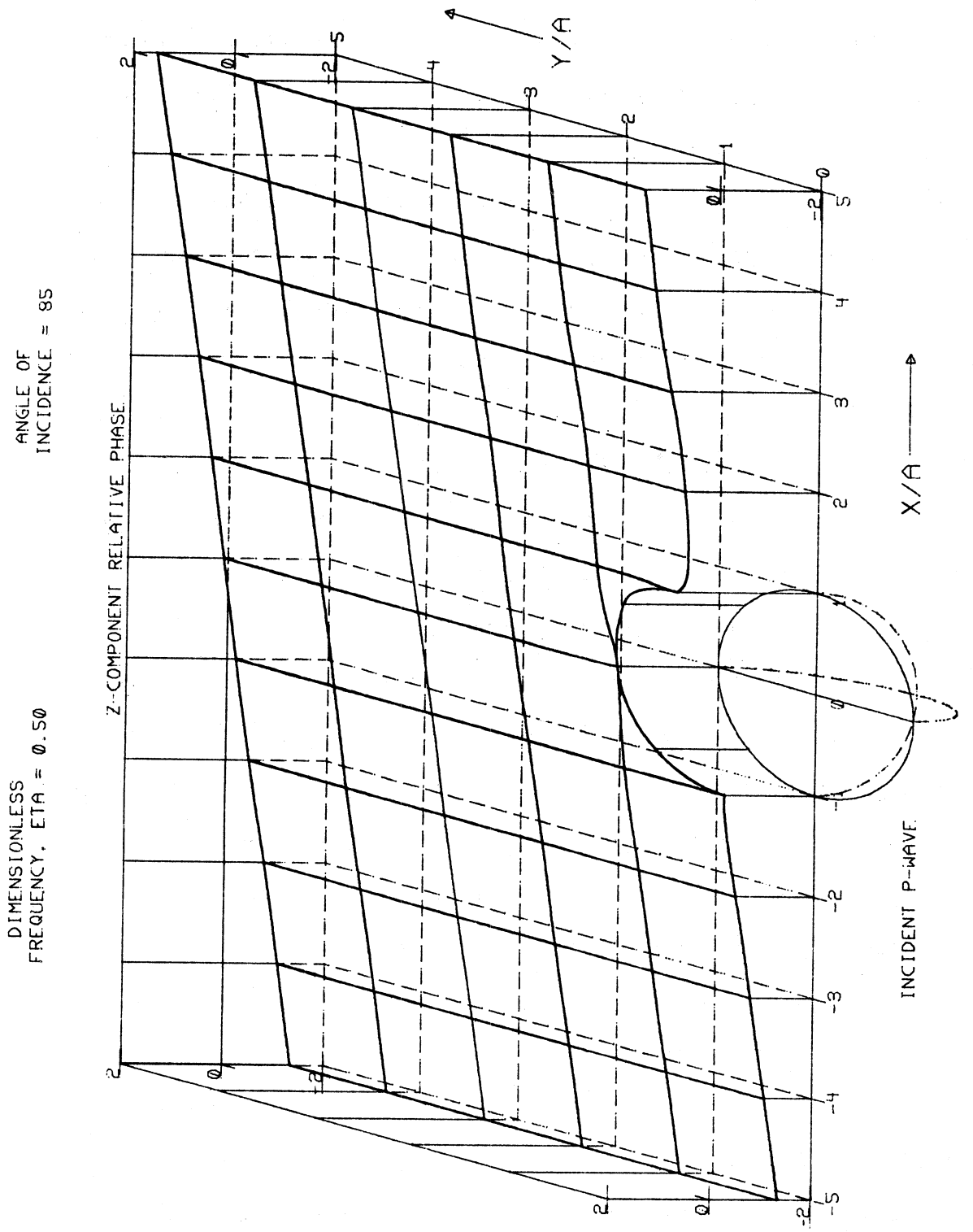

Figure 21

Phase/π

are plotted.

The point $(x/a, y/a) = (-1,0)$ corresponds to the leftmost rim of the canyon, and $(x/a, y/a) = (1,0)$ to the rightmost rim. The rim of the canyon is defined by $(x/a)^2 + (y/a)^2 = 1$.

The phase diagrams have been shifted arbitrarily to have a common zero phase at the point $(x/a, y/a) = (0,1)$. This is in agreement with the convention used in Reference 8. The phase values presented are in multiples of π. A phase of +1 in the phase diagrams thus correspond to a phase value of $+\pi$.

The displacement amplitudes shown illustrate several interesting features of the model. The most prominent one is that there are no points on the surface of the half-space, including points on the rim of the canyon, that lead to high amplification.

The case of vertical incidence ($\gamma = 0°$) leads to symmetric results for displacement amplitudes and phases, as the model is symmetric. The displacement amplitudes only slightly depart from the uniform half-space amplitude, which equals 2 for the vertical z-component and 0 for the horizontal x- and y-components. Likewise, the z-component phases are quite close to the straight lines for uniform half-space.

As γ increases from 0° to 90°, a progressively more complicated pattern of ground displacements and phases of all components is observed. For acute incidence ($\gamma > 0°$), the incident P-waves arrive from the 'left,' i.e., from the direction of negative x-axis. The left side of the canyon acts as a barrier, reflecting an appreciable amount of energy back in the direction from which it comes. This causes scattering

predominently from the canyon side near (x/a, y/a) = (-1,0), and a shadow zone is formed behind the canyon near (x/a, y/a) = (1,0). For large values of (x/a, y/a), i.e., at distances far from the canyon, the amplitudes of each component approach that of uniform half-space motions.

The phase diagrams show a similar trend. Abrupt jumps are observed most prominently at points near the canyon where the displacement amplitudes become very small. The points where such jumps occur have predominently torsional vibrations. Similarly, for large values of (x/a, y/a), the phases all tend to the linear phase relationship for uniform half space.

The case of grazing incidence ($\gamma = 90°$) is not presented, and is replaced by nearly grazing incidence ($\gamma = 85°$). This is because in uniform half-space, the case of grazing incident P-waves will result in zero motion everywhere.

The above observations are reminiscent of the analysis of SH-waves scattering from a semi-circular canyon in Reference 8, and a semi-elliptical canyon in Reference 12.

Excitation: Incident SV-Wave

The analysis for an incident transverse SV-wave is similar to the forgoing analysis. The plane SV-wave has its displacement and propagation vector again situated in the x-z plane, similar to the case of incident P-wave. It has angle of incidence δ, circular frequency ω and is represented by the displacement vector $\underset{\sim}{u}^{(i)}$, where

$$\underset{\sim}{u}^{(i)} = ik_\beta(-\cos\delta\ \underset{\sim}{e}_x + \sin\delta\ \underset{\sim}{e}_z)\exp ik_\beta(x\sin\delta + z\cos\delta)\ , \qquad (7.1)$$

of wavelength $\lambda_\beta = 2\pi/k_\beta$, where $k_\beta = \omega/\beta$ is the transverse wave number. The magnitude of the displacement vector, $|\underset{\sim}{u}^{(i)}|$, is k_β.

In the presence of only the free half-space boundary, the incident SV-wave is reflected from the plane free surface (z=0). Two separate cases are to be considered:

(i) incidence at or below the critical angle ($\delta \le \delta_{cr}$), and

(ii) incidence beyond the critical angle: total reflection ($\delta > \delta_{cr}$), where the critical angle, δ_{cr}, is given by

$$\delta_{cr} = \sin^{-1}(\beta/\alpha) \qquad (7.2)$$

Case (i) - Incidence at or below the critical angle ($\delta \le \delta_{cr}$):

In general, both reflected longitudinal (P) and transverse (SV) plane waves will be generated, with displacement vectors respectively given by

$$\text{(P):}\quad \underset{\sim}{u}_1^{(r)} = iK_1k_\alpha(\sin\gamma\ \underset{\sim}{e}_x - \cos\gamma\ \underset{\sim}{e}_z)\exp ik_\alpha(x\sin\gamma - z\cos\gamma) \qquad (7.3)$$

$$\text{(SV):}\quad \underset{\sim}{u}_2^{(r)} = iK_2k_\beta(\cos\delta\ \underset{\sim}{e}_x + \sin\delta\ \underset{\sim}{e}_z)\exp ik_\beta(x\sin\delta - z\cos\delta) \qquad (7.4)$$

where $k_\alpha = \omega/\alpha$ is the longitudinal wave number,

γ is the angle of reflection of the P-wave, and

K_1, K_2 are reflection coefficients given by

$$K_1 = \frac{-(\alpha/\beta)^2 \sin 4\delta}{\sin 2\gamma \sin 2\delta + (\alpha/\beta)^2 \cos^2 2\delta}$$

$$K_2 = \frac{\sin 2\gamma \sin 2\delta - (\alpha/\beta)^2 \cos^2 2\delta}{\sin 2\gamma \sin 2\delta + (\alpha/\beta)^2 \cos^2 2\delta} \qquad (7.5)$$

Following the analysis in Appendix I and its use in the foregoing sections, the incident and reflected displacement vectors can be represented by spherical potentials of the form

$$\Phi^{(i)} = 0$$

$$\Psi^{(i)} = \sum_{m,n} k_\beta B_{mn}^{(i)} j_n(k_\beta r) P_n^m(\mu) \sin m\phi$$

$$\chi^{(i)} = \sum_{m,n} C_{mn}^{(i)} j_n(k_\beta r) P_n^m(\mu) \cos m\phi$$

$$\Phi^{(r)} = \sum_{m,n} A_{mn}^{(r)} j_n(k_\alpha r) P_n^m(\mu) \cos m\phi$$

$$\Psi^{(r)} = \sum_{m,n} k_\beta B_{mn}^{(r)} j_n(k_\beta r) P_n^m(\mu) \sin m\phi$$

$$\chi^{(r)} = \sum_{m,n} C_{mn}^{(r)} j_n(k_\beta r) P_n^m(\mu) \cos m\phi \quad , \qquad (7.6)$$

where the summation is for $m,n = 0,1,2, \ldots$ and $m \le n$. With spherical angles $(u,v) = (\delta,0)$, $(\pi-\delta,0)$ for the incident and reflected SV-waves, respectively, the coefficients take the form

$$B_{mn}^{(i)} = i\delta_{mn}(-c_{mnx}^{o} \cos\delta + c_{mnz}^{o} \sin\delta)/\sqrt{n(n+1)}$$

$$C_{mn}^{(i)} = \delta_{mn}\,(-b_{mnx}{}^{e}\cos\delta + b_{mnz}{}^{e}\sin\delta)/\sqrt{n(n+1)}$$

$$A_{mn}^{(r)} = \delta_{mn}\,P_n^m(-\cos\gamma)K_1$$

$$B_{mn}^{(r)} = iK_2\delta_{mn}\,(c_{mnx}{}^{o}\cos\delta + c_{mnz}{}^{o}\sin\delta)/\sqrt{n(n+1)}$$

$$C_{mn}^{(r)} = K_2\delta_{mn}\,(b_{mnx}{}^{e}\cos\delta + b_{mnz}{}^{e}\sin\delta)/\sqrt{n(n+1)}\quad , \qquad (7.7)$$

where the terms used in the expressions are given in Appendix I.

Case (ii) - Incidence beyond the critical angle ($\delta > \delta_{cr}$)

In this case, the reflected waves take the form:

$$\underset{\sim}{u}_1^{(r)} = ik_\beta S(\sin\delta\ \underset{\sim}{e}_x - i\nu\ \underset{\sim}{e}_z)\exp(k_\beta \nu z)\exp i(-\xi + k_\beta x\sin\delta)$$

$$\underset{\sim}{u}_2^{(r)} = -ik_\beta(\cos\delta\ \underset{\sim}{e}_x + \sin\delta\ \underset{\sim}{e}_z)\exp(-2i\xi)\exp ik_\beta(x\sin\delta - z\cos\delta)\ , \qquad (7.8)$$

where

$$S = \frac{-\sin 4\delta}{(\cos^4 2\delta + 4\nu^2\sin^2 2\delta\sin^2\delta)^{1/2}}$$

$$\nu = \frac{(\kappa^2\sin^2\delta - 1)^{1/2}}{\kappa}\quad , \text{ and}$$

$$\tan\xi = \frac{2\nu\sin 2\delta\ \sin\delta}{\cos^2 2\delta}\quad . \qquad (7.9)$$

There is no reflected plane P-wave as before. $(7.8)_1$ represents a dilational disturbance that propagates along the boundary and decreases exponentially with distance from it. $(7.8)_2$ represents a plane reflected SV-wave, which has no change in amplitude, but a change in its phase relative to the incident wave.

As in case (i), the incident and reflected waves are to be represented

in terms of spherical wave functions. The incident SV-wave, $\underset{\sim}{u}^{(i)}$, corresponds to $\Psi^{(i)}$, $\chi^{(i)}$, while the plane reflected SV-wave, $\underset{\sim}{u}_2^{(i)}$, corresponds to $\Psi^{(r)}$, $\chi^{(r)}$ exactly as they are in equation (7.6), where

$$K_2 = -\exp(-2i\xi) \quad . \tag{7.10}$$

The reflected 'P'-wave, $\underset{\sim}{u}_1^{(r)}$, corresponds to the potential $\Phi^{(r)}$, which can first be expressed in the form

$$\Phi^{(r)} = K_1 \exp i k_\alpha(-c_\gamma z + s_\gamma x) \quad , \tag{7.11}$$

where

$$s_\gamma = (\alpha/\beta)\sin\delta$$

$$c_\gamma = (1 - s_\gamma^2)^{1/2} = i(s_\gamma^2 - 1)^{1/2} \quad , \text{ and}$$

$$K_1 = \frac{-(\alpha/\beta)^2 \sin 4\delta}{2s_\gamma\, c_\gamma \sin 2\delta + (\alpha/\beta)^2 \cos^2\delta} \quad . \tag{7.12}$$

The exponent of (7.11) is similar to that of (7.3), with s_γ, c_γ in place of $\sin\gamma$, $\cos\gamma$. For $\delta_{cr} < \delta$, $s_\gamma > 1$ and c_γ is imaginary, corresponding to the sine and cosine of a complex angle. (7.11) is to be expanded in terms of spherical wave functions. In terms of spherical co-ordinate (r,θ,ϕ), (7.11) takes the form

$$\Phi^{(r)} = K_1 \exp i k_\alpha r(-c_\gamma\cos\theta + s_\gamma\sin\theta\cos\phi) \quad . \tag{7.13}$$

Let

$$z_1 = -c_\gamma \quad ,$$

$$z_2 = \cos\theta \quad , \text{ and}$$

$$z = -c_\gamma\cos\theta + s_\gamma\sin\theta\cos\phi \quad ,$$

then

$$s_\gamma = (1 - c_\gamma^{\,2})^{1/2} = i(z_1^{\,2} - 1)^{1/2} \quad ,$$

$$\sin\theta = (1 - \cos^2\theta)^{1/2} = i(z_2^{\,2} - 1)^{1/2} \quad ,$$

$$z = z_1 z_2 - (z_1^{\,2} - 1)^{1/2}(z_2^{\,2} - 1)^{1/2}\cos\phi \quad , \tag{7.14}$$

and

$$\Phi^{(r)} = K_1 \exp i\, k_\alpha r z \quad . \tag{7.15}$$

Using equation (10.1.47) in reference [14], (7.15) has the following expansion:

$$\Phi^{(r)} = K_1 \sum_{n=0}^{\infty} (2n+1)\, i^n\, j_n(k_\alpha r) P_n(z) \quad . \tag{7.16}$$

Equation (15.7) of reference [15] states the following additional theorem for Legendre polynomials:

"Let n be a natural number, z_1, z_2 and ϕ be arbitrary complex numbers, and z be given by (7.14) above, then

$$P_n(z) = \sum_{m=0}^{n} \varepsilon_m \frac{(n-m)!}{(n+m)!} P_n^{\,m}(z_1) P_n^{\,m}(z_2)\cos m\phi \quad ." \tag{7.17}$$

In our case, (7.17) takes the form

$$P_n(z) = \sum_{m=0}^{n} \varepsilon_m \frac{(n-m)!}{(n+m)!} P_n^{\,m}(-c_\gamma) P_n^{\,m}\cos\theta)\cos m\phi \quad . \tag{7.18}$$

Using (7.18), (7.16) becomes

$$\Phi^{(r)} = \sum_{m,n} A_{mn}^{\,(r)} j_n(k_\alpha r) P_n^{\,m}(\cos\theta)\cos m\phi \quad , \tag{7.19}$$

with

$$A_{mn}^{\,(r)} = \varepsilon_m i^n (2n+1) \frac{(n-m)!}{(n+m)!} P_n^{\,m}(-c_\gamma) K_1 \quad , \tag{7.20}$$

where $m,n = 0,1,2, \ldots,$ with $m \le n$ in the summation.

The expression for $A_{mn}^{(r)}$ in (7.20) is in the same form as the $A_{mn}^{(r)}$ in (7.7), with cosγ replaced by the imaginary number c_γ. This completes the expansion for case (ii).

In both cases (i) and (ii), the resulting displacement vector

$$\underset{\sim}{u}^{(i+r)} = \underset{\sim}{u}^{(i)} + \underset{\sim 1}{u}^{(r)} + \underset{\sim 2}{u}^{(r)} \tag{7.21}$$

satisfies the stress-free boundary conditions

$$\sigma_{zz} = \sigma_{zx} = \sigma_{zy} = 0 \qquad \text{at } z=0 \ , \tag{7.22}$$

and the reflected waves take the form

$$\underset{\sim 1}{u}^{(r)} = iK_1 k_\alpha (s_\gamma \, \underset{\sim x}{e} - c_\gamma \, \underset{\sim z}{e}) \exp i k_\alpha (x \, s_\gamma - z \, c_\gamma) \tag{7.23}$$

$$\underset{\sim 2}{u}^{(r)} = iK_2 k_\beta (\cos\delta \, \underset{\sim x}{e} + \sin\delta \, \underset{\sim z}{e}) \exp i k_\beta (x \sin\delta - z \cos\delta) \ . \tag{7.24}$$

Solution of the Problem -- Results

In the presence of the canyon, the two types of outgoing spherical (longitudinal and transverse) waves that are reflected back into the medium are given by

$$\Phi^{(s)} = \sum_{m,n} A_{mn}^{(3)} z_n^{(3)}(k_\alpha r) P_n^m(\mu)\cos m\phi$$

$$\Psi^{(s)} = \sum_{m,n} k_\beta B_{mn}^{(3)} z_n^{(3)}(k_\beta r) P_n^m(\mu)\sin m\phi$$

$$\chi^{(s)} = \sum_{m,n} C_{mn}^{(3)} z_n^{(3)}(k_\beta r) P_n^m(\mu)\cos m\phi \quad , \qquad (8.1)$$

which are identical with (2.1). Using the analysis in Appendix II, and applying the boundary conditions of a spherical cavity in an infinite medium subjected to incident SV-waves, the expansion coefficients are given by the equations:

$$\begin{bmatrix} E_{11}^{(3)} & E_{13}^{(3)} \\ E_{41}^{(3)} & E_{43}^{(3)} \end{bmatrix} \begin{Bmatrix} A_{mn}^{(3)} \\ C_{mn}^{(3)} \end{Bmatrix} = -C_{mn}^{(i)} \begin{Bmatrix} E_{13}^{(1)} \\ E_{43}^{(1)} \end{Bmatrix} ,$$

and

$$B_{mn}^{(3)} = -\left(E_{42}^{(1)}/E_{43}^{(3)}\right) B_{mn}^{(i)} \quad , \qquad (8.2)$$

for $m,n = 0,1,2 \ldots$ and $m \leq n$.

In the presence of both the plane free boundary and the hemispherical canyon, the additional waves that are generated are represented by

$$\Phi^{(R)} = \sum_{j,m,n} A_{mn}^{(j)} z_n^{(j)}(k_\alpha r) P_n^m(\mu)\cos m\phi$$

$$\psi^{(R)} = \sum_{j,m,n} k_\beta B_{mn}^{(j)} z_n^{(j)}(k_\beta r) P_n^m(\mu)\sin m\phi$$

$$\chi^{(R)} = \sum_{j,m,n} C_{mn}^{(j)} z_n^{(j)}(k_\beta r) P_n^m(\mu)\cos\phi \quad , \tag{8.3}$$

where $j=1,2$, and $m,n=0,1,2, \ldots$, with $m \leq n$. (8.3) is again identical with (2.2). The boundary conditions to be satisfied are that of (3.8) and (3.10), repeated here

(3.8):
$$\sigma_{rr}^{(r)} + \sigma_{rr}^{(R)} = 0$$

$$\sigma_{r\theta}^{(r)} + \sigma_{r\theta}^{(R)} = 0$$

$$\sigma_{r\phi}^{(r)} + \sigma_{r\phi}^{(R)} = 0 \quad , \text{ at } r=a$$

and

(3.10):
$$\sigma_{zz}^{(s)} + \sigma_{zz}^{(R)} = 0$$

$$\sigma_{zx}^{(s)} + \sigma_{zx}^{(R)} = 0$$

$$\sigma_{zy}^{(s)} + \sigma_{zy}^{(R)} = 0 \quad , \text{ at } z=0 \quad .$$

Applying the boundary conditions, identical sets of equations are obtained for the unknowns

$$\{A_{mn}^{(j)}, B_{mn}^{(j)}, C_{mn}^{(j)}\} \qquad j=1,2;\ m,n=0,1,2, \ldots \quad m \leq n \ ,$$

namely, equations (4.1), (4.16), (4.19) and (4.21).

The same steps of numerical calculation are carried out as in the foregoing analysis, and the results are presented in Figures 22 through 49. They represent typical characteristics of amplitudes and phases of

surface displacements at dimensionless points (x/a, y/a) near the canyon for angles of incidence $\delta = 0°$, 30°, 45°, 60°, 75° and 85°. The values of dimensionless frequency, η, and Poisson's ratio, ν, are again 0.5 and 0.25, respectively.

In the absence of the hemisperical canyon, the surface displacement amplitude of each component in the uniform half-space would be no more than 2, for incident SV-wave of unit amplitude. The x-component amplitude is 2 for the case of a vertically incident plane SV-wave ($\delta = 0°$). Also, for $\delta < 90°$, the phase angles ϕ_x, ϕ_z would both be

$$\phi_x = \phi_z = k_\beta \sin\delta\, x \quad , \tag{8.4}$$

again a linear function of x, this time with a steeper slope $k_\beta \sin\delta$ as compared to $k_\alpha \sin\gamma$ for the case of incident P-waves.

The value $\nu = 0.25$ used corresponds to $\kappa = \alpha/\beta = \sqrt{3}$, and the critical angle, δ_{cr}, is given by

$$\delta_{cr} = \sin^{-1}(1/\sqrt{3}) = 35°16' \quad . \tag{8.5}$$

The angles of incidence $\delta = 0°$ and 30° thus correspond to cases of incidence below the critical angle ($\delta < \delta_{cr}$), while the angles of incidence $\delta = 45°$, 60°, 75°, and 85° correspond to cases of incidence beyond critical angle ($\delta > \delta_{cr}$). For $\delta = 45$, the reflected P-wave vanishes, and the incident SV-wave is reflected as an SV-wave in the free-field. Thus, $\delta = 0°$, 30°, and 45° correspond to the case of harmonic incident and reflected plane waves of uniform amplitude in the free-field. The case of $\delta = 60°$, 75°, and 85° correspond to the presence of inhomogeneous plane waves with a complex propagation vector and varying amplitudes even in the free-field. The case of $\delta = 90°$ will result in zero motion

everywhere in the free-field, and thus is excluded in the present analysis.

The following table gives the amplitudes and phases of the motion at the surface of the free-field for plane incident SV-waves at angle δ, and $\nu = 0.25$.

Angle of Incidence, δ	Amplitude $\lvert u_x \rvert$	Amplitude $\lvert u_z \rvert$	Phase $\frac{\lvert \phi_x \rvert}{(x/a)}$	Phase $\frac{\lvert \phi_z \rvert}{(x/a)}$
0°	2.0	0.	0.	-
30°	1.732	1.	.250π	.250π
45°	0.	1.414	-	.354π
60°	0.5	1.118	.433π	.433π
75°	0.423	0.731	.484π	.484π
85°	0.170	0.279	.498π	.498π
90°	0.	0.	-	-

(8.6)

The motion in the y direction is uniformly zero in the free-field since the displacement vector of the incident waves are in the x-z plane.

The presence of the canyon changes the uniformity and results in non-zero motion in all three components. The case of vertical incidence ($\delta = 0°$) again leads to symmetric results for displacement amplitudes and phases. A progressively more complicated pattern of ground displacements and phases of all components is observed as δ increases from 0° to 90° in the creation of amplification and shadow zones in the vicinity of the canyon. The amplitudes of each component again approach that of free-field motions at comparably large distances from the canyon.

The phase diagrams show a similar trend. The phase angles in the free-field have a steeper slope $k_\beta \sin\delta$ as compared to $k_\alpha \sin\gamma$ for the

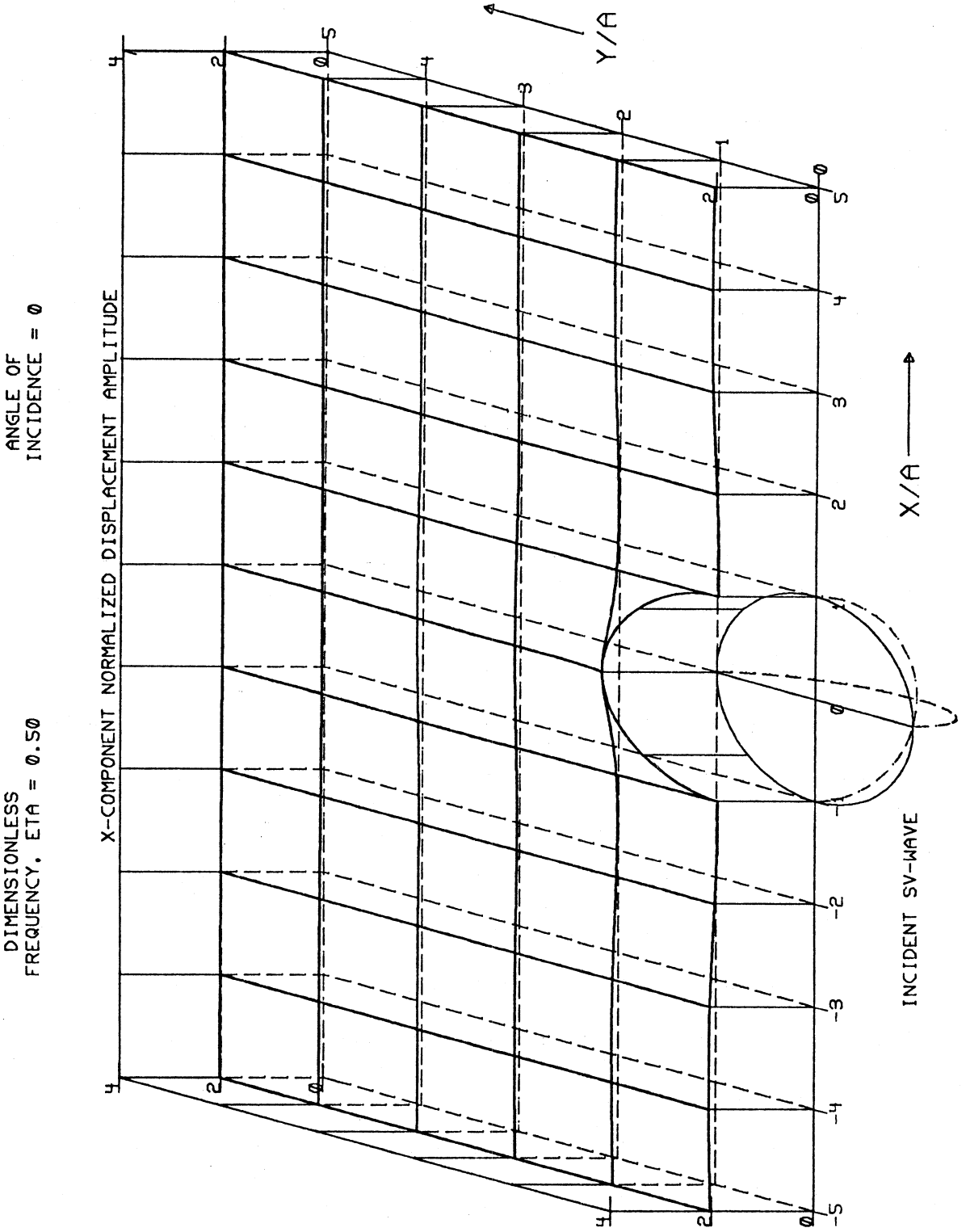

Figure 22

Free-Field Amplitude, $|u_x| = 2$

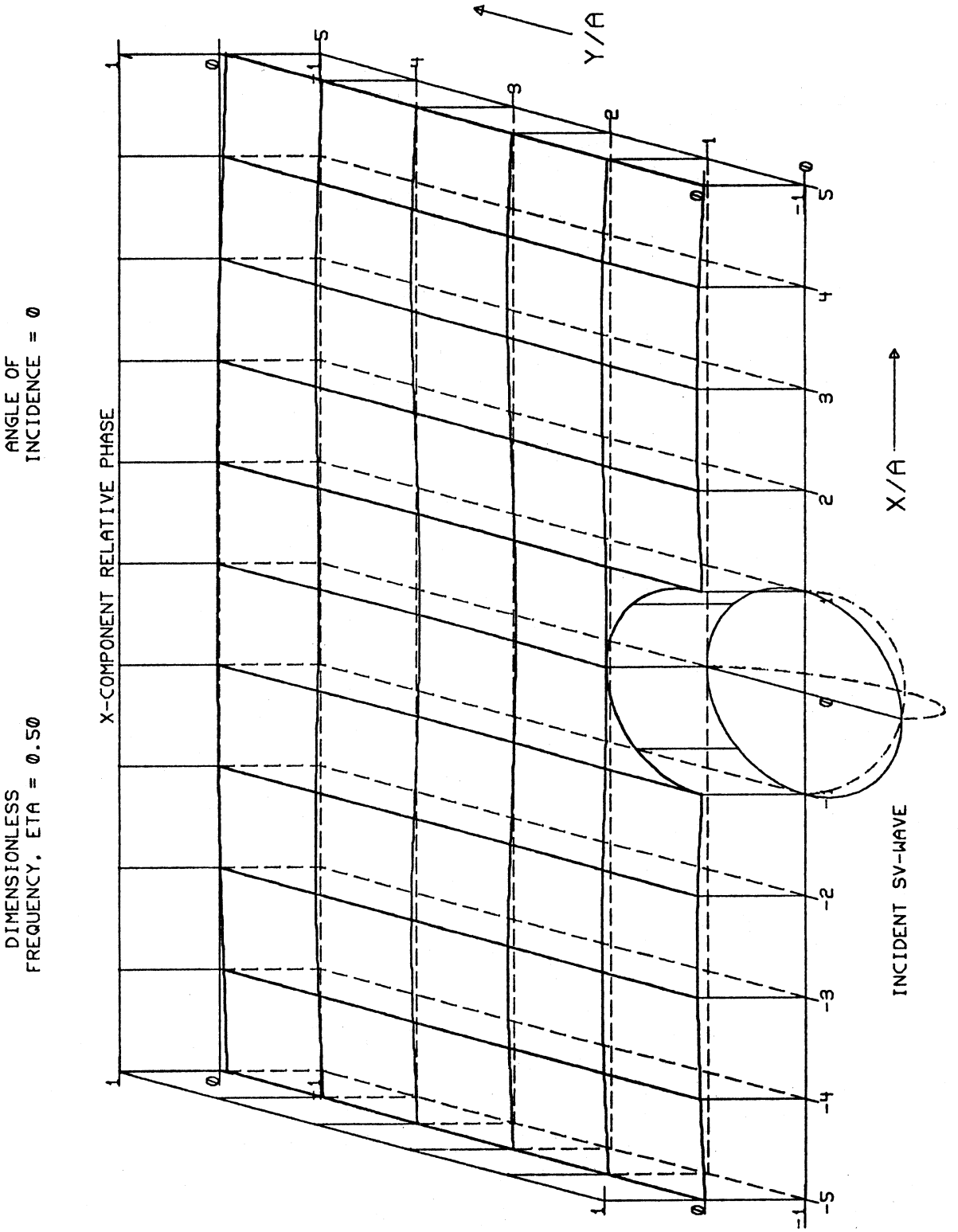

Figure 23

Phase/π

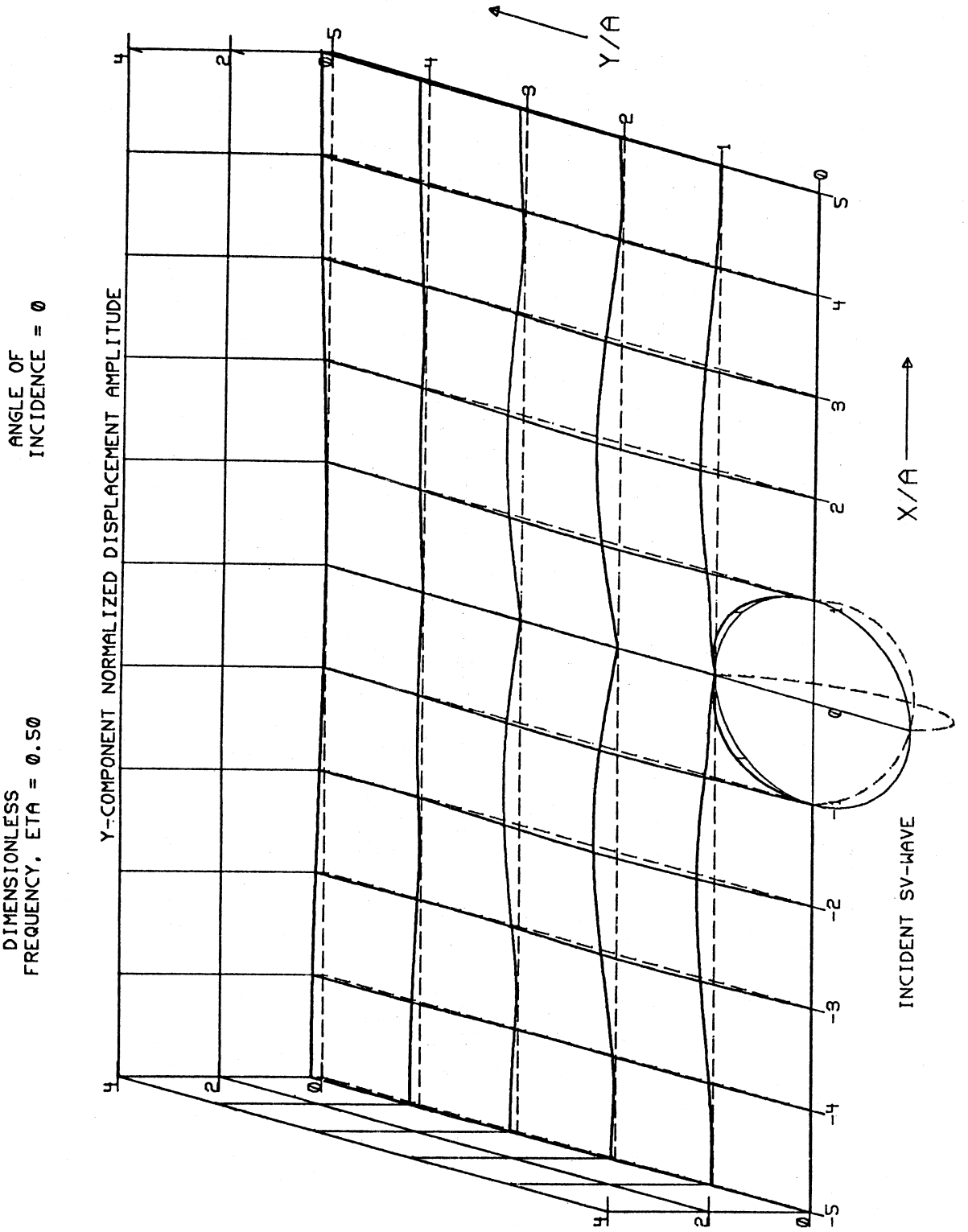

Figure 24

Free-Field Amplitude, $|u_y| = 0$

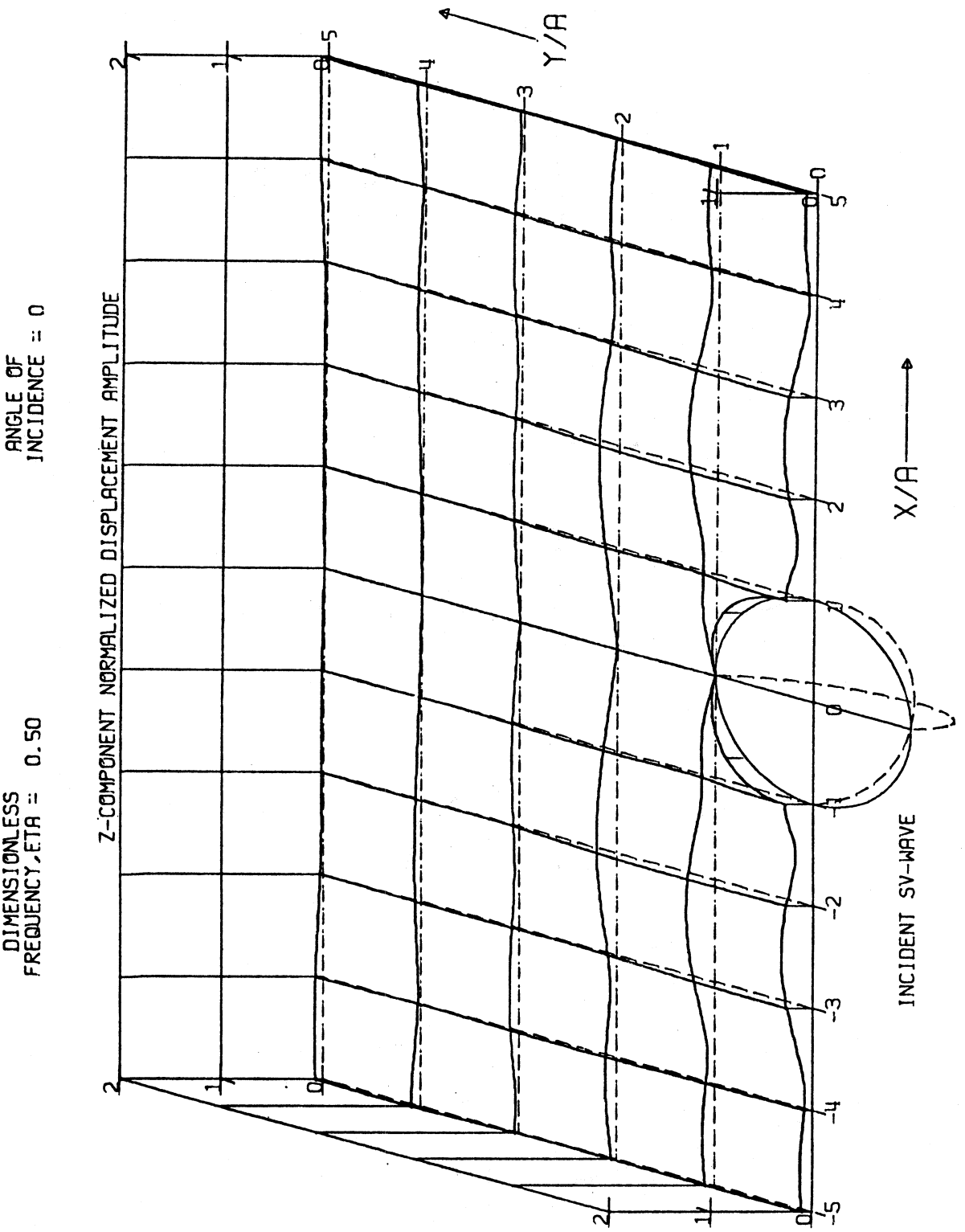

Figure 25

Free-Field Amplitude, $|u_z| = 0$

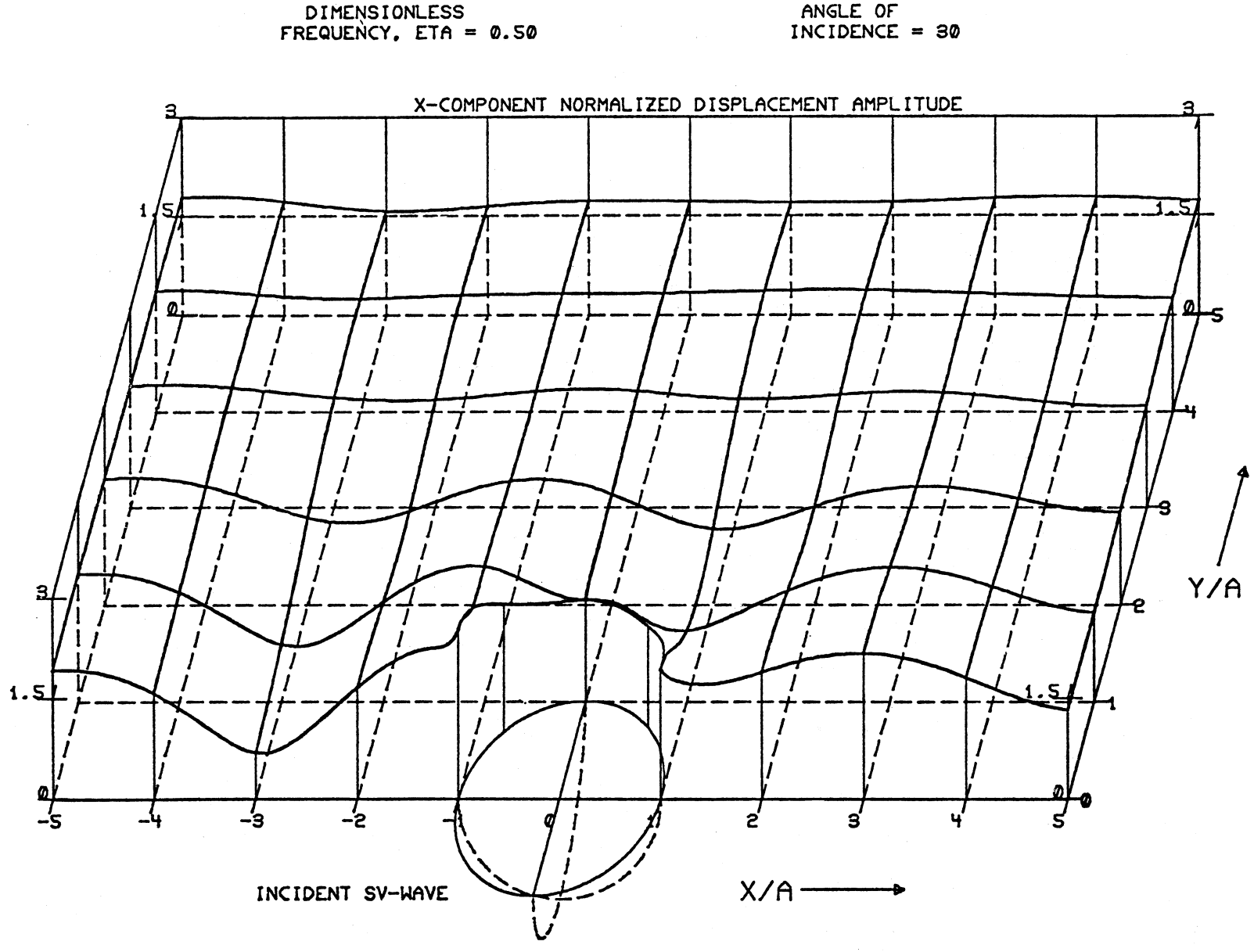

Figure 26

Free-Field Amplitude, $|u_x| = 1.732$

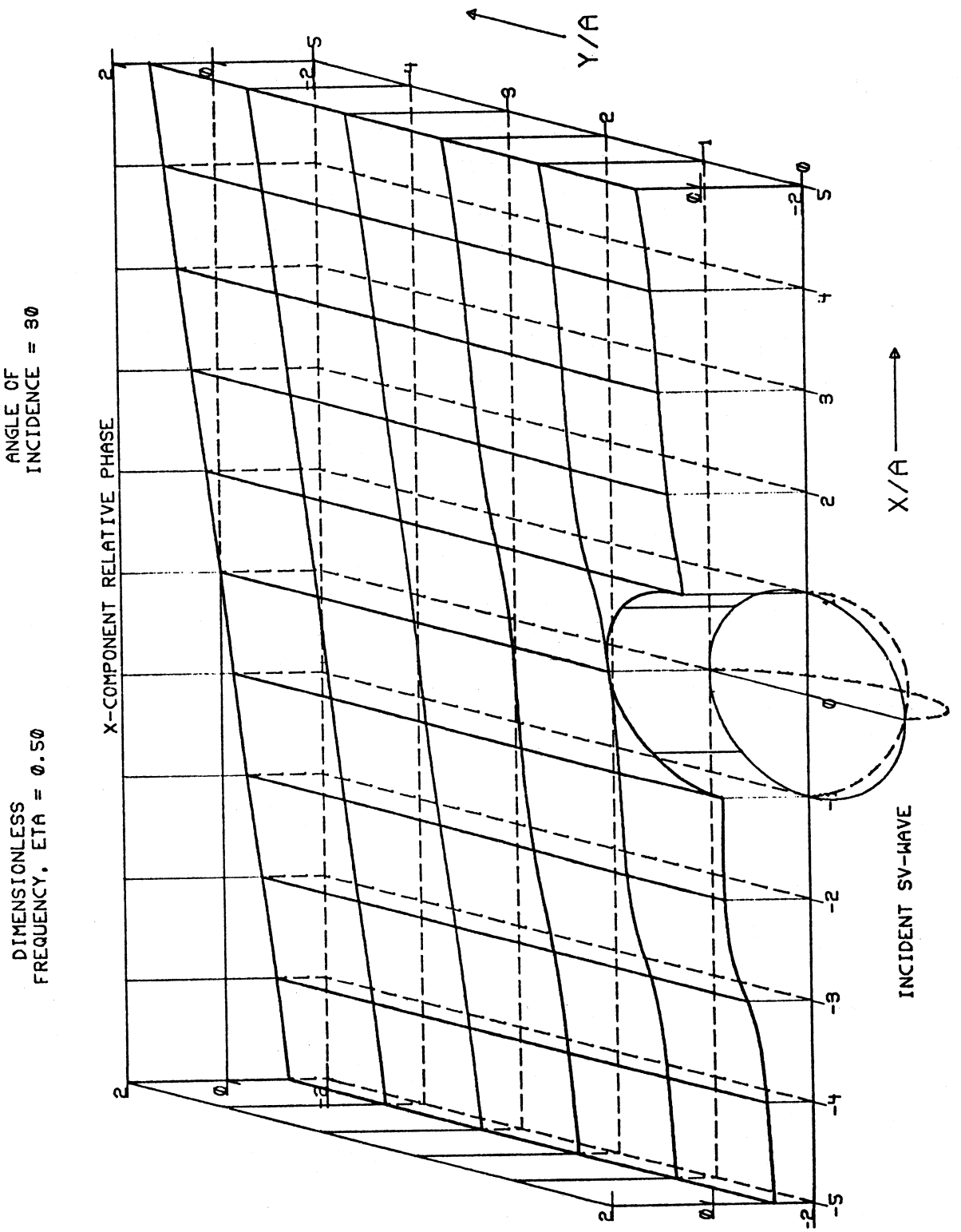

Figure 27

Phase/π

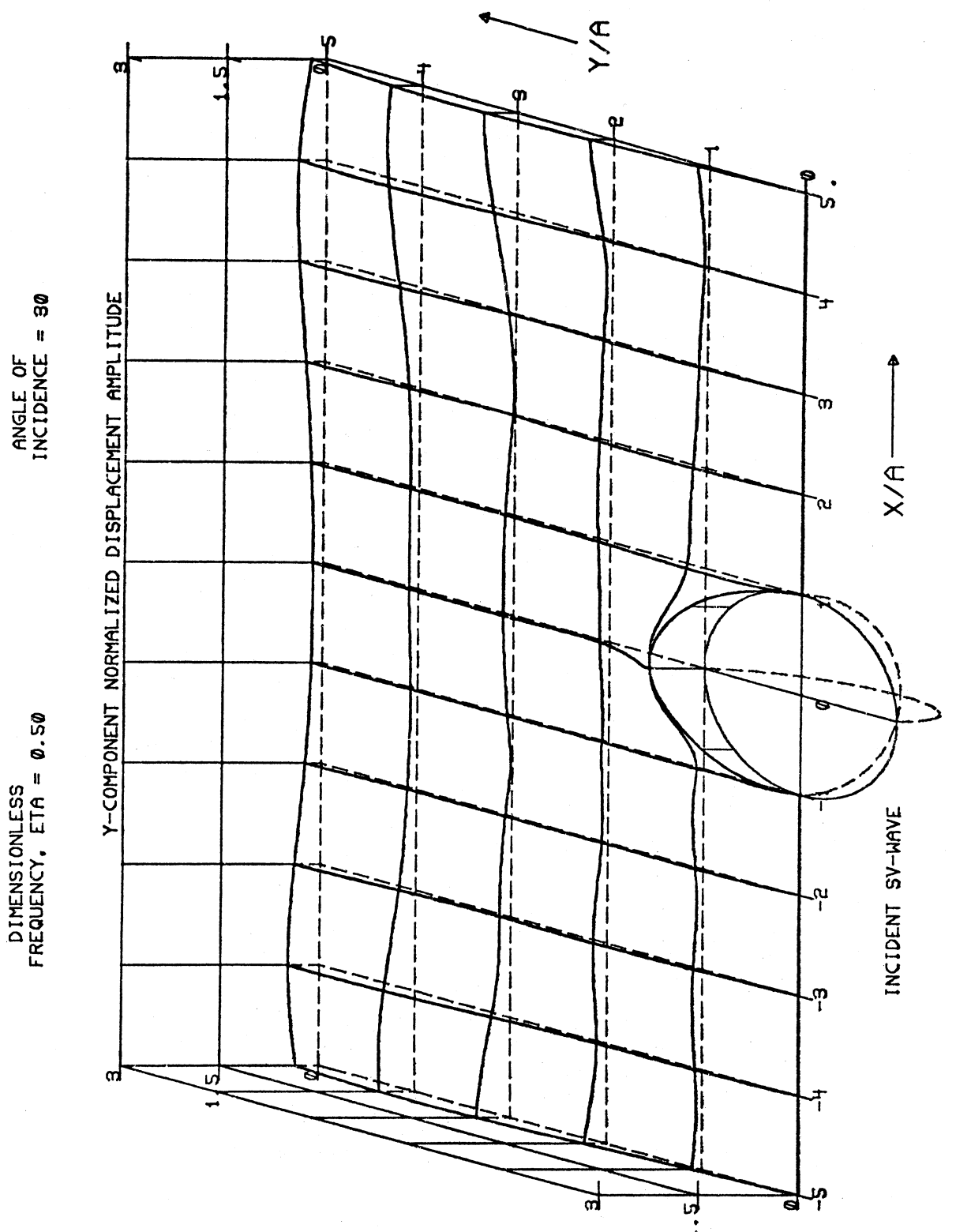

Figure 28

Free-Field Amplitude, $|u_y| = 0$

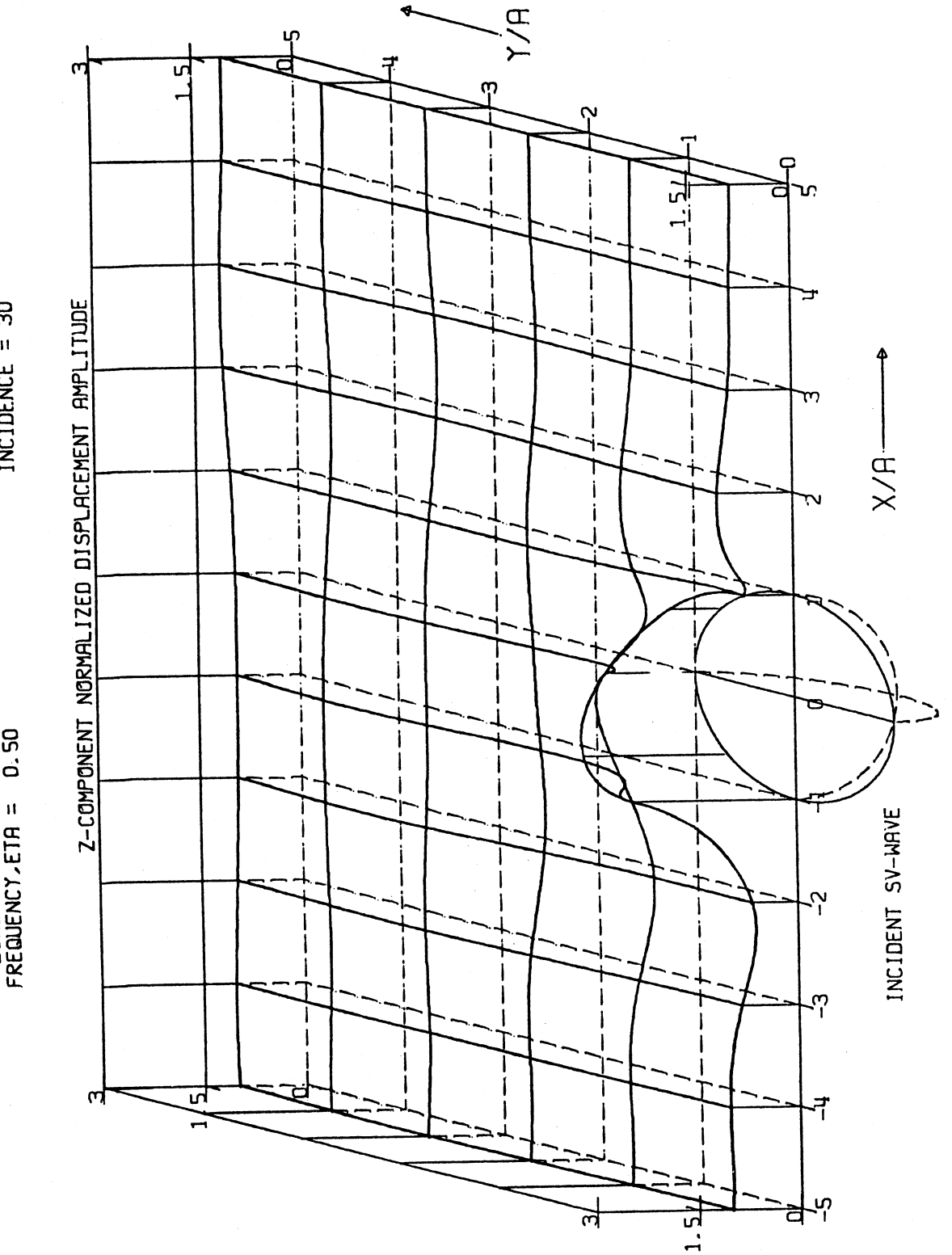

Figure 29

Free-Field Amplitude, $|u_z| = 1$

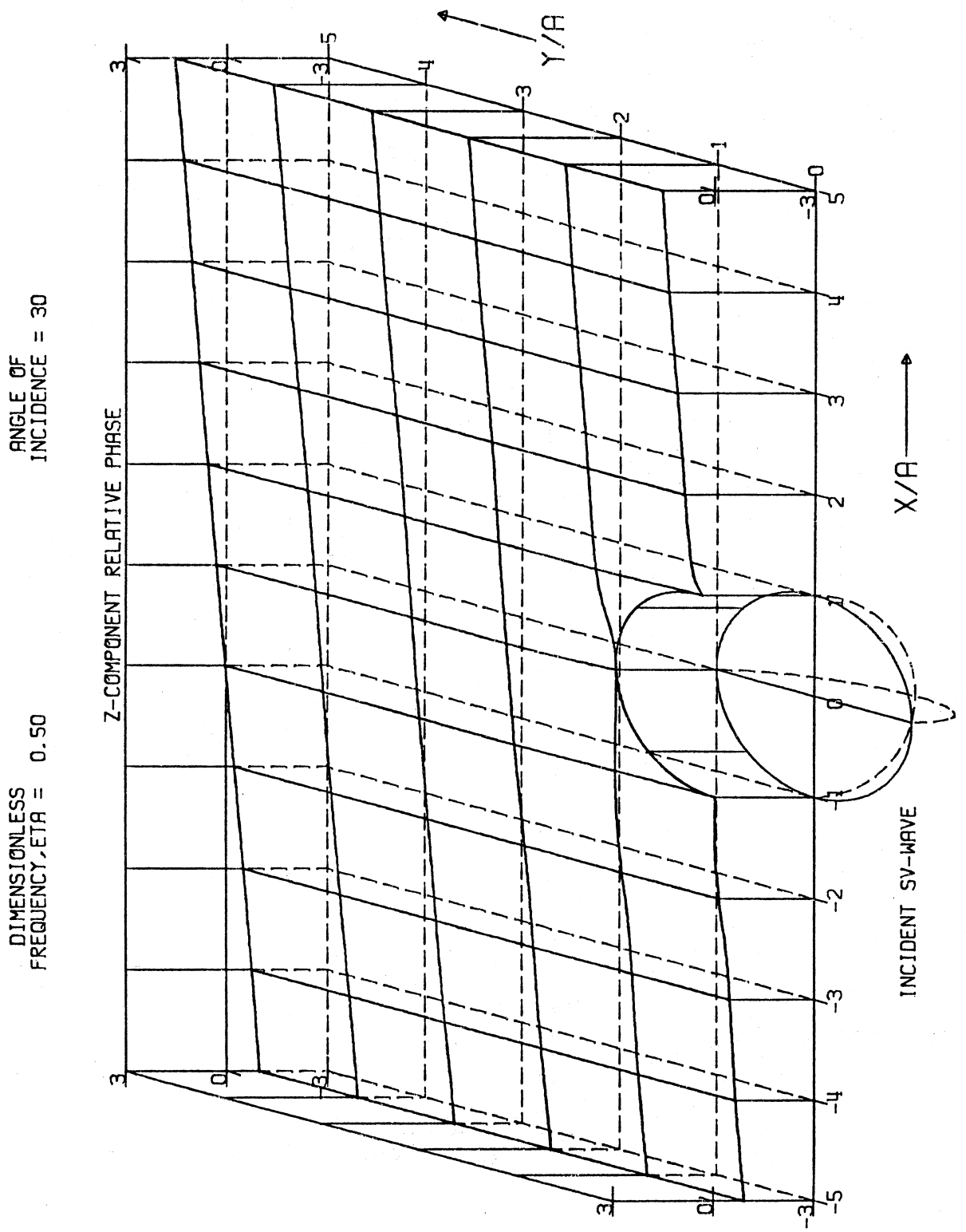

Figure 30

Phase/π

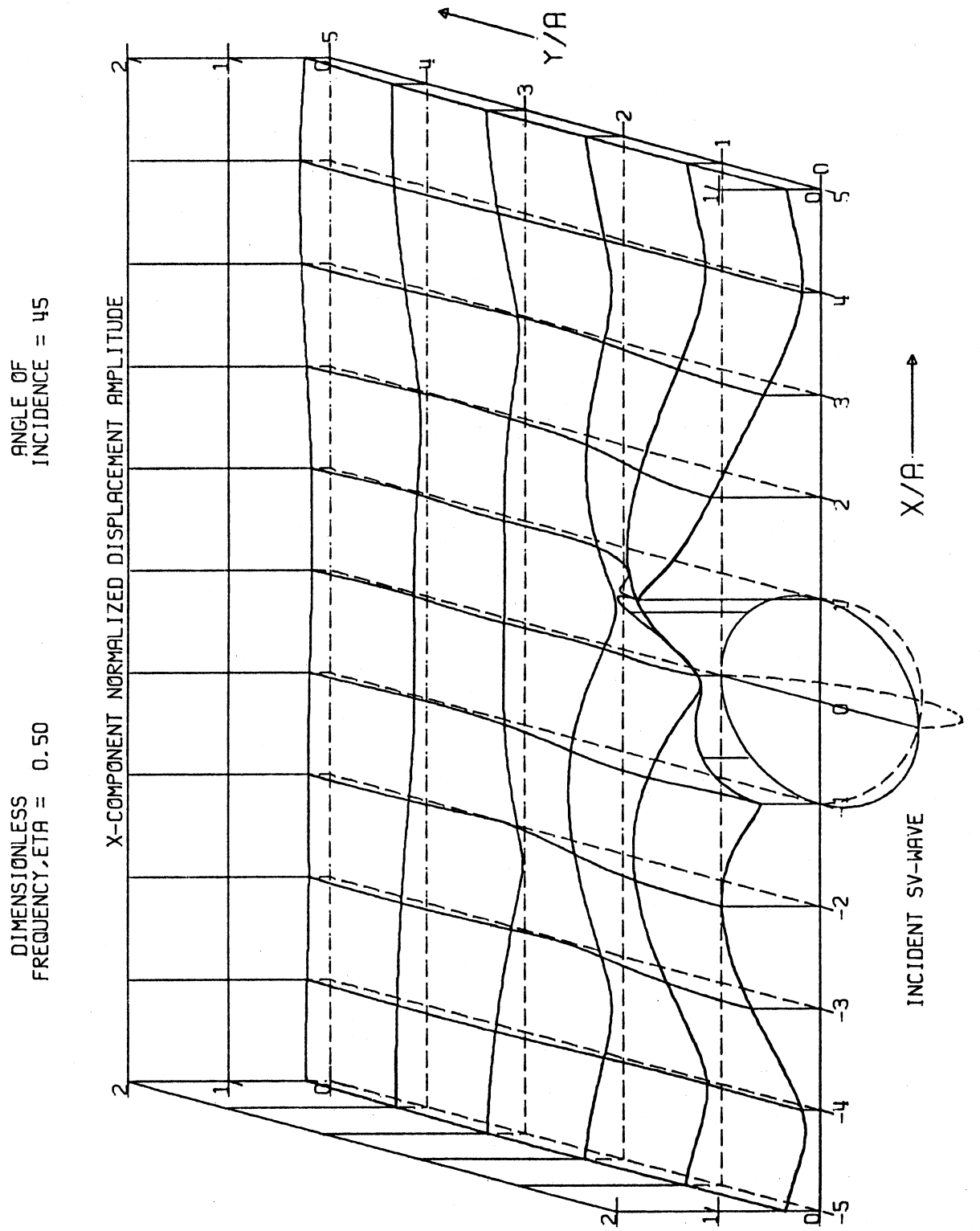

Figure 31

Free-Field Amplitude, $|u_x| = 0$

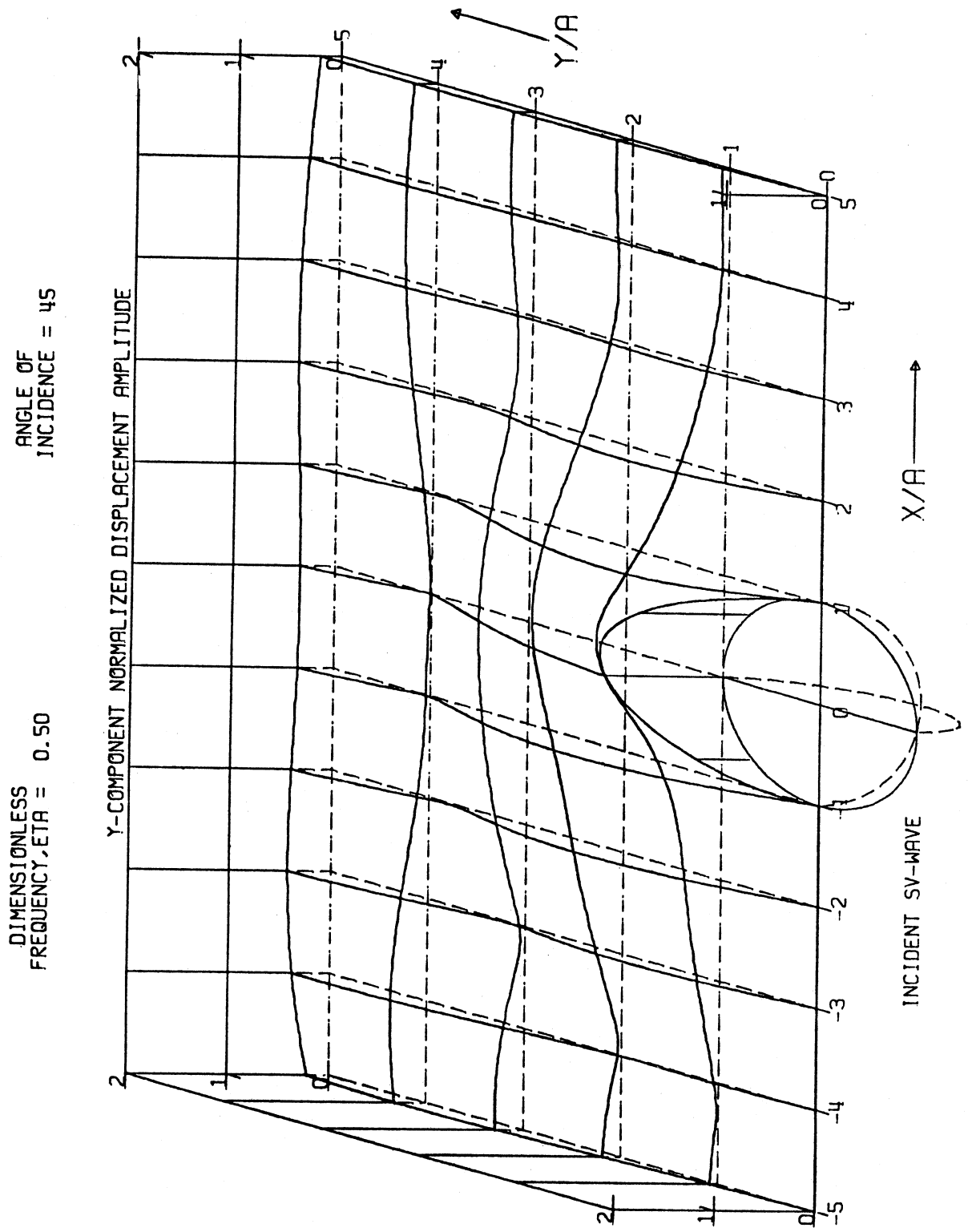

Figure 32

Free-Field Amplitude, $|u_z| = 0$

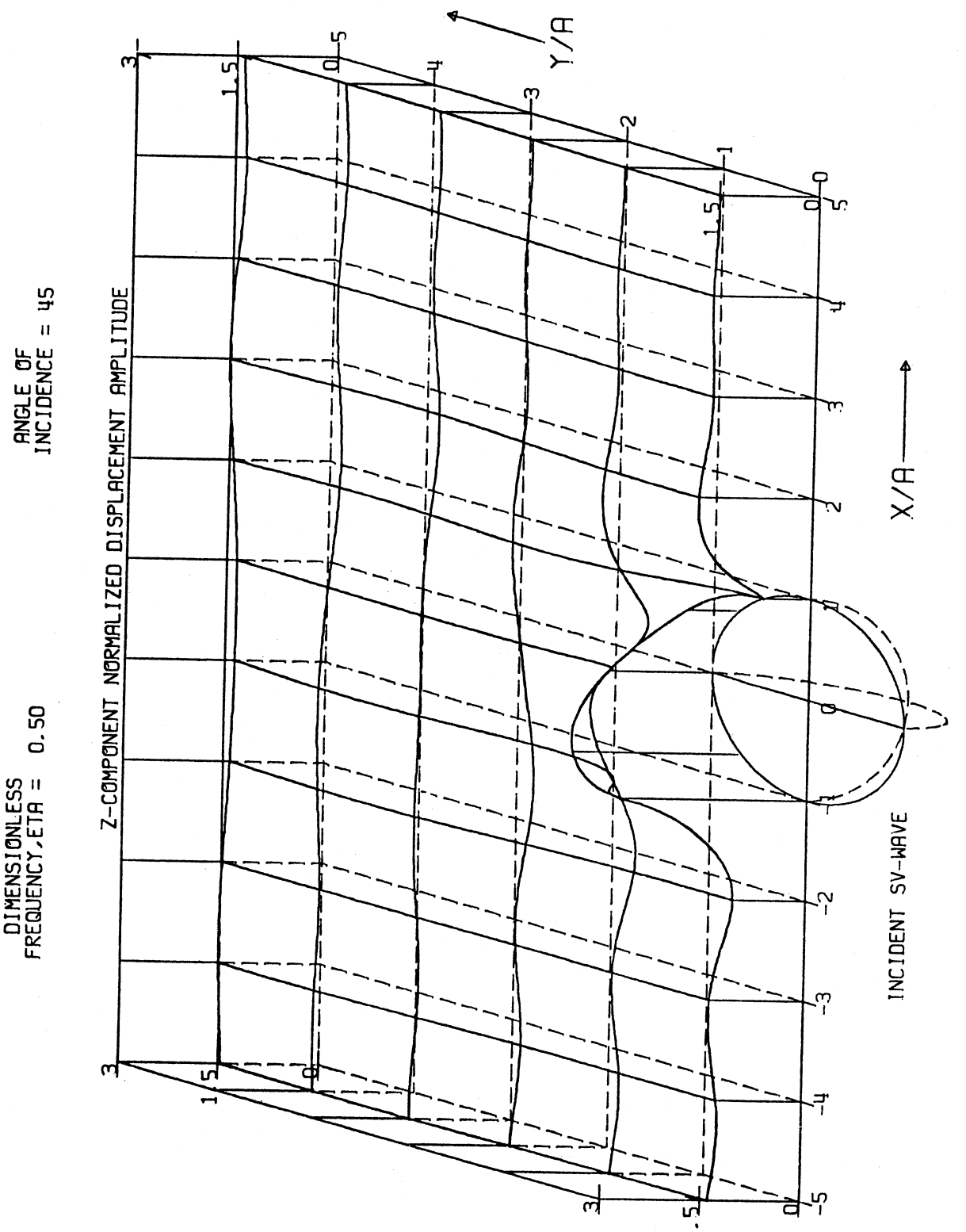

Figure 33

Free-Field Amplitude, $|u_z| = 1.414$

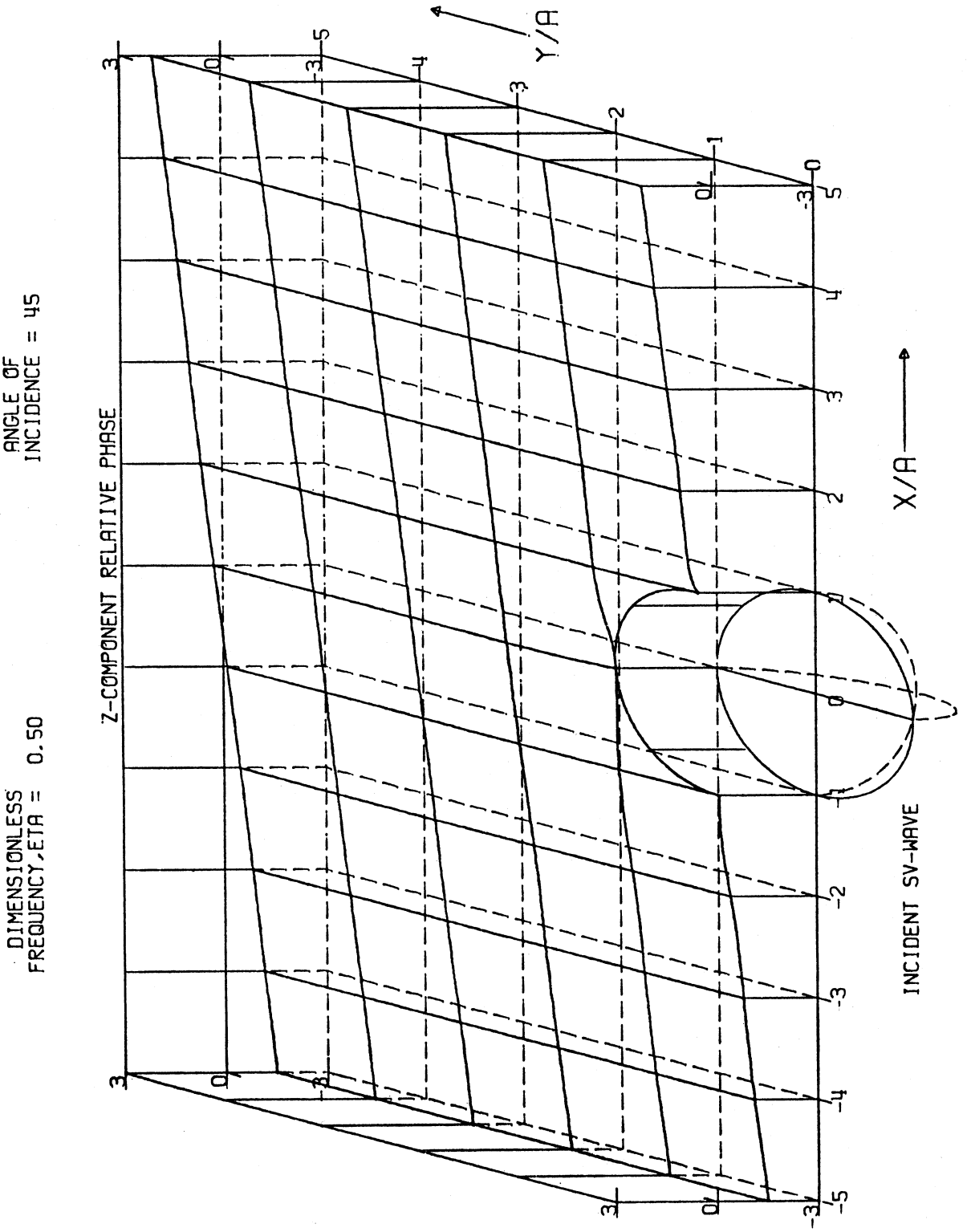

Figure 34

Phase/π

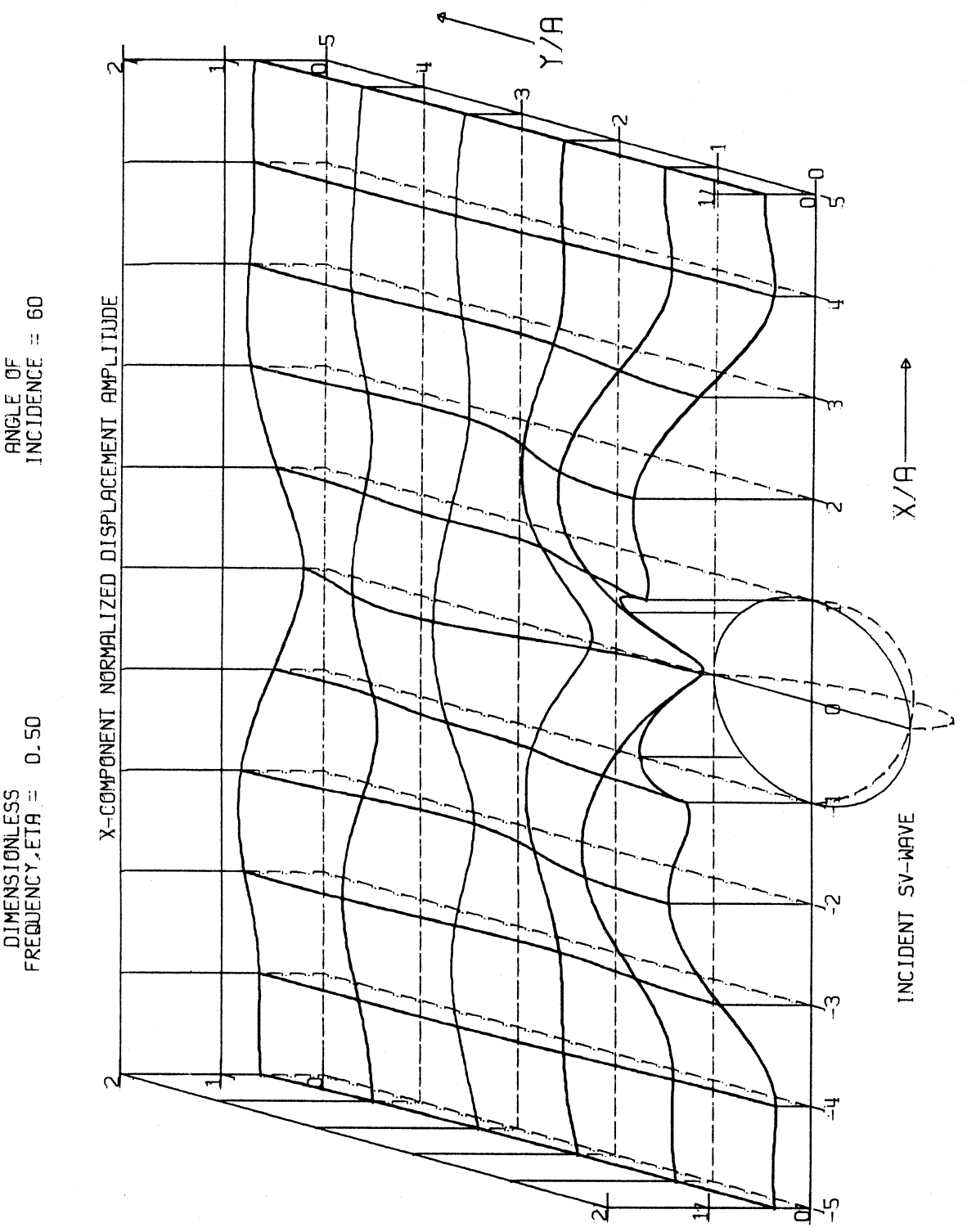

Figure 35

Free-Field Amplitude, $|u_x| = 0.5$

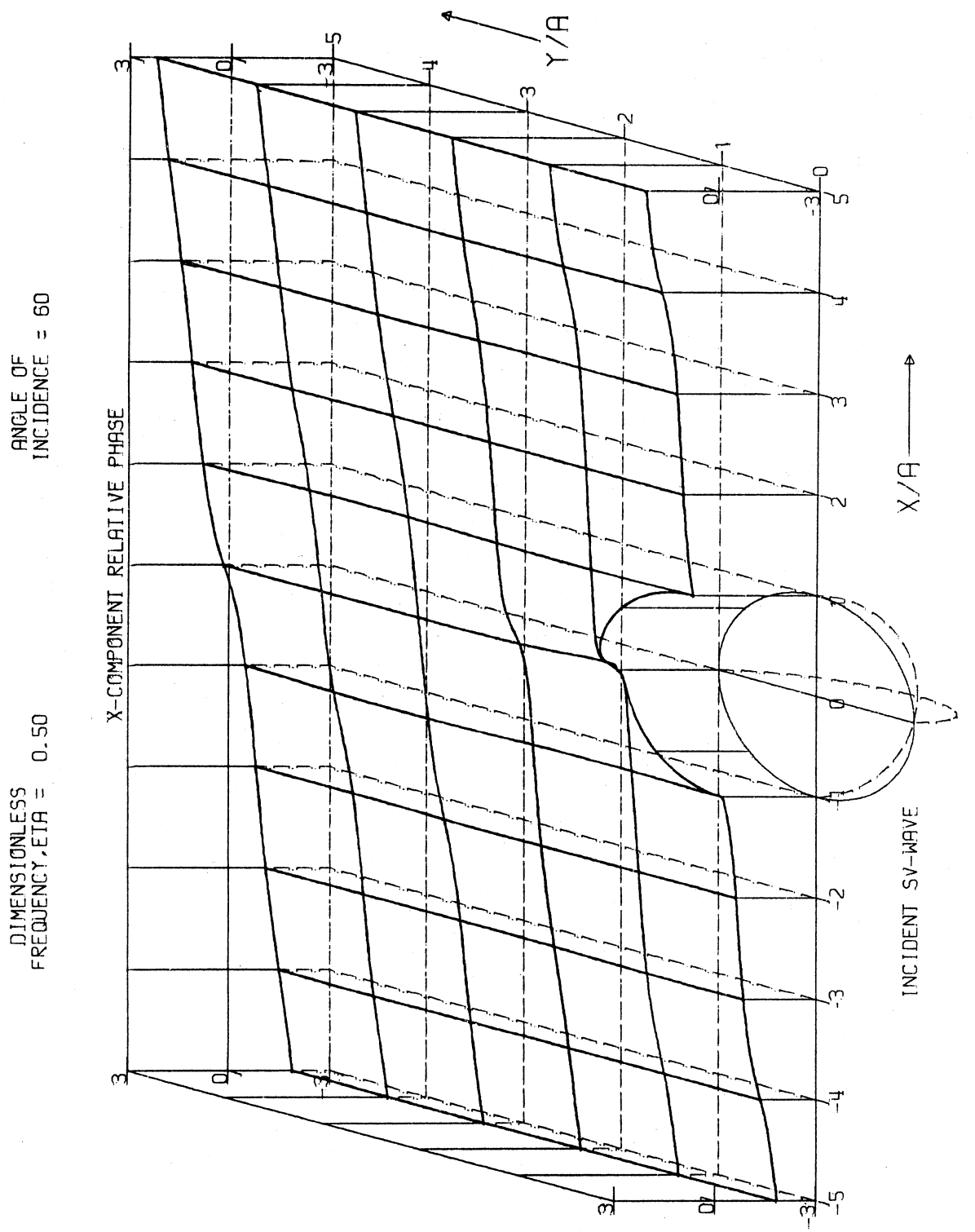

Figure 36

Phase/π

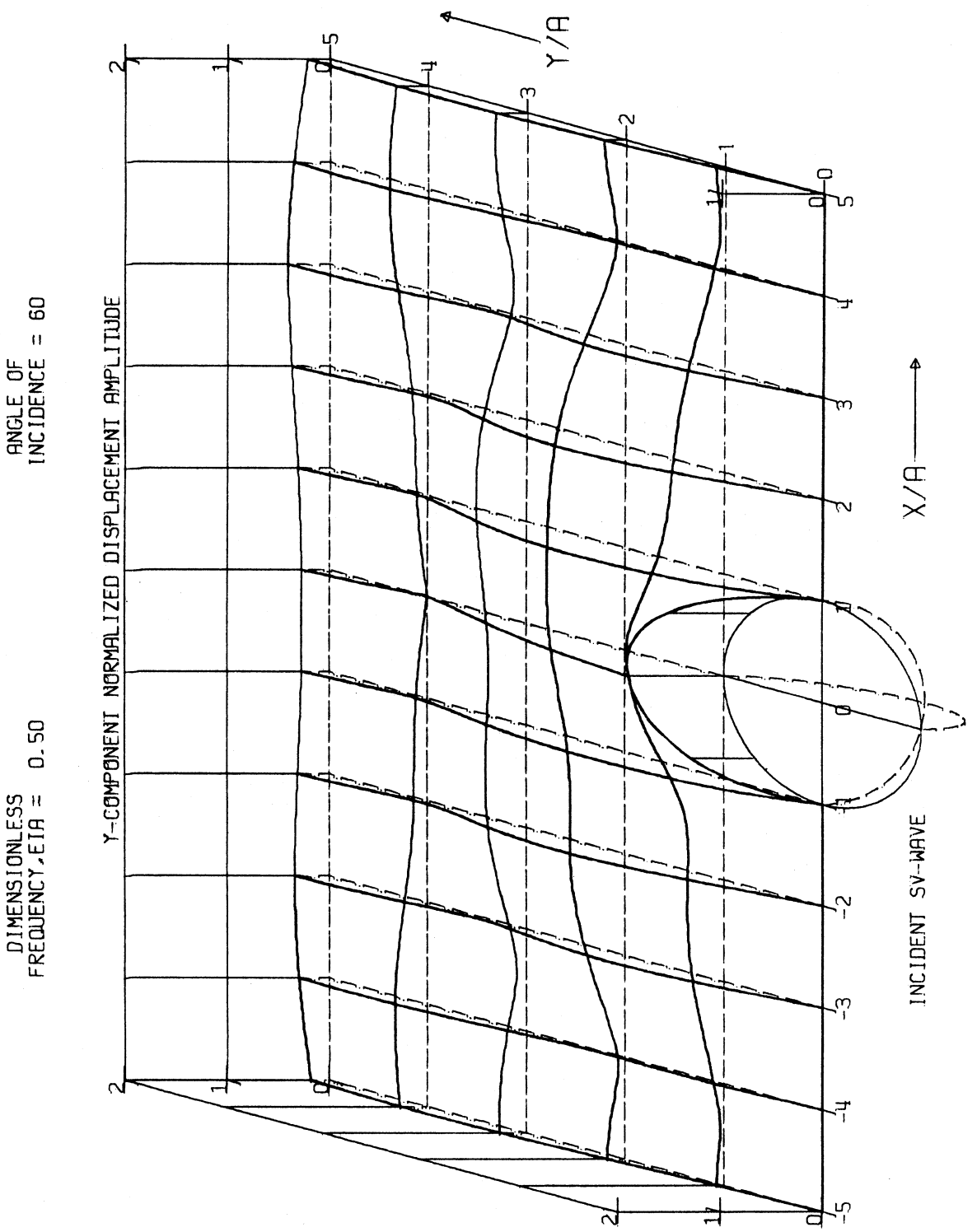

Figure 37

Free-Field Amplitude, $|u_y| = 0$

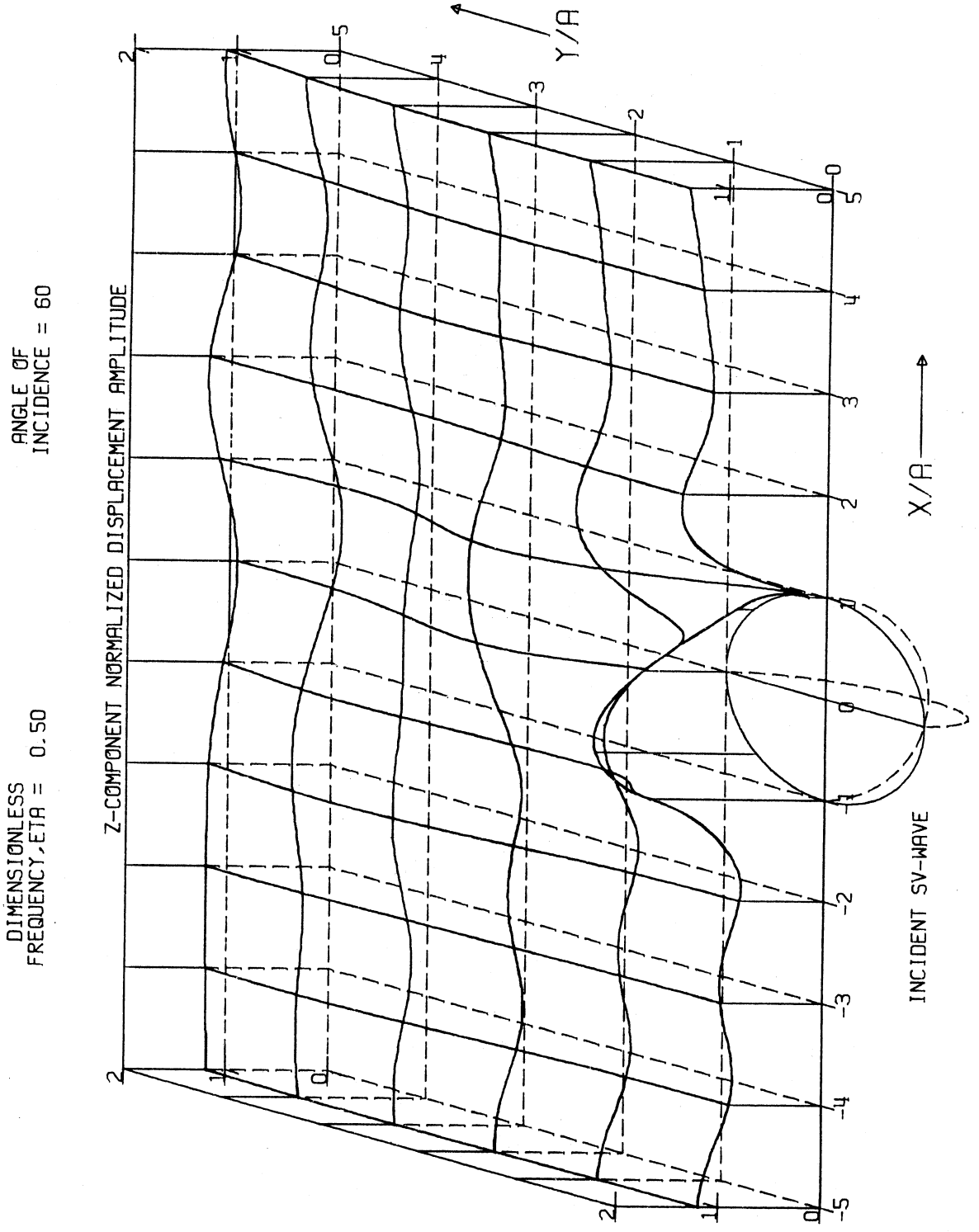

Figure 38

Free-Field Amplitude, $|u_z| = 1.118$

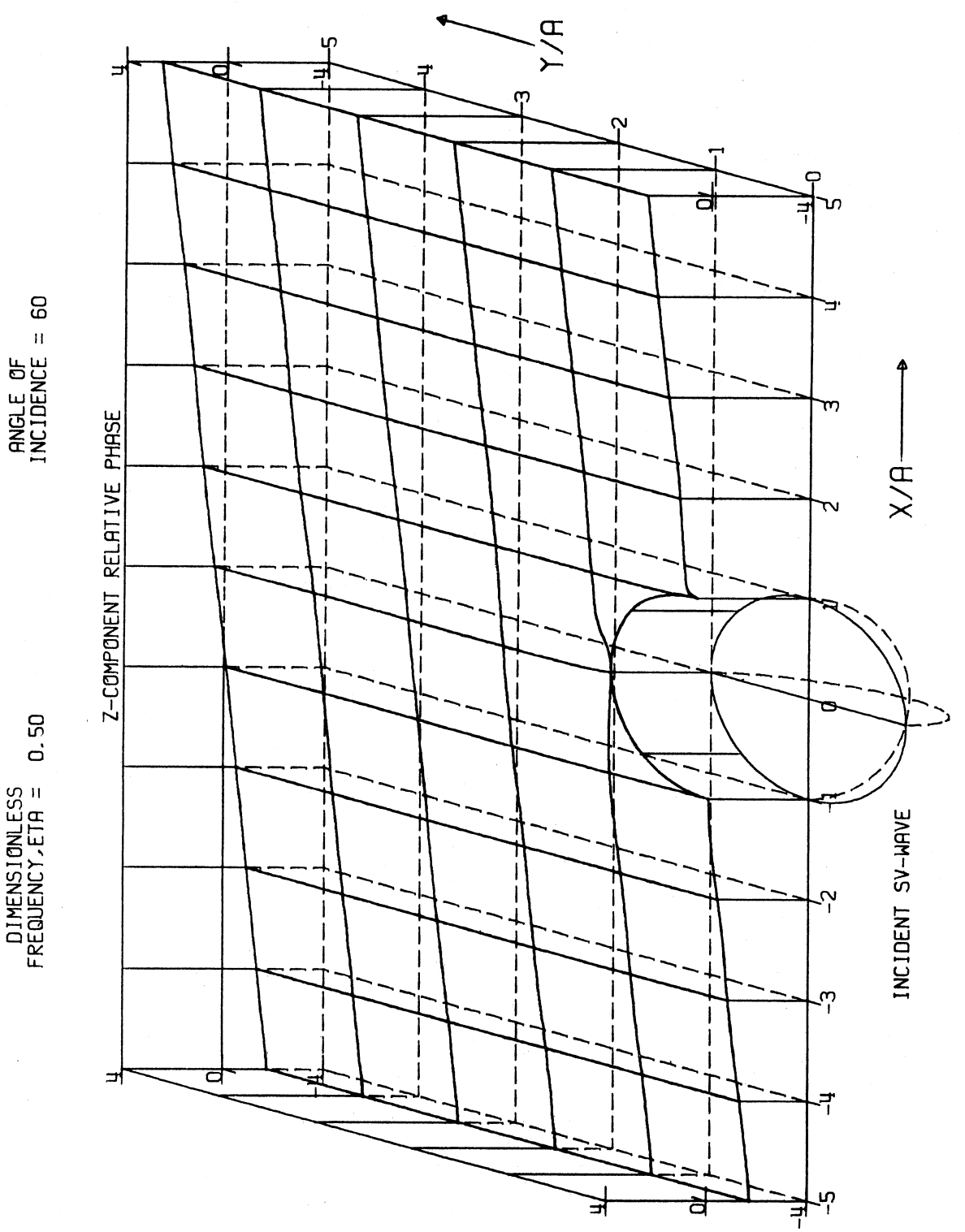

Figure 39

Phase/π

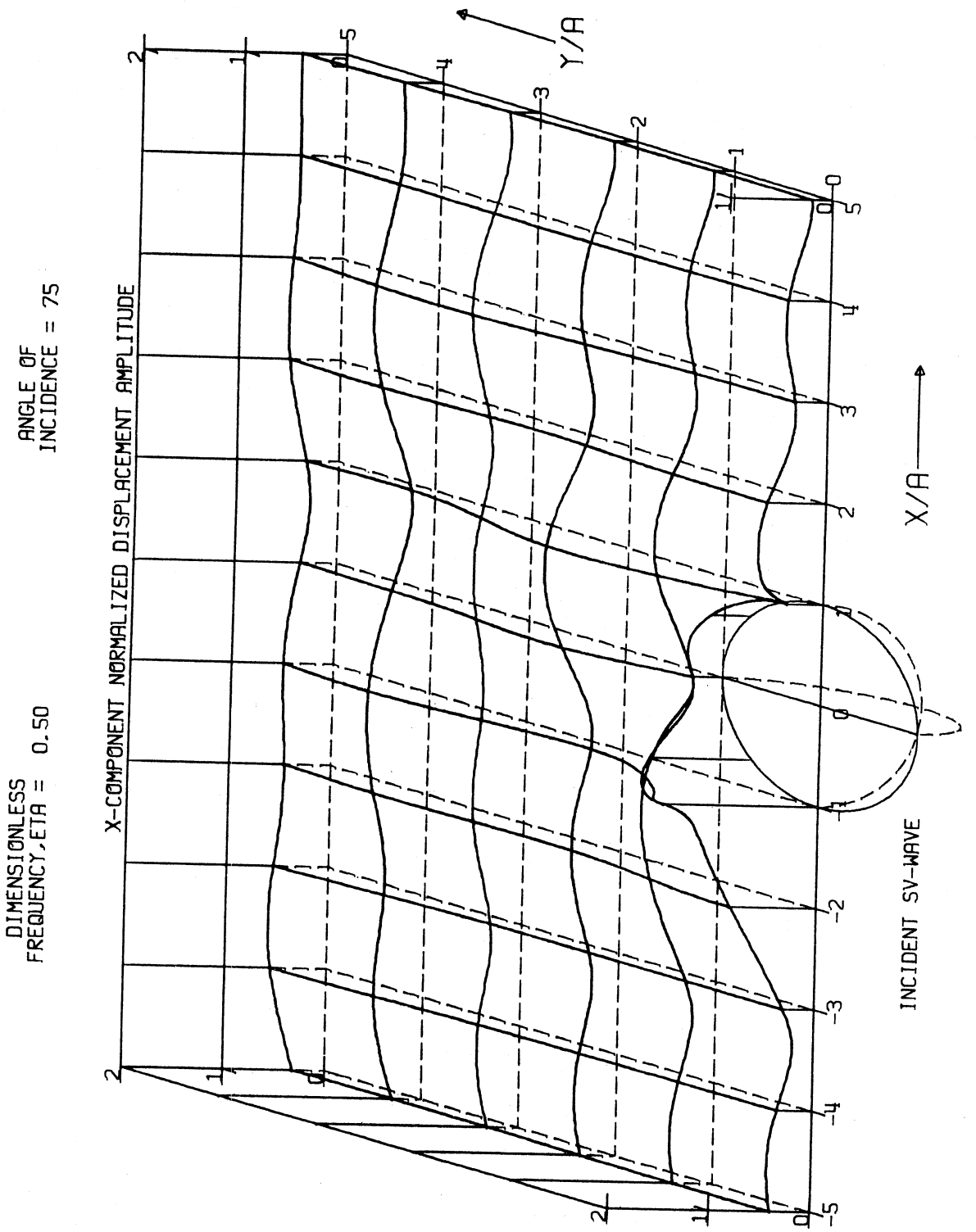

Figure 40

Free-Field Amplitude, $|u_x| = 0.423$

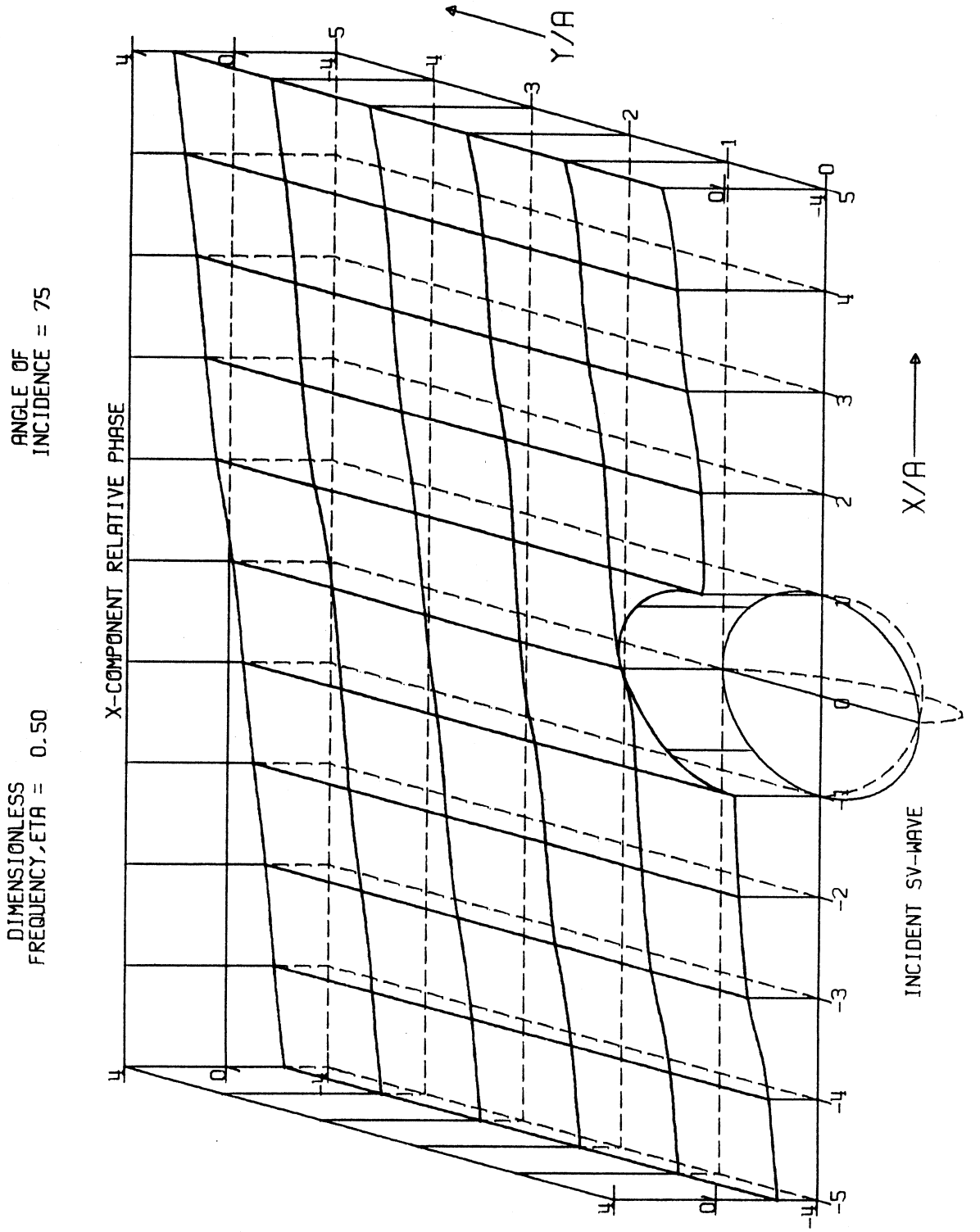

Figure 41

Phase/π

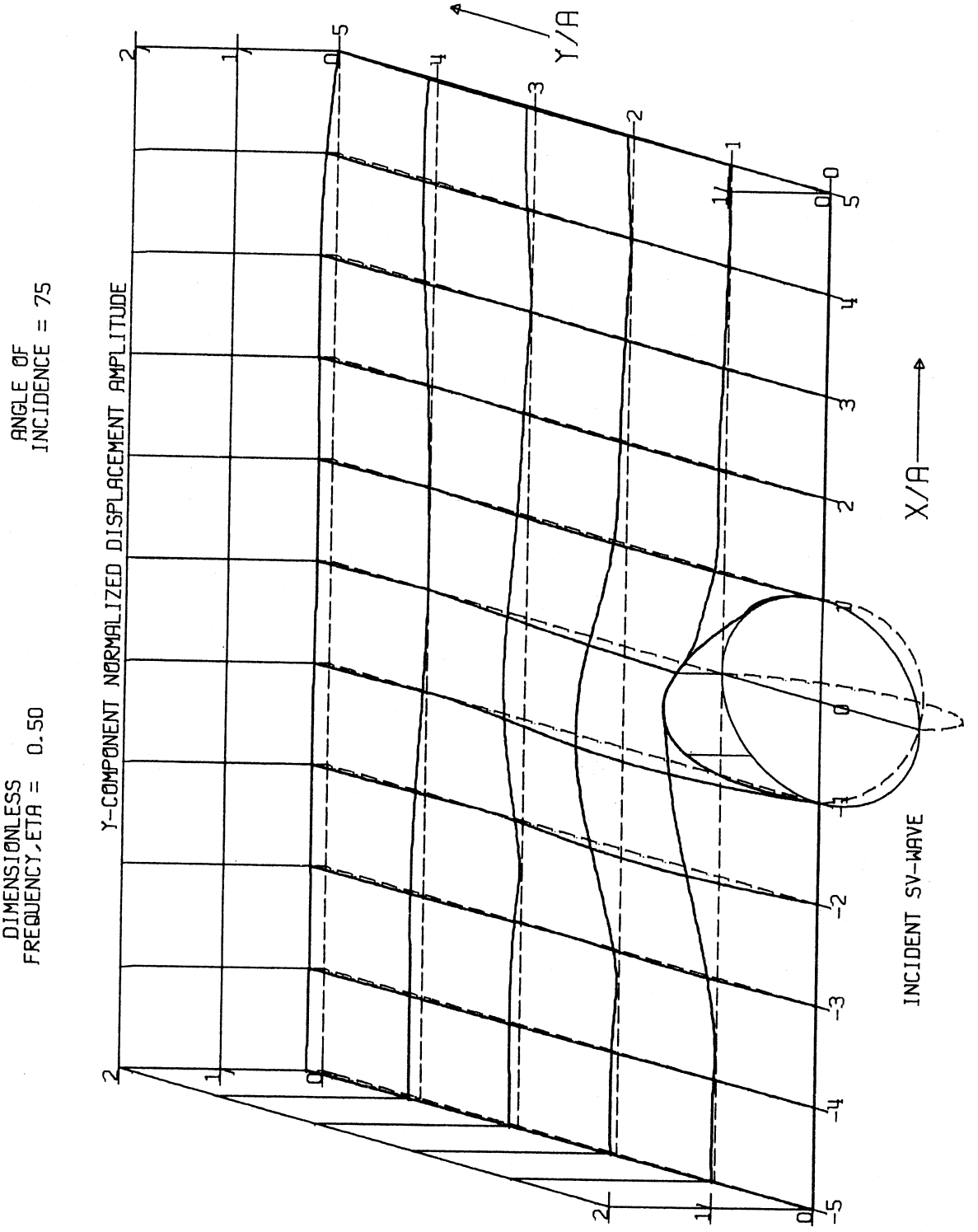

Figure 42

Free-Field Amplitude, $|u_y| = 0$

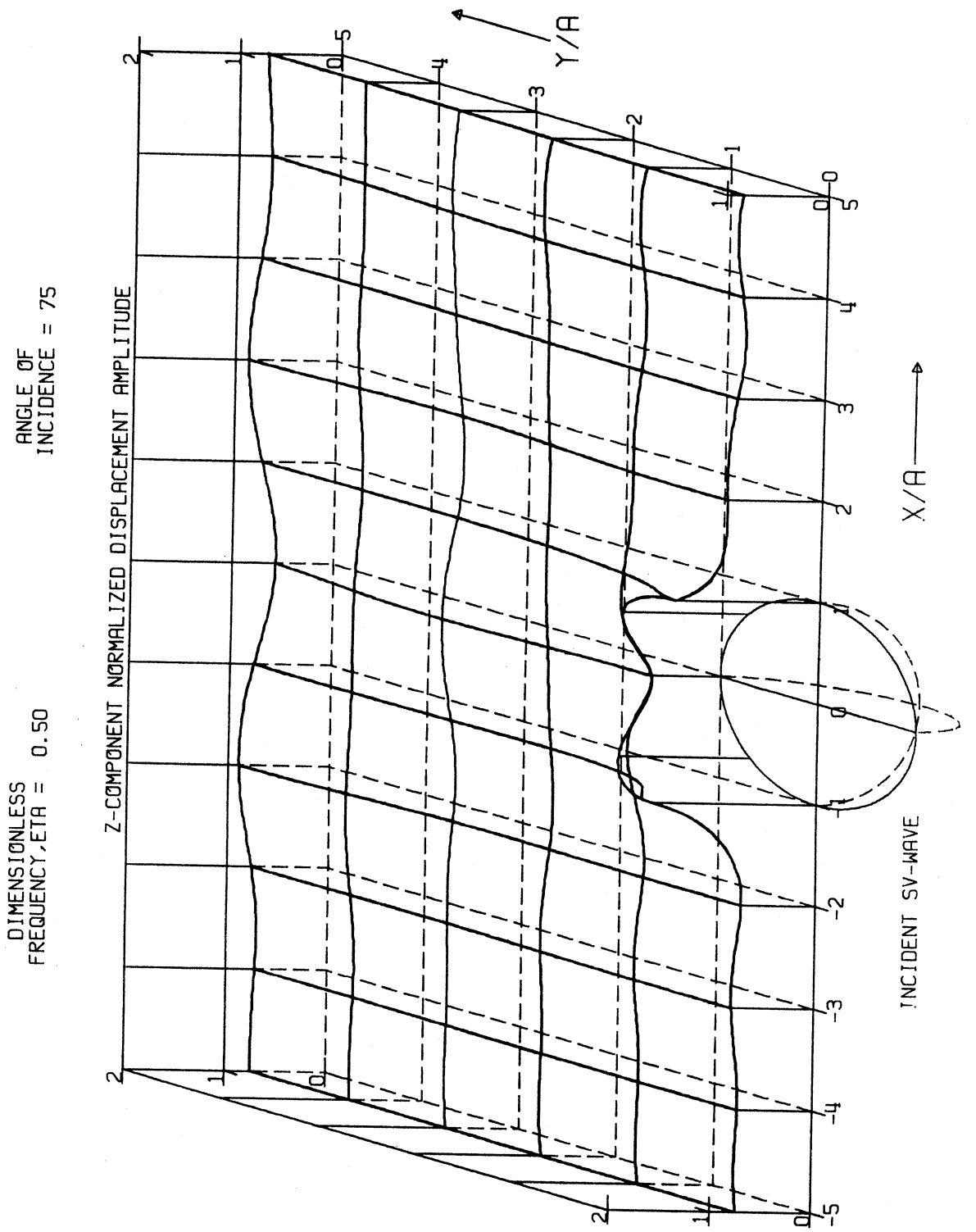

Figure 43

Free-Field Amplitude, $|u_z| = 0.731$

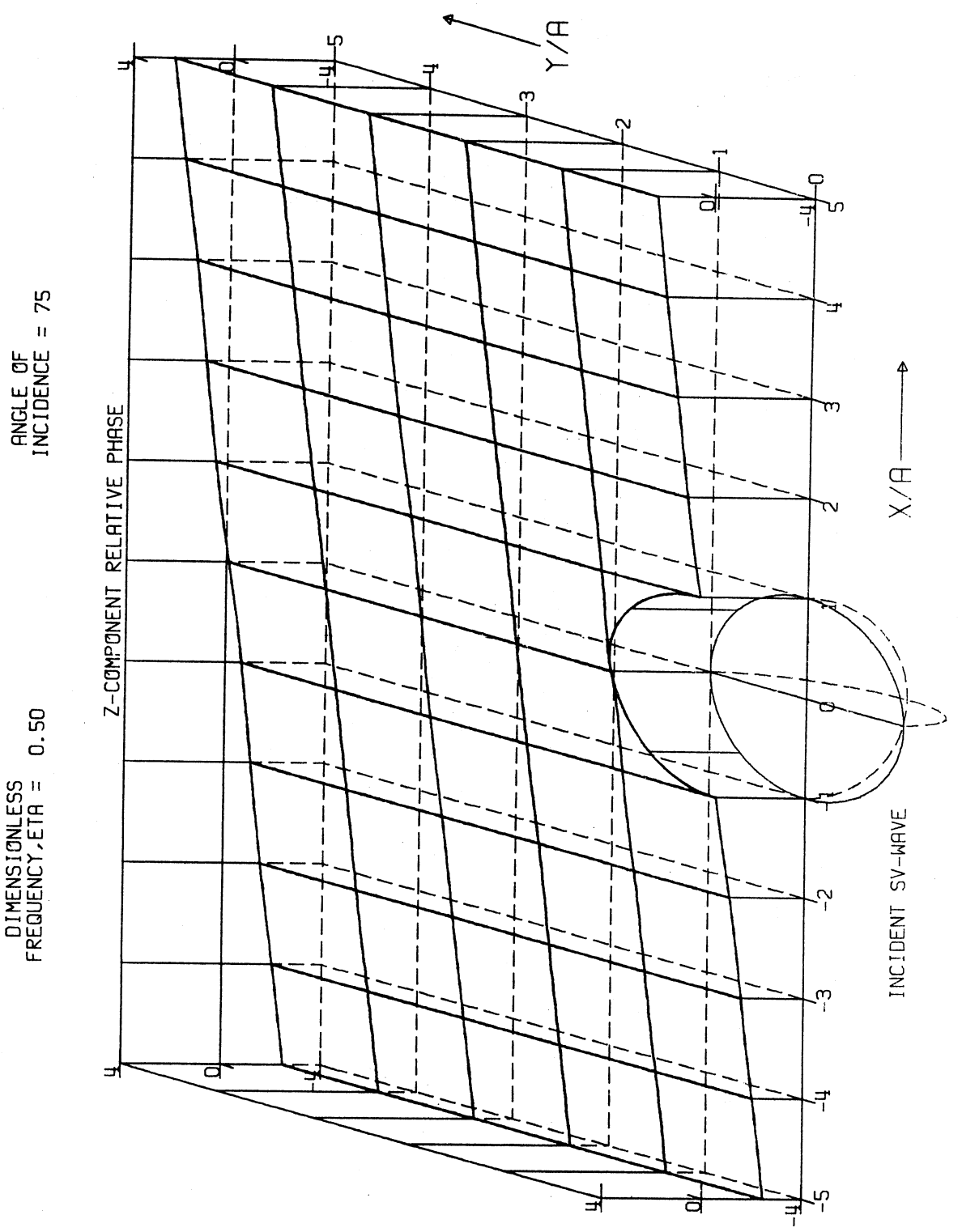

Figure 44

Phase/π

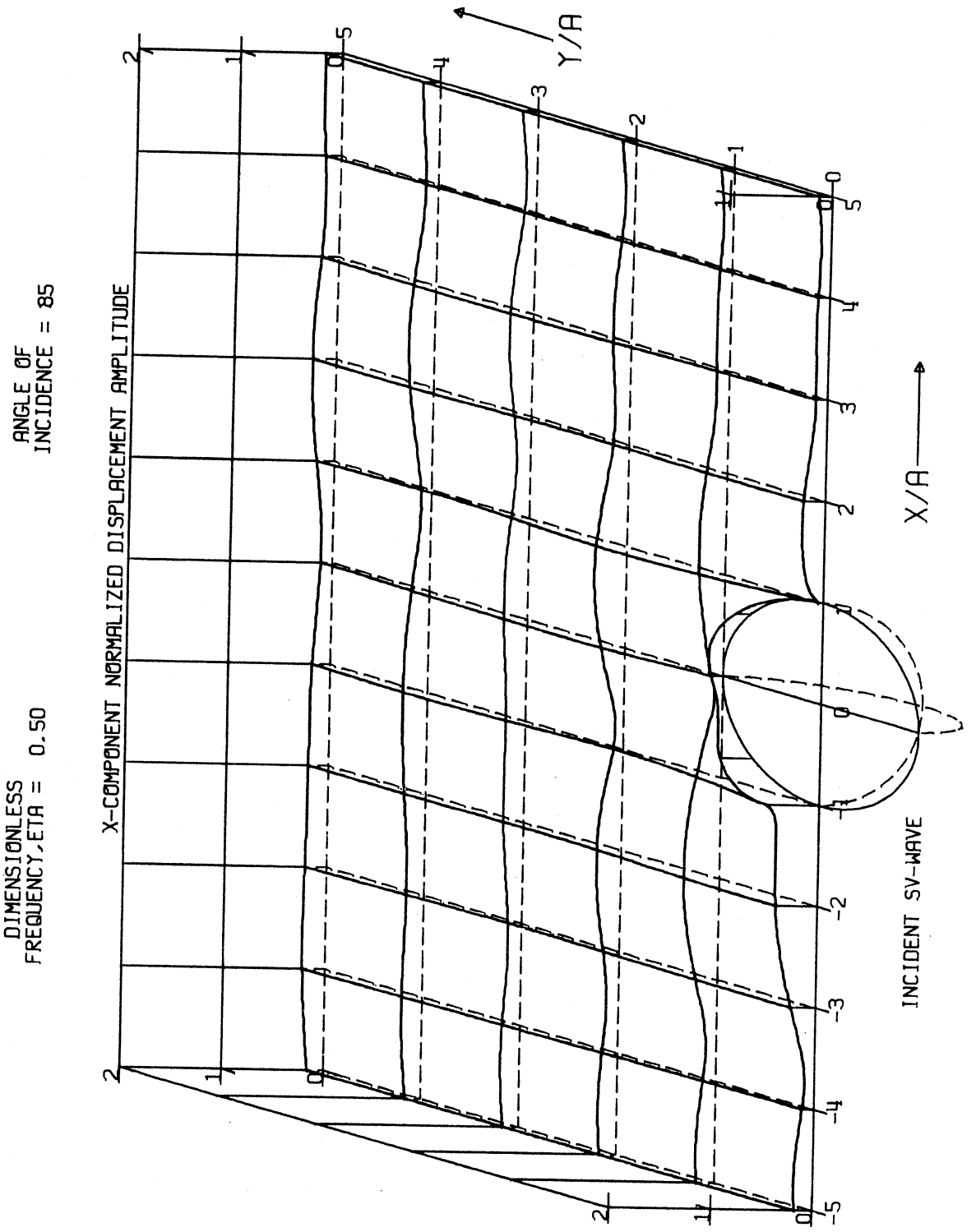

Figure 45

Free-Field Amplitude, $|u_x| = 0.170$

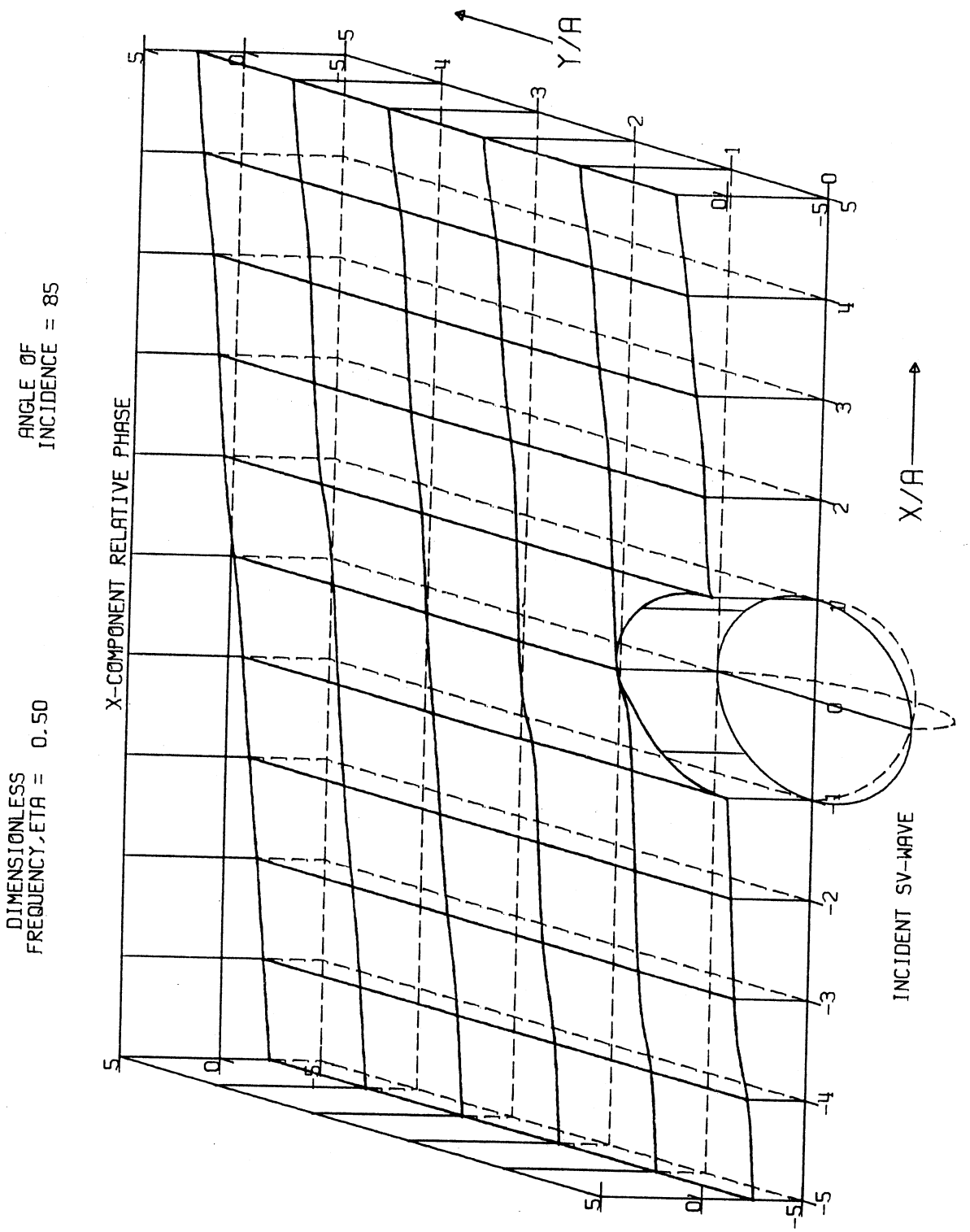

Figure 46

Phase/π

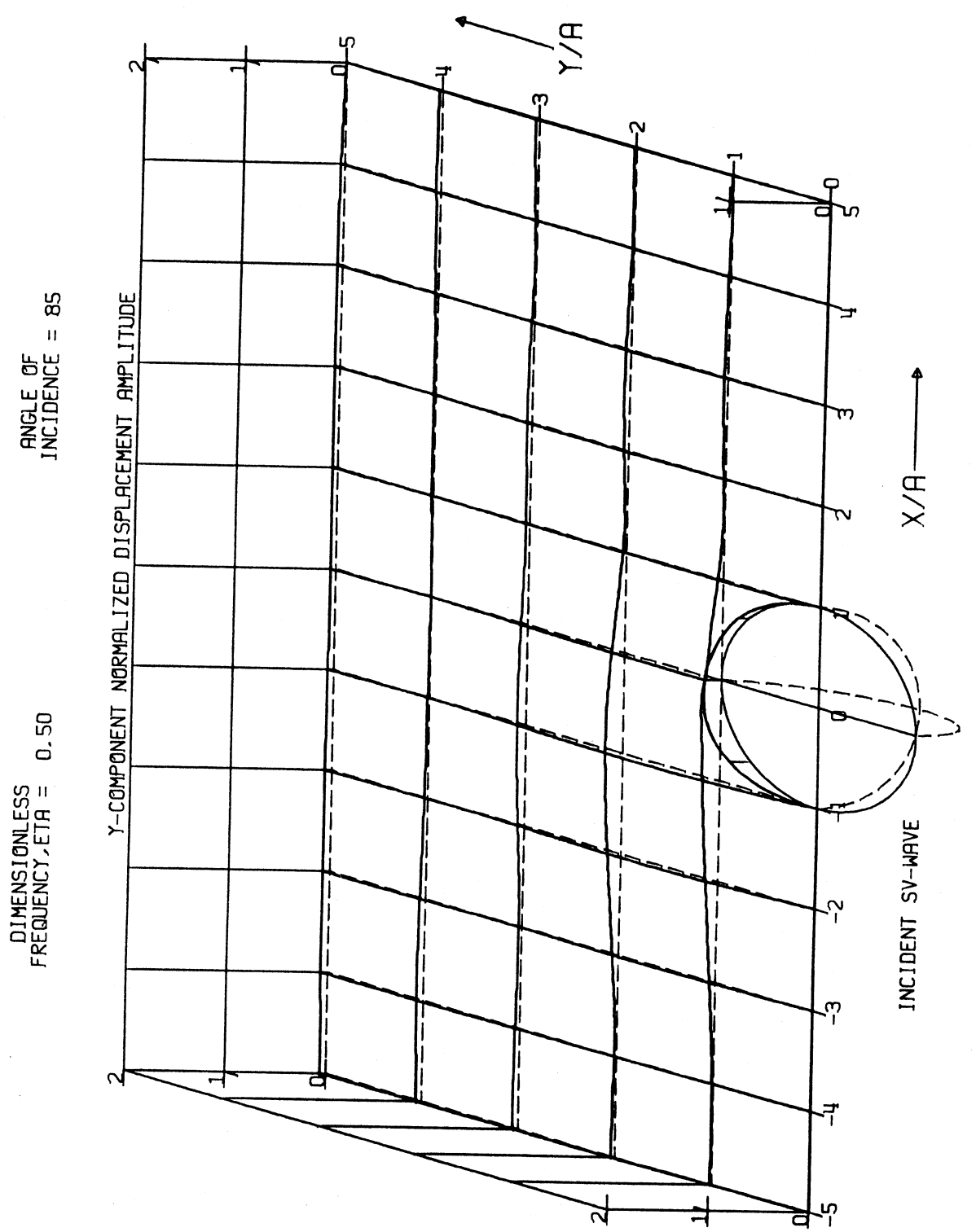

Figure 47

Free-Field Amplitude, $|u_y| = 0$

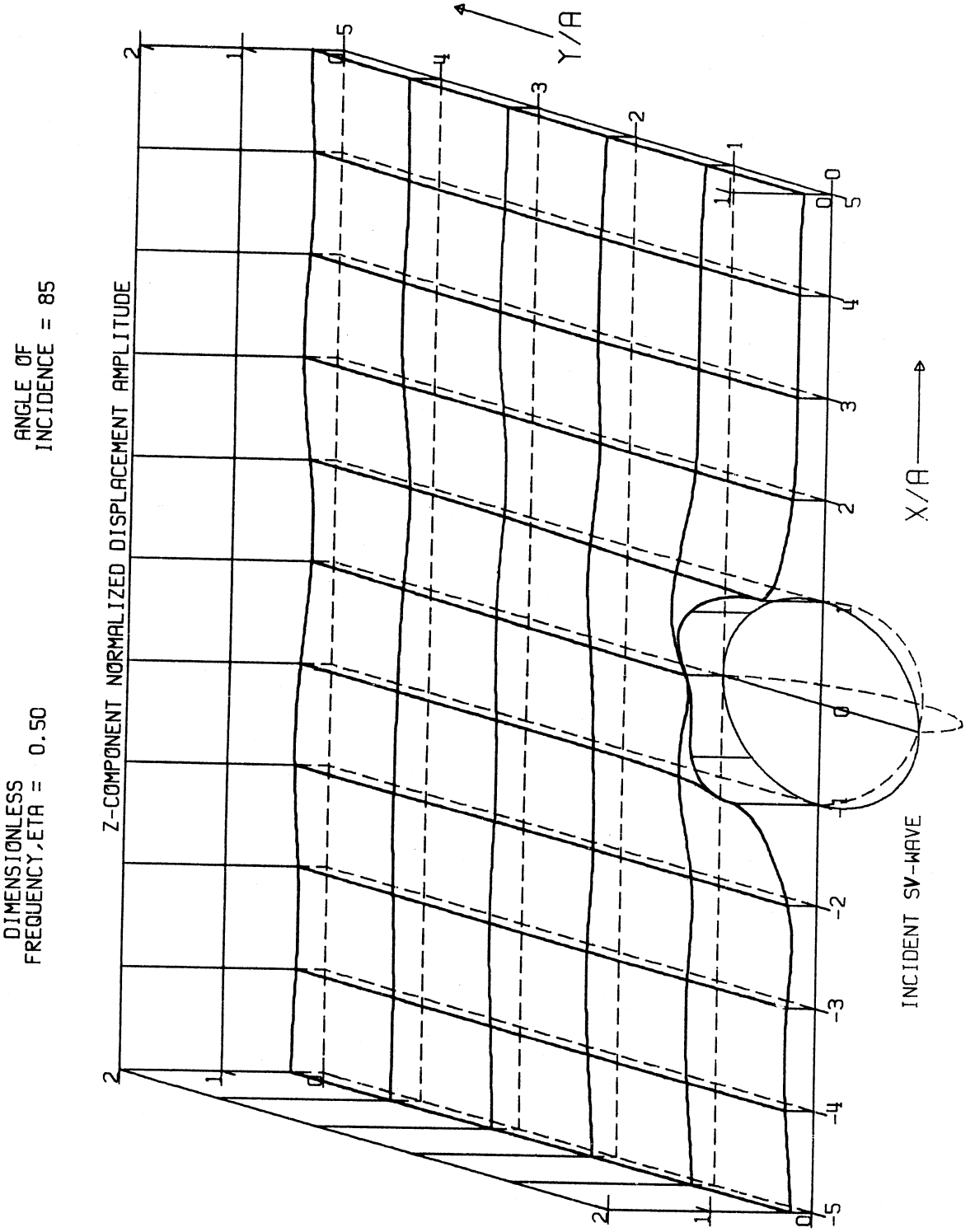

Figure 48

Free-Field Amplitude, $|u_z| = 0.279$

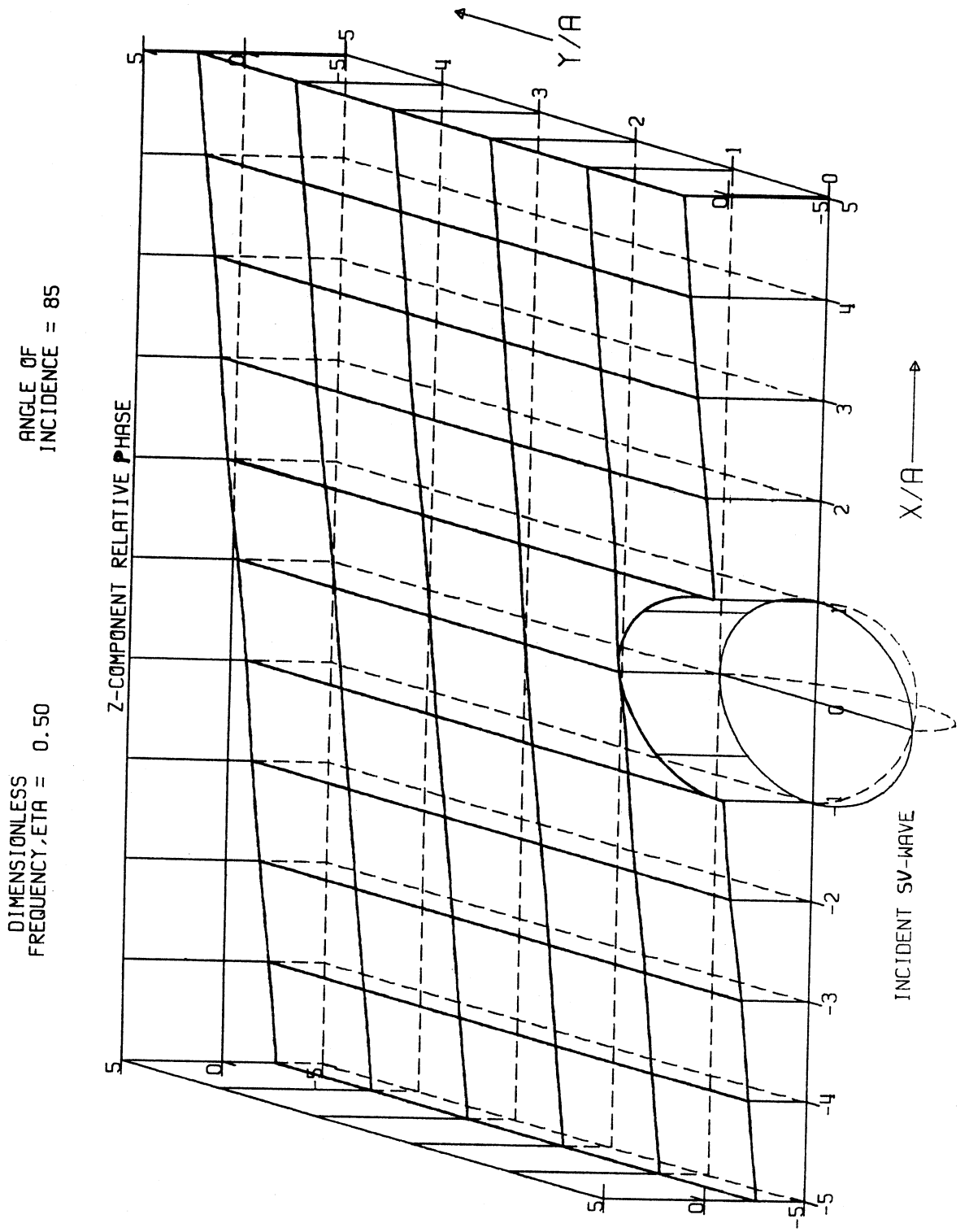

Figure 49

Phase/π

case of incident P-waves. For $\delta = 60°$, prominent, abrupt jumps of magnitude as large as π are observed. These jumps are most prominent at places where displacement amplitudes become very small or close to zero. The motions of the points on opposite sides of the jump are $180°$ out of phases. They are points experiencing predominantly torsional vibrations. Similarly, the phases again approach the linear phase relationship with x at comparably large distances from the canyon.

Excitation: Incident SH-Wave

The analysis for incident transverse SH-wave is similar to the forgoing analysis for P- and SV-waves. The plane SH-wave has its propagation vector again situated in the x-z plane, but the displacement vector is in the y-direction. It has angle of incidence δ, circular frequency ω and is represented by the displacement vector $\underset{\sim}{u}^{(i)}$, where

$$\underset{\sim}{u}^{(i)} = i k_\beta \underset{\sim}{e}_y \exp i k_\beta (x \sin\delta + z \cos\delta) \quad , \tag{9.1}$$

with wave number k_β and magnitude $|\underset{\sim}{u}^{(i)}| = k_\beta$. $\underset{\sim}{e}_y$ is the unit vector in the y-direction.

In the presence of only the free half-space boundary, the incident SH-wave is reflected from the plane free surface ($z = 0$) as SH-wave with angle of reflection same as the angle of incidence. The reflected displacement vector is given by

$$\underset{\sim}{u}^{(r)} = ik_\beta \underset{\sim}{e}_y \exp i k_\beta (x \sin\delta - z \cos\delta) \quad , \tag{9.2}$$

with the same phase and magnitude as $\underset{\sim}{u}^{(i)}$ along the boundary. There is no reflected P- nor SV-wave.

In terms of displacement spherical potentials, $\underset{\sim}{u}^{(i)}$ corresponds to $\Psi^{(i)}$, $\chi^{(i)}$ and $\underset{\sim}{u}^{(r)}$ corresponds to $\Psi^{(r)}$, $\chi^{(r)}$. The potentials are given by

$$\Phi^{(i)} = 0$$

$$\Psi^{(i)} = \sum_{m,n} k_\beta B_{mn}^{(i)} j_n(k_\beta r) P_n^m(\mu) \cos m\phi$$

$$\chi^{(i)} = \sum_{m,n} C_{mn}^{(i)} j_n(k_\beta r) P_n^m(\mu) \sin m\phi$$

$$\Phi^{(r)} = 0$$

$$\Psi^{(r)} = \sum_{m,n} k_\beta B_{mn}^{(r)} j_n(k_\beta r) P_n^m(\mu) \cos m\phi$$

$$\chi^{(r)} = \sum_{m,n} C_{mn}^{(r)} j_n(k_\beta r) P_n^m(\mu) \sin m\phi \quad , \tag{9.3}$$

where the summation is for $m,n = 0,1,2,\ldots$ and $m \leq n$. The coefficients take the form for incident wave, $(u,v) = (\delta,0)$ and

$$B_{mn}^{(i)} = i\delta_{mn} c_{mny}^{e} / \sqrt{n(n+1)}$$

$$C_{mn}^{(i)} = \delta_{mn} b_{mny}^{o} / \sqrt{n(n+0)} \quad , \tag{9.4}$$

while for reflected waves, $(u,v) = (\pi-\delta,0)$ and

$$B_{mn}^{(r)} = i\delta_{mn} c_{mny}^{e} / \sqrt{n(n+1)}$$

$$C_{mn}^{(r)} = \delta_{mn} b_{mny}^{o} / \sqrt{n(n+1)} \quad , \tag{9.5}$$

where the terms in the expressions are given in Appendix I.

The resulting displacement vector is

$$\underset{\sim}{u}^{(i+r)} = \underset{\sim}{u}^{(i)} + \underset{\sim}{u}^{(r)} \quad , \tag{9.6}$$

again satisfying the stress-free boundary conditions

$$\sigma_{zz} = \sigma_{zx} = \sigma_{zy} = 0 \tag{9.7}$$

The resulting potentials from incident SH-waves have one major difference with those for incident P- or SV-waves. For incident P- or SV-waves, the Φ- and χ-potentials are even functions of ϕ, with

factors $\cos m\phi$, while the Ψ-potentials are odd functions of ϕ with factors $\sin m\phi$. It is vice versa for incident SH-waves, which has its displacement vector in the y-direction. The Φ- and χ-potentials are now odd functions of ϕ, with factors $\sin m\phi$, while the Ψ-potentials are even functions of ϕ, with factors $\cos m\phi$.

In the presence of the canyon, outgoing spherical waves are reflected back into the medium. They are represented by the potentials $\Phi^{(r)}$, $\Psi^{(s)}$ and $\chi^{(s)}$ given by

$$\Phi^{(s)} = \sum_{m,n} A_{mn}^{(3)} z_n^{(3)}(k_\alpha r) P_n^m(\mu) \sin m\phi$$

$$\Psi^{(s)} = \sum_{m,n} k_\beta B_{mn}^{(3)} z_n^{(3)}(k_\beta r) P_n^m(\mu) \cos m\phi$$

$$\chi^{(s)} = \sum_{m,n} C_{mn}^{(3)} z_n^{(3)}(k_\beta r) P_n^m(\mu) \sin m\phi \quad , \tag{9.8}$$

in the same form as those in (8.1), with the sine and cosine terms switched. The coefficients $\left\{A_{mn}^{(3)}, B_{mn}^{(3)}, C_{mn}^{(3)}\right\}$ $m,n = 0,1,2, \ldots$ with $m \le n$, identically satisfy the equations in (8.2).

In the presence of both the plane free boundary and the hempispherical canyon, additional spherical waves are generated, being represented by

$$\Phi^{(R)} = \sum_{j,m,n} A_{mn}^{(j)} z_n^{(j)}(k_\alpha r) P_n^m(\mu) \sin m\phi$$

$$\Psi^{(R)} = \sum_{j,m,n} k_\beta B_{mn}^{(j)} z_n^{(j)}(k_\beta r) P_n^m(\mu) \cos m\phi$$

$$\chi^{(R)} = \sum_{j,m,n} C_{mn}^{(j)} z_n^{(j)}(k_\beta r) P_n^m(\mu) \sin m\phi \tag{9.9}$$

where $j = 1,2$, and $m,n = 0,1,2,\ldots$, with $m \leq n$. (9.9) is in the same form as (8.3) with the sine and cosine terms switched. The six sets of unknowns $\left\{A_{mn}^{(j)}, B_{mn}^{(j)}, C_{mn}^{(j)}\right\}$ $j = 1,2$, $m,n = 0,1,2,\ldots$ $m \leq n$, again satisfy the identical set of equations, namely (4.1), (4.16), (4.19) and (4.21).

The same steps in the numerical calculations are carried out as in the foregoing analysis for P- and SV-waves; and the results are presented in Figures 50 through 65. They represent typical characteristics of amplitudes and phases of surface displacements at dimensionless points $(x/a, y/a)$ near the canyon for angles of incidence $\delta = 0°$, $30°$, $60°$ and $85°$. Again, the values $\eta = 0.5$ and $\nu = 0.25$ are used.

In the absence of the hemispherical canyon, the free-field surface displacement amplitude for incident SH-wave of unit amplitude is two for the y-component and 0 for the x- and z-components for all angles of incidence. The y-component phase is given by

$$\phi_y = k_\beta \sin\delta\, x \quad , \tag{9.10}$$

where δ is the angle of incidence. The presence of the canyon changes the above uniformity and results in non-zero motion in all three components. Similar results are obtained as in the cases of incident P- and SV-waves. Scattering and diffraction of waves around the canyon result in the creation of amplification and shadow zones. Similar results are obtained for phase changes.

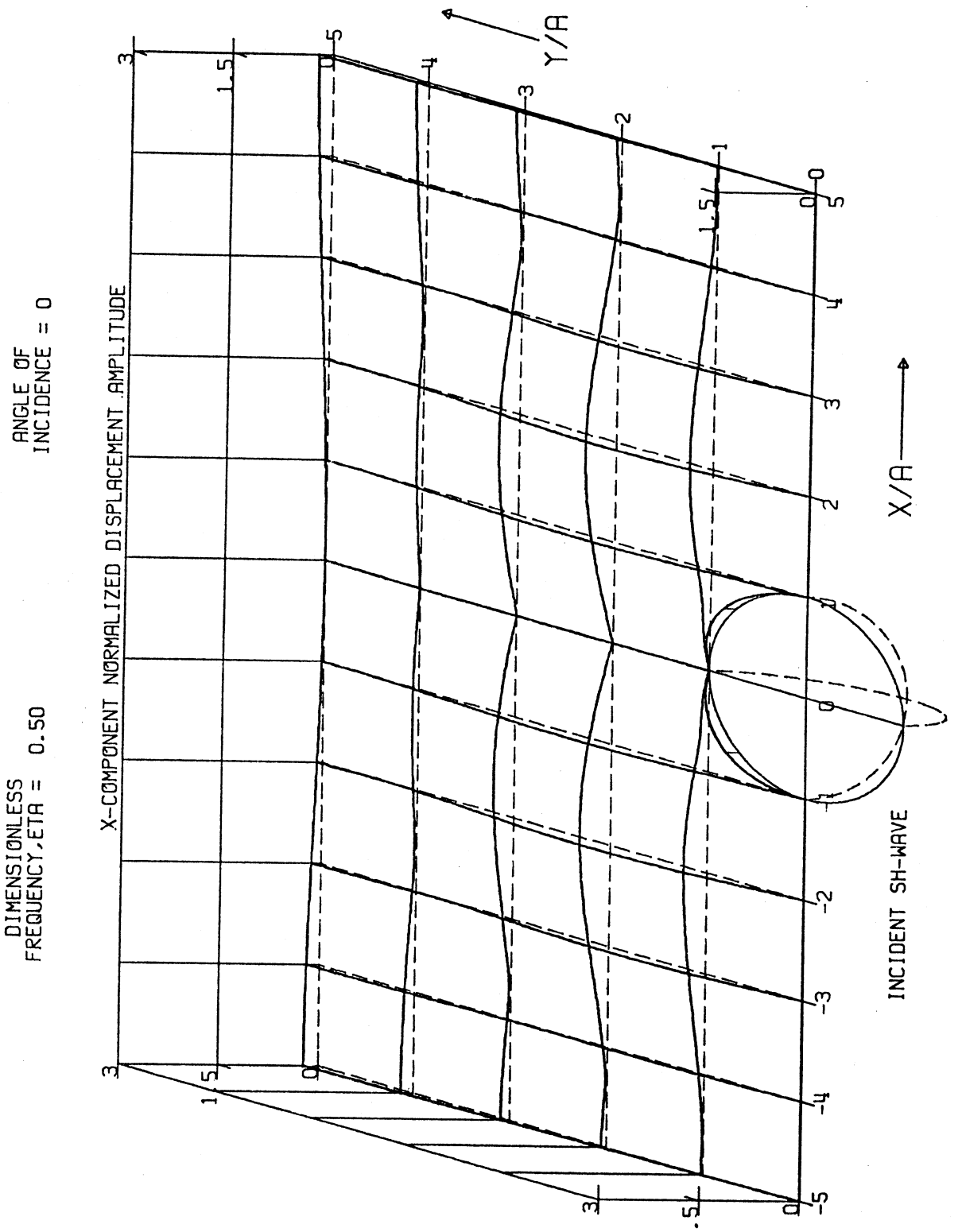

Figure 50

Free-Field Amplitude, $|u_x| = 0$

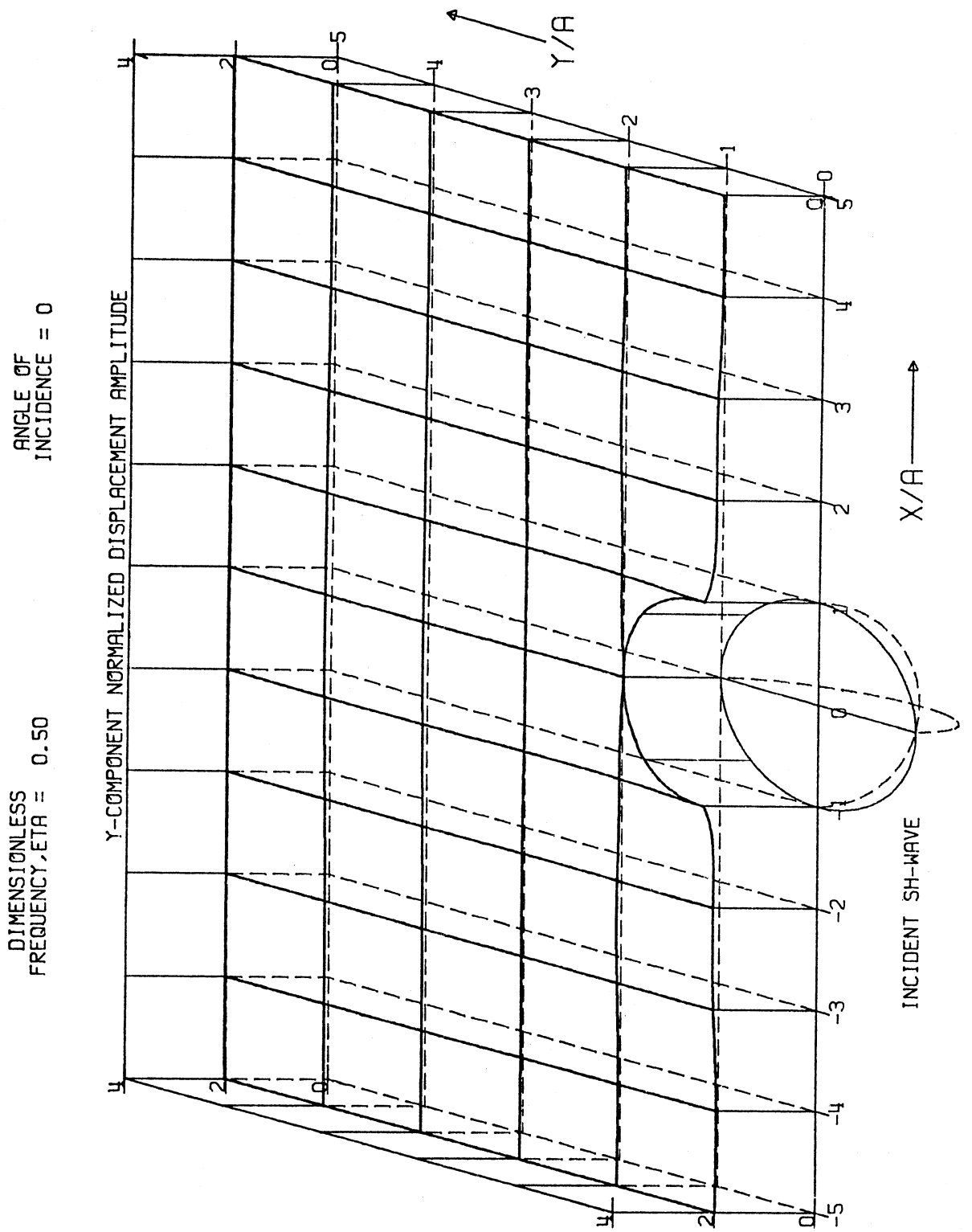

Figure 51

Free-Field Amplitude, $|u_z| = 2$

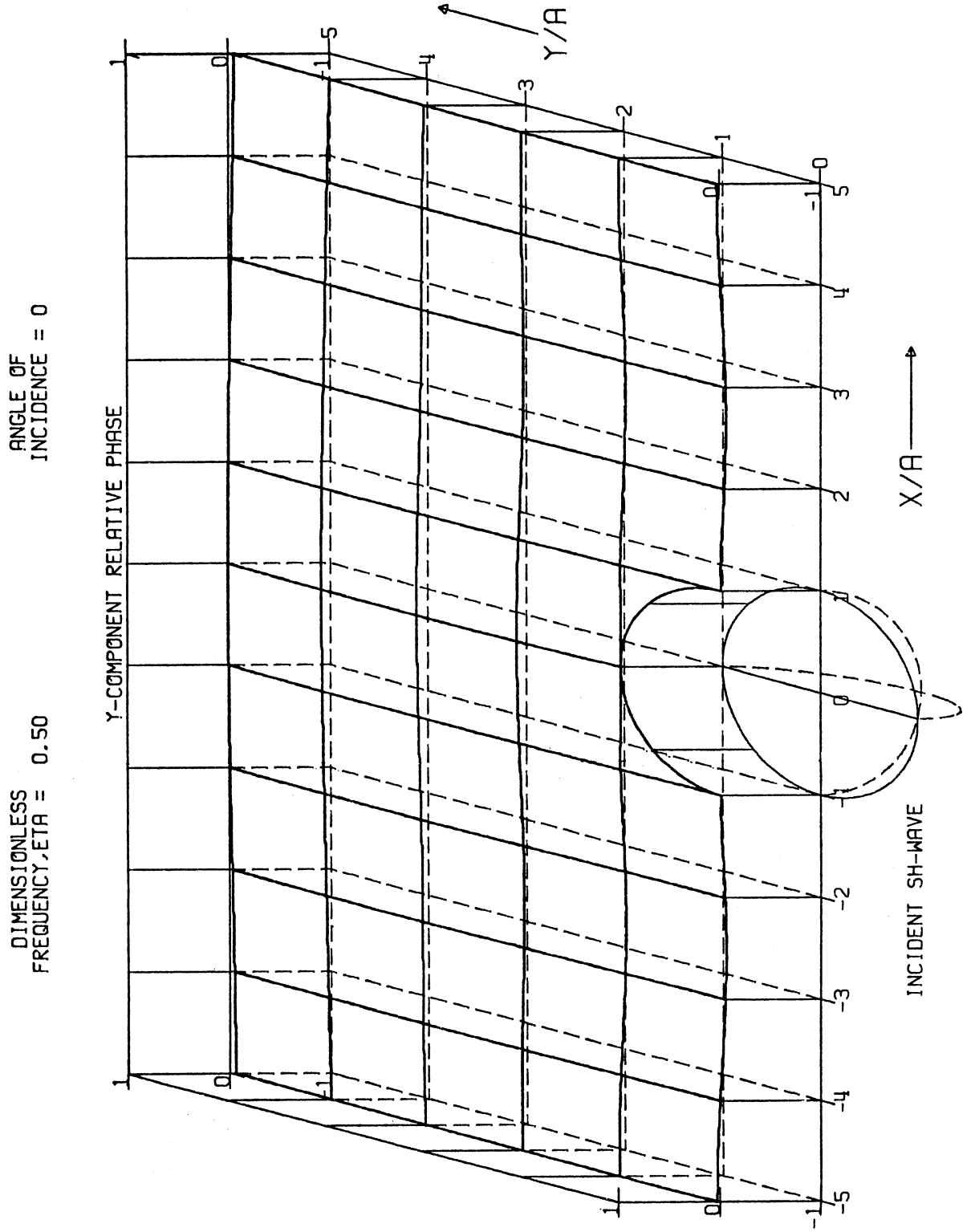

Figure 52

Phase/π

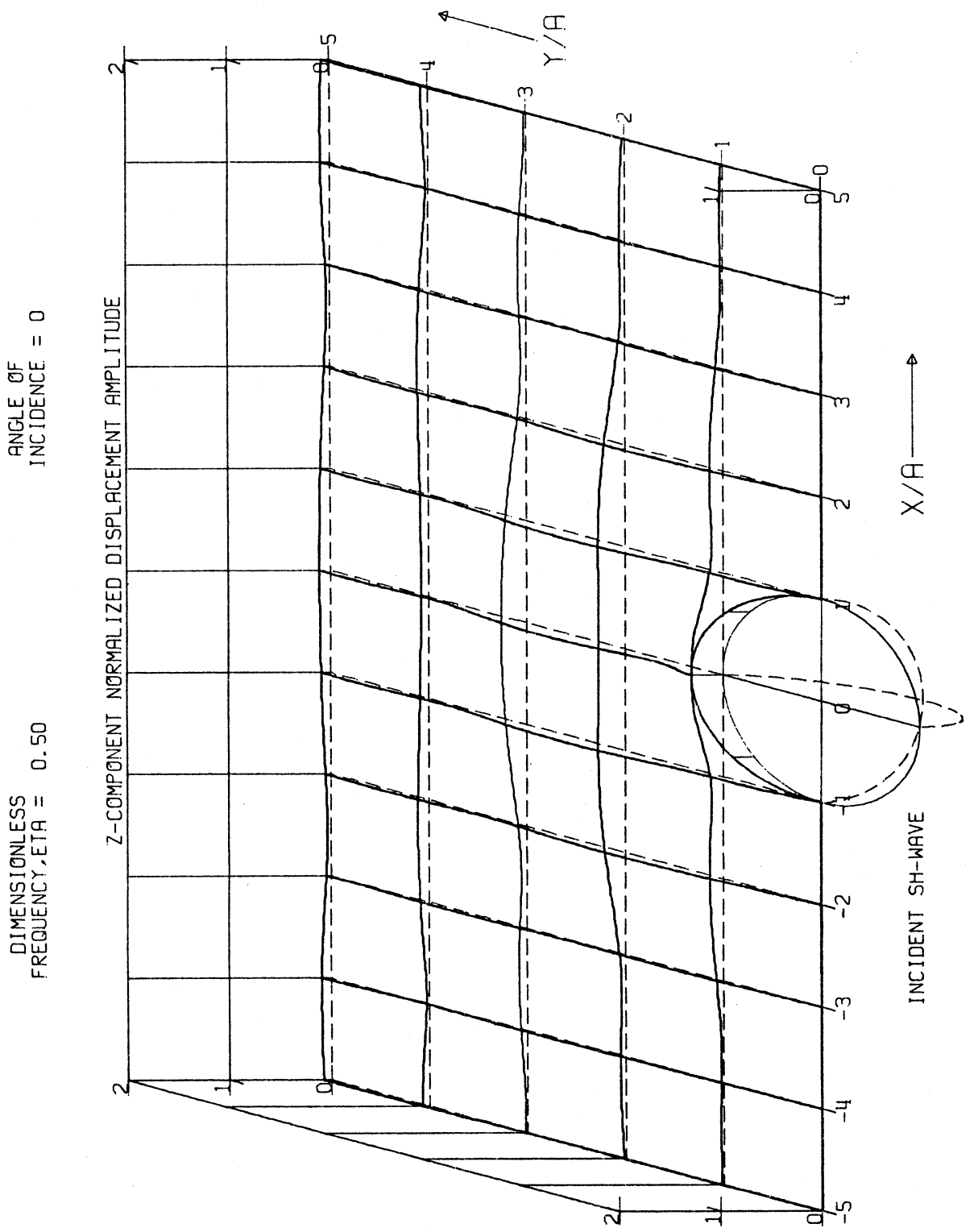

Figure 53

Free-Field Amplitude, $|u_z| = 0$

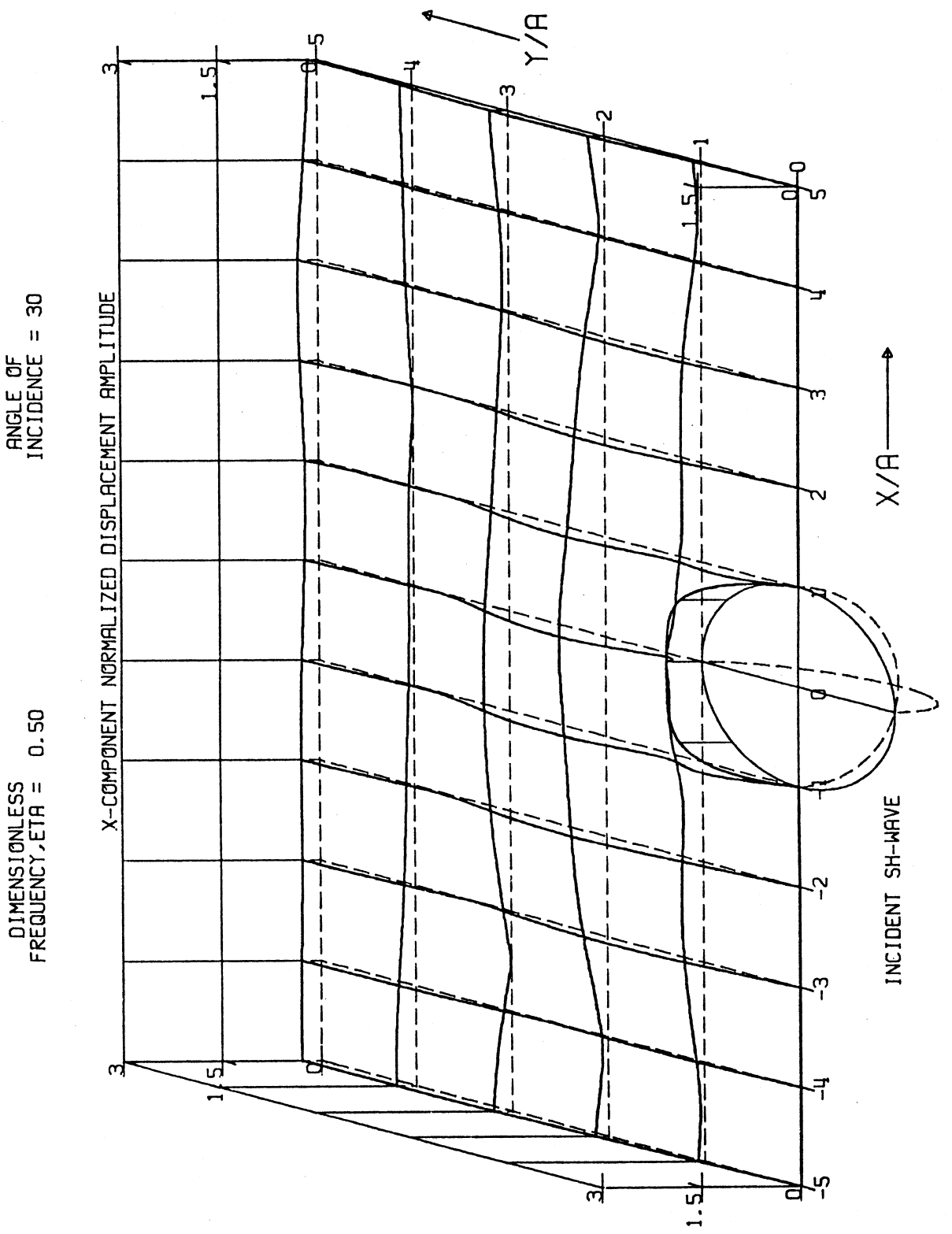

Figure 54

Free-Field Amplitude, $|u_x| = 0$

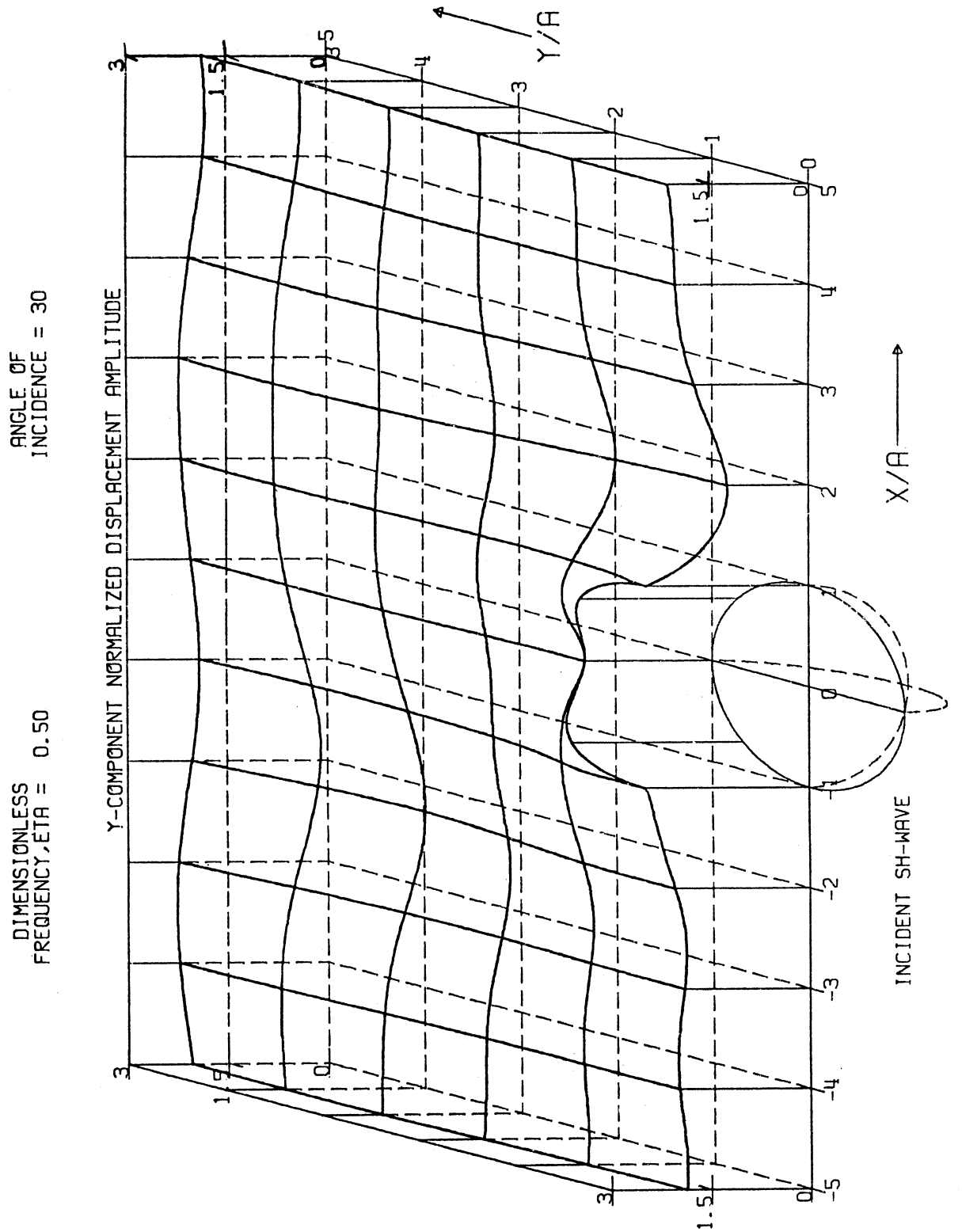

Figure 55

Free-Field Amplitude, $|u_y| = 2$

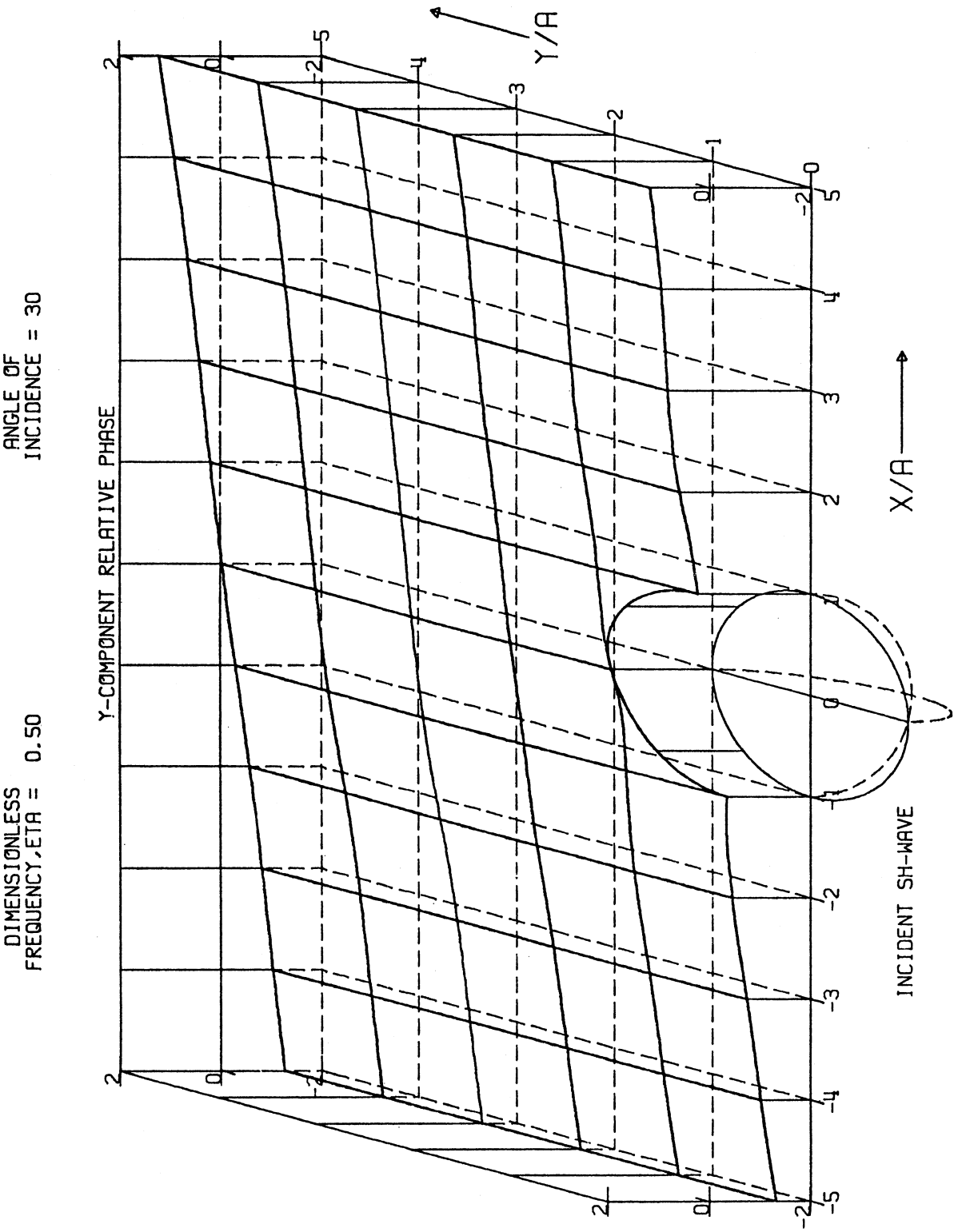

Figure 56

Phase/π

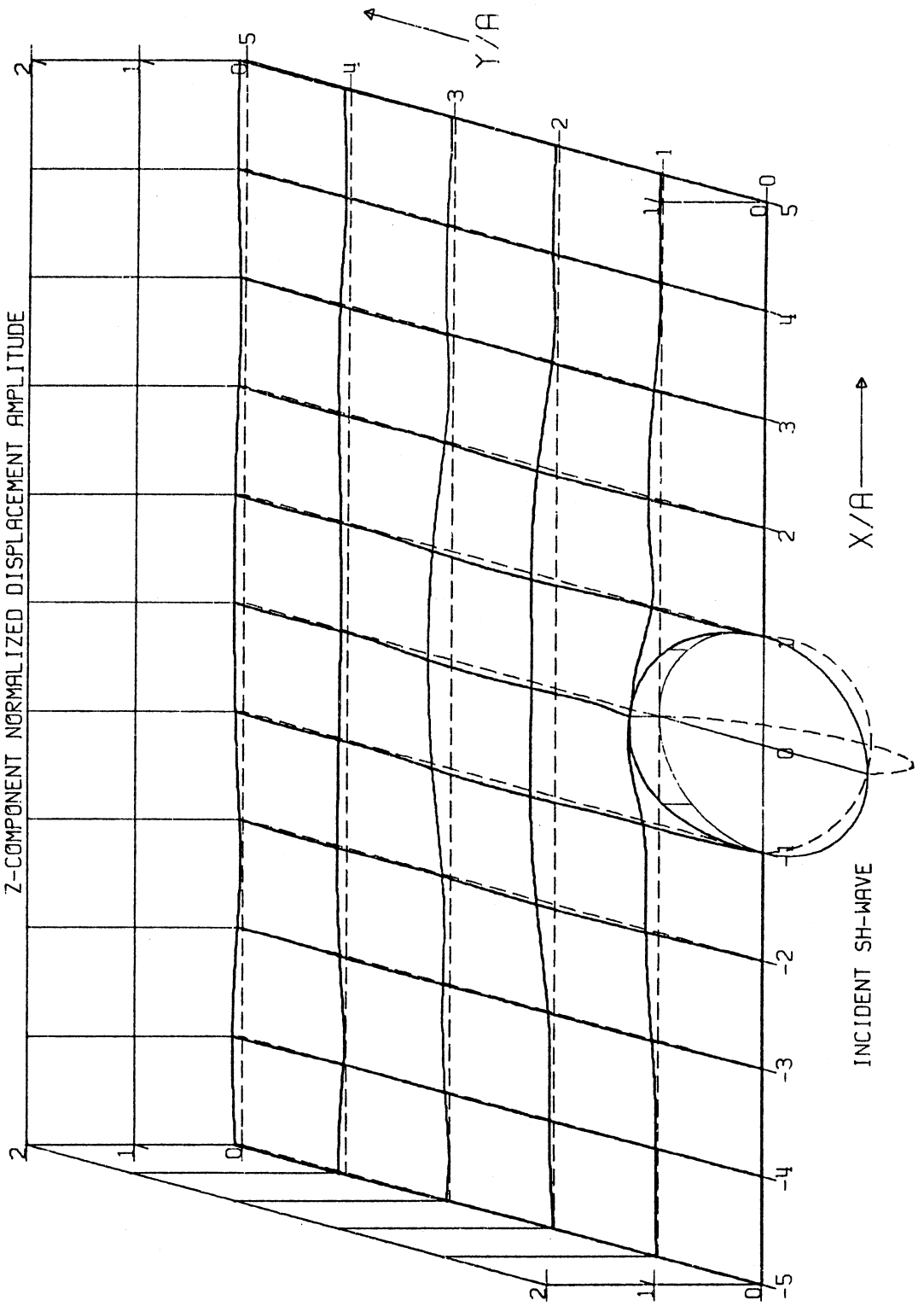

Figure 57

Free-Field Amplitude, $|u_z| = 0$

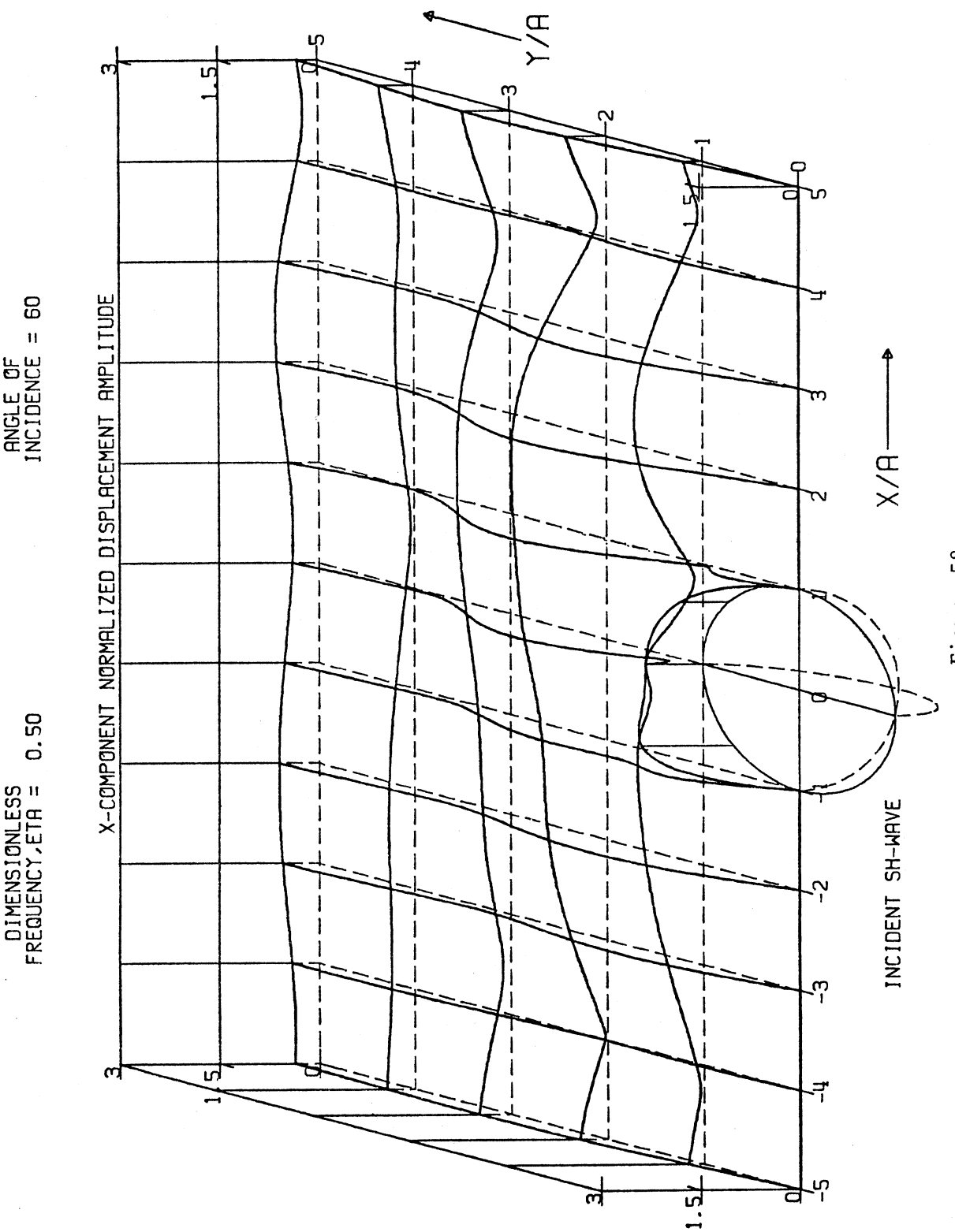

Figure 58

Free-Field Amplitude, $|u_x| = 0$

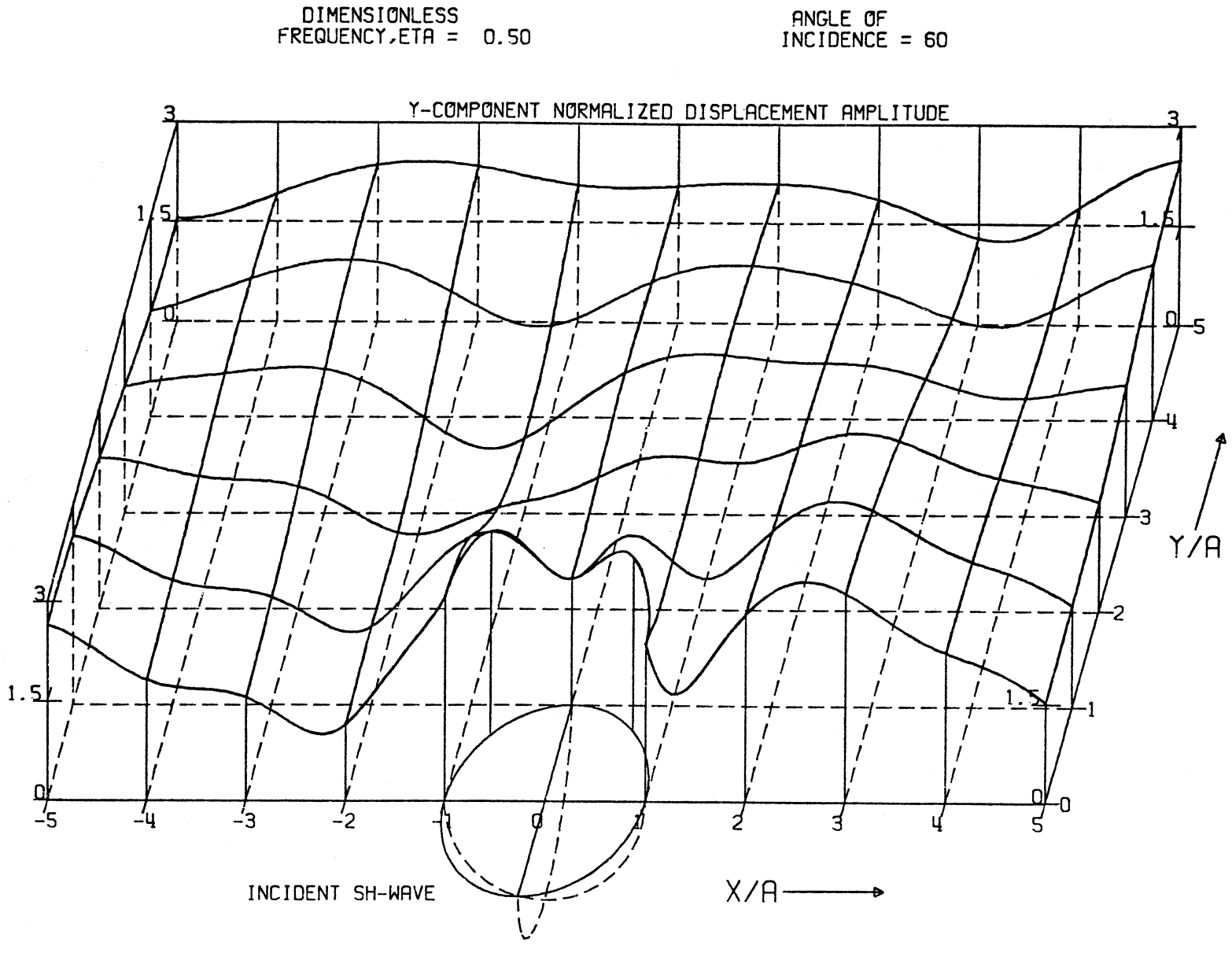

Figure 59

Free-Field Amplitude, $|u_z| = 2$

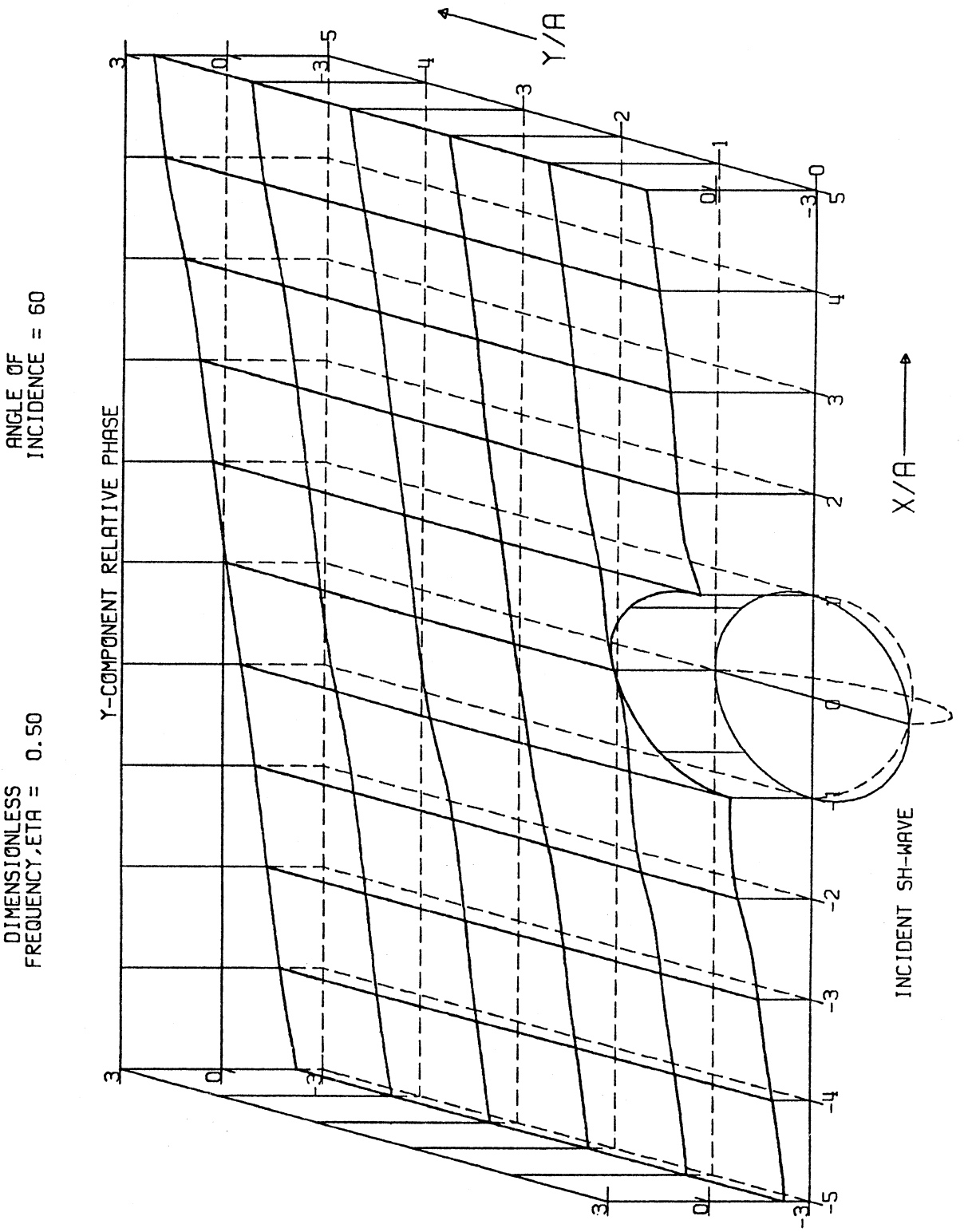
DIMENSIONLESS
FREQUENCY,ETA = 0.50
ANGLE OF
INCIDENCE = 60
Y-COMPONENT RELATIVE PHASE
Y/A
X/A
INCIDENT SH-WAVE
Phase/π

Figure 60

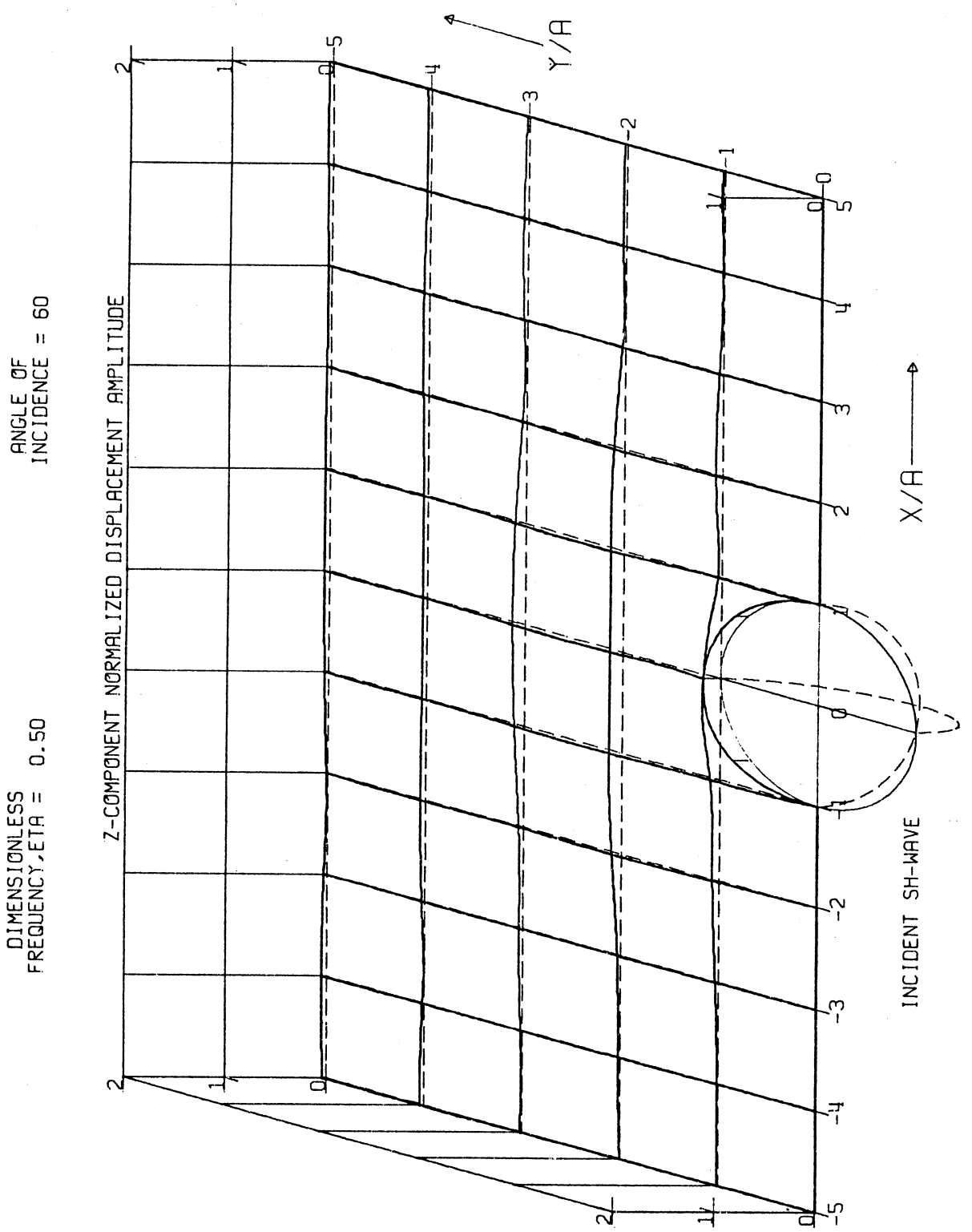

Figure 61

Free-Field Amplitude, $|u_z| = 0$

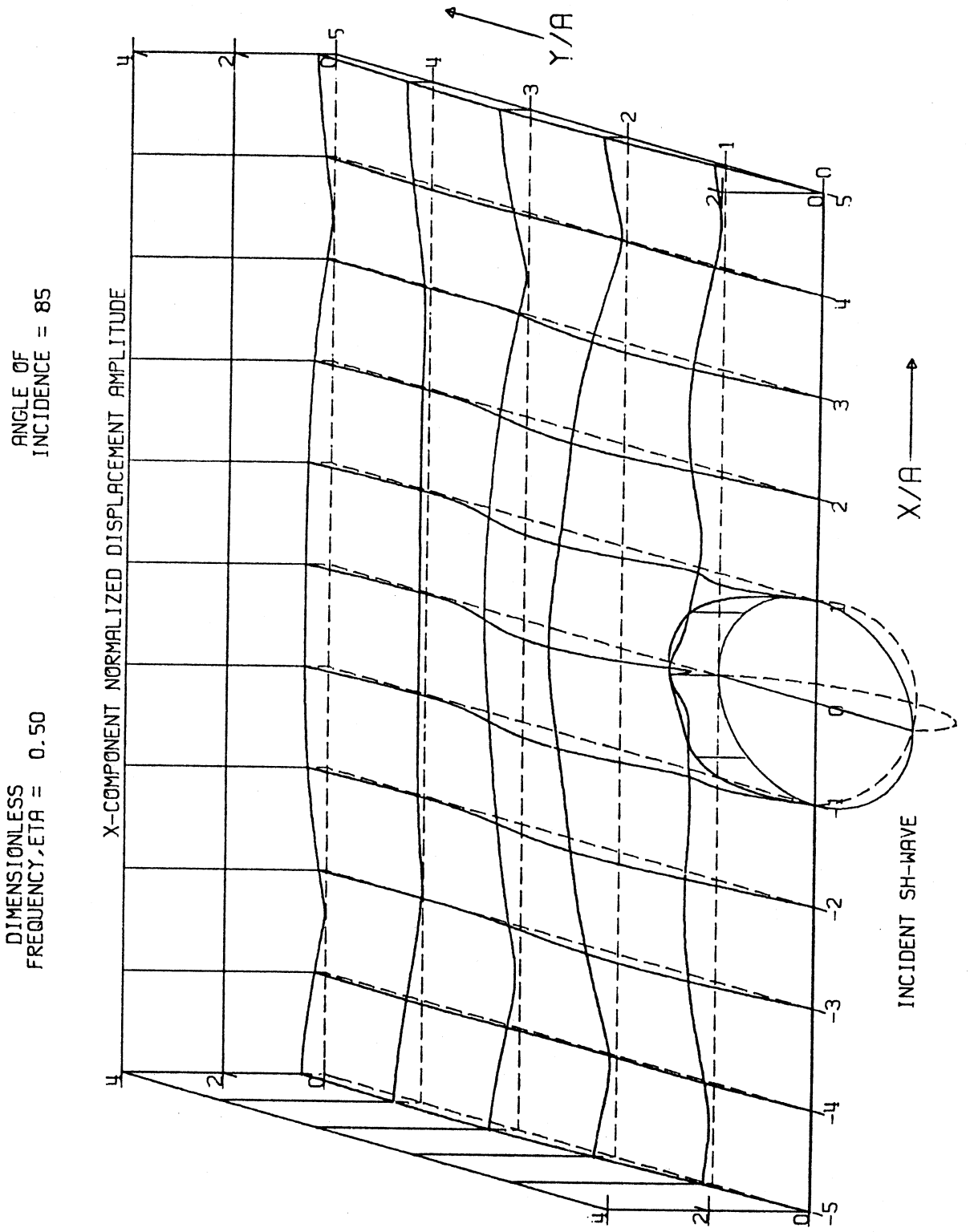

Figure 62

Free-Field Amplitude, $|u_x| = 0$

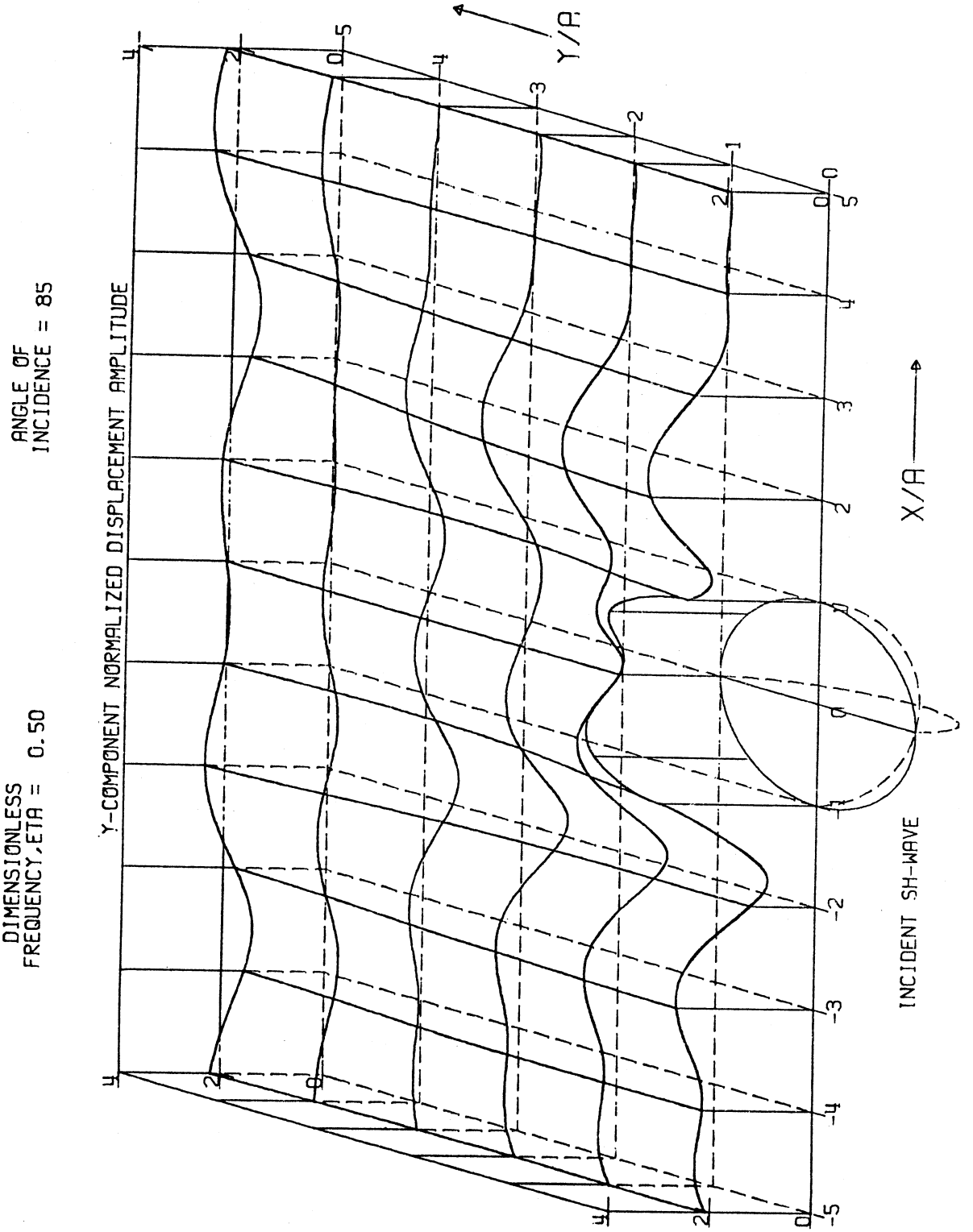

Figure 63

Free-Field Amplitude, $|u_y| = 2$

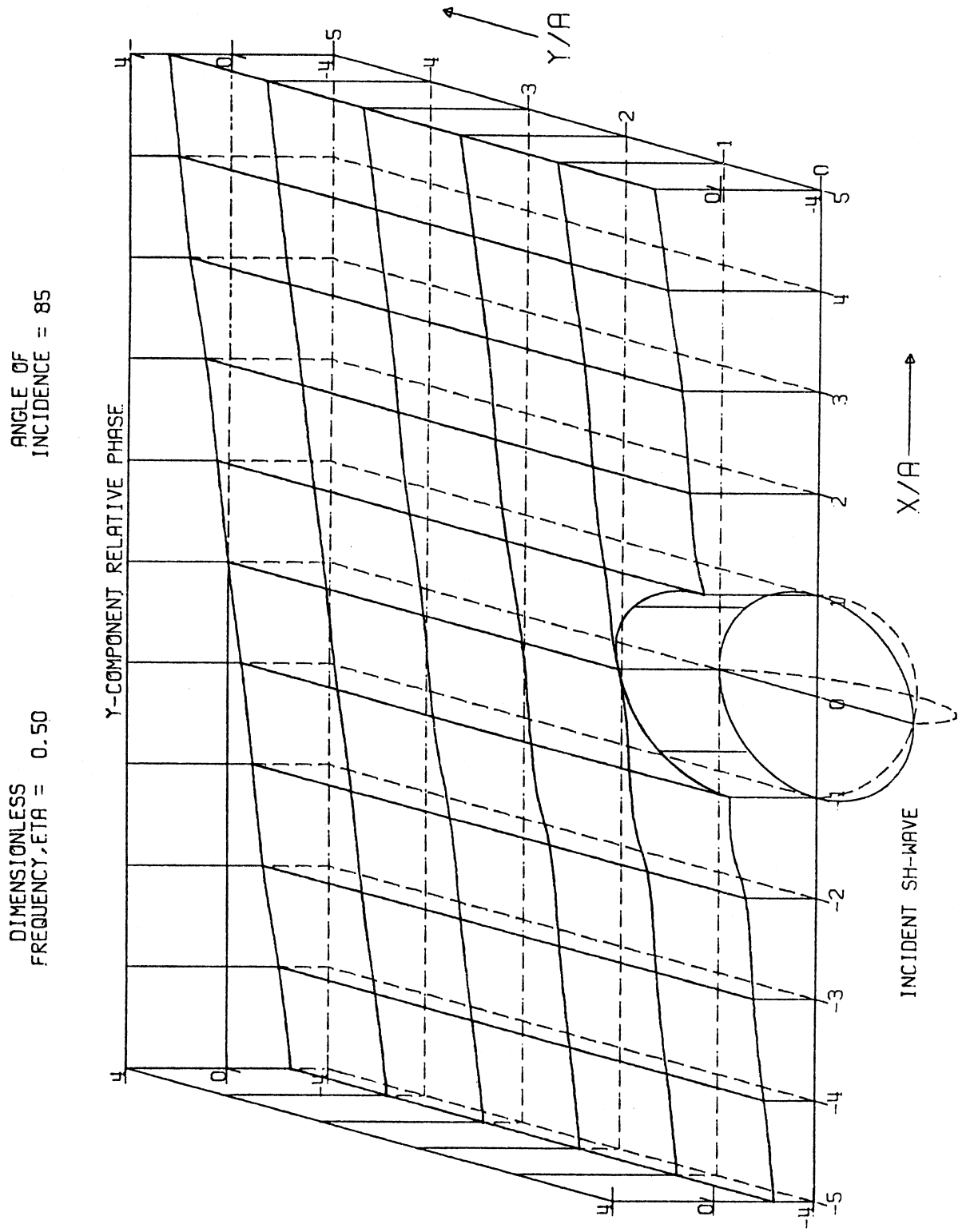
DIMENSIONLESS
FREQUENCY,ETA = 0.50
ANGLE OF
INCIDENCE = 85
Y-COMPONENT RELATIVE PHASE
Y/A
X/A
INCIDENT SH-WAVE
Phase/π

Figure 64

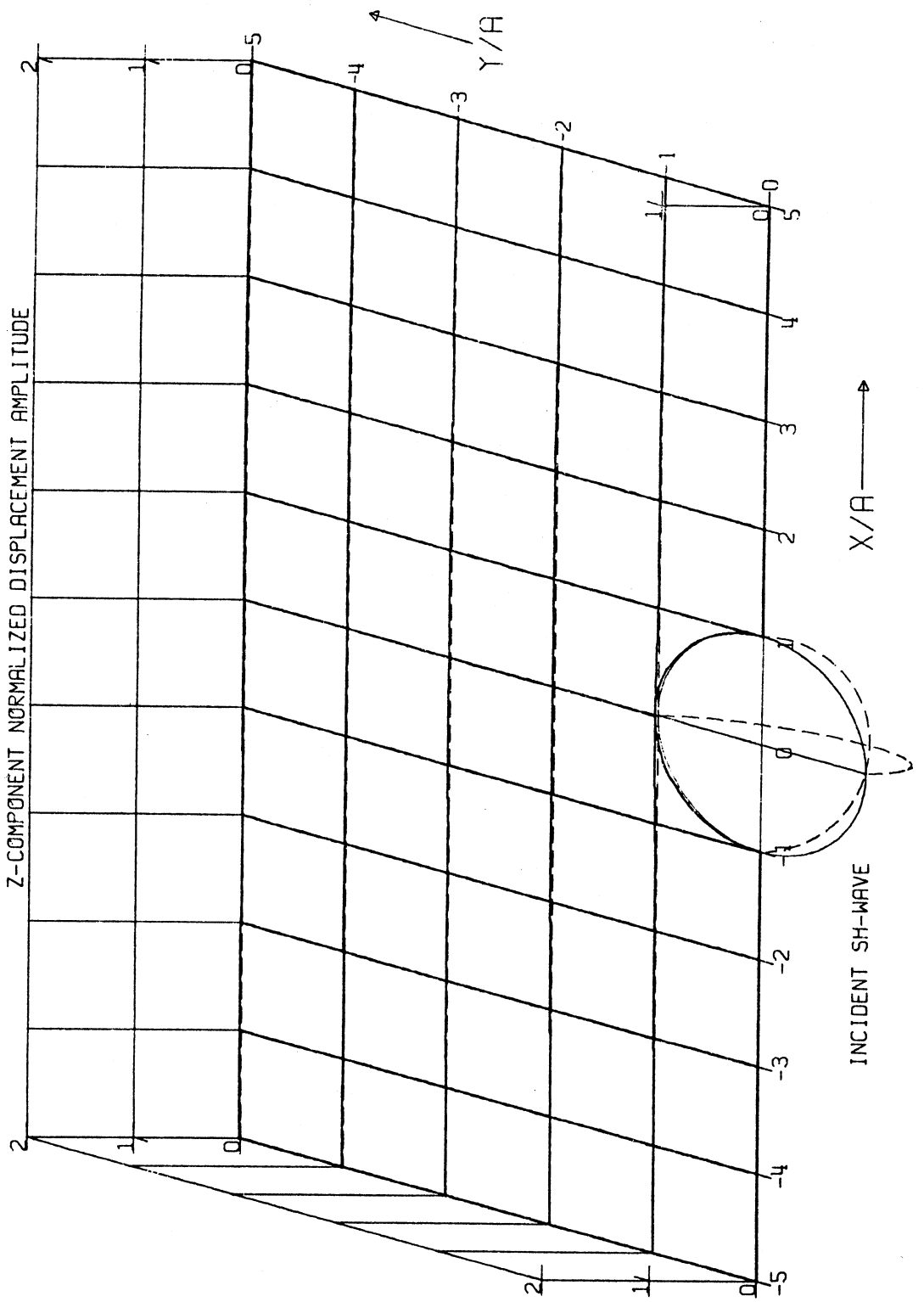

Figure 65

Free-Field Amplitude, $|u_z| = 0$

Conclusions

Some of the principal observations that emerge from the analysis above may be summarized as follows:

1) The surface displacement amplitudes at all points around the canyon is no higher than four, for incident plane P-, SV- and SH-waves. The resulting amplification of surface displacements is thus no higher than two.

2) The pattern and amplitudes of surface displacements depend significantly on the direction of incident waves. For acute angles of incidence, amplification and shadow zones are observed around the canyon.

3) Similarly, significant phase changes are observed close to the canyon at points where the motion is small.

4) The principal role of the ratio of the diameter of the canyon to the wavelength of the incident plane waves is that it determines the extent to which the above-mentioned effects are developed.

ACKNOWLEDGEMENTS

I would like to express my thanks for Professor M.D. Trifunac for his many valuable remarks, encouragement and helpful suggestions, to Professor B.A. Troesch for critical reading of the manuscript. Their critical review and constructive criticism led to numerous additions, changes and improvements in the final manuscript.

This research has been supported in part by contracts from the U.S. Geological Survey and the U.S. Nuclear Regulatory Commission.

References

1. P.M. Morse and H. Feshbach, "Methods of Theoretical Physics," McGraw-Hill, New York (1953).

2. C.C. Mow and Y.H. Pao, "The Diffraction of Elastic Waves and Dynamic Stress Concentrations," Rand Report, R-482-PR (1971).

3. A.C. Eringen and E.S. Suhubi, "Elastodynamics, Vol. II: Linear Theory," Academic Press, New York, 1975.

4. Knopoff, L., "Scattering of Compressional Waves by Spherical Obstacles," Geophysics, Vol. 24, No. 1, February, 1959.

5. Knopoff, L., "Scattering of Shear Waves by Sperhical Obstacles," Geophysics, Vol. 24, No. 2, April, 1959.

6. Ying, C.F. and R. Truell, "Scattering of Plane Longitudinal Waves by a Spherical Obstacle in an Isotropic Elastic Solid," J. Appl. Phys., Vol. 27, No. 9, September, 1956.

7. Einsprich, N.G., E.J. Witterholt, and R. Truell, "Scattering of a Plane Transverse Wave by a Spherical Obstacle in an Elastic Medium," J. Appl. Phys., Vol. 31, No. 5, May 1960.

8. M.D. Trifunac, "Scattering of Plane SH-Waves by a Semi-Cylindrical Canyon," Int. J. Earthq. Structural Dynamics, 1, 267-281 (1973).

9. M.D. Trifunac, "Surface Motion of a Semi-Cylindrical Alluvial Valley for Incident Plane SH-Waves," Bull. Seism. Soc. Am., 61, 1755-1770 (1971).

10. V.W. Lee, "On Deformations Near Circular Underground Cavity Subjected to Incident Plane SH-Waves," Proc. of Symposium on Applications of Computer Methods in Engineering, Vol. II, U.S.C., 951-962 (August, 1977).

11. V.W. Lee, M.D. Trifunac, "On Deformations Near Circular Underground Tunnel Subjected to Incident Plane SH-Waves," submitted for publication.

12. H.L. Wong, M.D. Trifunac," Scattering of Plane SH-Waves by a Semi-Elliptical Canyon," Earthq. Eng. and Structural Dynamics, Vol. 3, 157-169 (1974).

13. J.E. Luco, H.L. Wong and M.D. Trifunac, "A Note on the Dynamic Response of Rigid Embedded Foundations," Earthq. Eng. and Structural Dynamics, Vol. 4, 119-127 (1975).

14. Abramowitz, M,, and Stegan, I.A., (editors), "Handbook of Mathematical Functions, with Formulas, Graphs, and Mathematical Tables," Dover 0-486-61272-4, New York.

15. Whittaker, E.T., and Watson, G.N., "A Course of Modern Analysis," MacMillan Company, New York, (1943).

16. Watson, G.N., "A Treatise of the Theory of Bessel Functions," MacMillan Company, New York, (1944).

17. Gradshteyn, Z.S., and Ryzhik, I.W., "Table of Integrals, Series and Products," Academic Press, New York (1965).

18. Stratton, J.A., "Electromagnetic Theory," McGraw-Hill, 1941.

19. Achenbach, J.D., "Wave Propagation in Elastic Solids," American Elsevier Publishing Company, Inc., New York.

APPENDIX I

Plane Wave Expansion

A vector harmonic plane wave propagating in an arbitrary direction has the displacement vector $\underset{\sim}{u}$ given by

$$\underset{\sim}{u} = \underset{\sim}{a} \exp i\ (\underset{\sim}{k}\cdot\underset{\sim}{r} - \omega t) \qquad \text{(A1.1)}$$

where

$\underset{\sim}{a}$ is the displacement amplitude vector,

$\underset{\sim}{k}$ is the propagation vector,

$\underset{\sim}{r}$ is the position vector,

ω is the harmonic frequency, and

t is the time coordinate.

A representation of such vector plane waves in terms of elementary spherical wave functions is next examined. In spherical co-ordinates, any given displacement vector can be decomposed into three independent spherical wave components,

$$\underset{\sim}{u} = \underset{\sim}{L} + \underset{\sim}{M} + \underset{\sim}{N} \qquad \text{(A1.2)}$$

each satisfying the vector Helmholtz equation. $\underset{\sim}{L}$ is the longitudinal component, while $\underset{\sim}{M}$ and $\underset{\sim}{N}$ are the transverse components with zero divergence. They are related to the scalar spherical potential functions as follows:

$$\underset{\sim}{L} = \frac{1}{k_\alpha}\,\text{grad}(\Phi)$$

$$\underset{\sim}{M} = \text{curl}(\underset{\sim}{r}\Psi)$$

$$\underset{\sim}{N} = \frac{1}{k_\beta}\,\text{curl curl}(\underset{\sim}{r}\chi) \qquad \text{(A1.3)}$$

where

$k_\alpha = \omega/\alpha$ is the longitudinal wave number, and

$k_\beta = \omega/\beta$ is the transverse wave number.

(A1.3) has the corresponding set of three basic solutions of the first kind, finite at $r = 0$,

$$\underset{\sim}{L}^1_{\substack{e\\o}\,mn} = \frac{1}{k_\alpha}\ \text{grad}\left(j_n(k_\alpha r)P_n^m(\mu)\begin{matrix}\cos\\ \sin\end{matrix} m\phi\right)$$

$$\underset{\sim}{M}^1_{\substack{e\\o}\,mn} = \text{curl}\left(\underset{\sim}{r}\, j_n(k_\beta r)P_n^m(\mu)\begin{matrix}\cos\\ \sin\end{matrix} m\phi\right)$$

$$\underset{\sim}{N}^1_{\substack{e\\o}\,mn} = \frac{1}{k_\beta}\ \text{curl}\left(\underset{\sim}{M}^1_{\substack{e\\o}\,mn}\right)$$

where

$$\mu = \cos\theta \quad . \tag{A1.4}$$

The label e (even) or o (odd) designates whether the even (real) or odd (imaginary) part of the azimuth function $\exp(im\phi)$ is to be employed. The index m appears as the "upper" index for the spherical harmonics and also as the index for the azimuth function. The index n appears as the index for the radial functions. The range of m,n is 0 to ∞, with $m \leq n$. The superscript (1) indicates that the radial functions used are those which are non-singular at the origin (j_n). These basic solutions are given in Morse and Feshbach, reference (1).

The most general series expansion for a vector plane wave propagating in the direction $\underset{\sim}{k}$ with angles u, v is given by the dyadic

$$\mathcal{F} e^{i\underset{\sim}{k}\cdot\underset{\sim}{r}} = \sum_{\sigma,m,n} \delta_{mn} \left\{ -i \underset{\sim}{P}_{mn}^{\sigma}(u,v) \underset{\sim}{L}_{\sigma mn}^{1}(r) + \frac{1}{\sqrt{n(n+1)}} \left[\underset{\sim}{c}_{mn}^{\sigma}(u,v) \underset{\sim}{M}_{\sigma mn}^{1}(r) - i \underset{\sim}{b}_{mn}^{\sigma}(u,v) \underset{\sim}{N}_{\sigma mn}^{1}(r) \right] \right\}$$

where

$$\delta_{mn} = \varepsilon_m i^n (2n+1)(n-m)!/(n+m)! \quad , \qquad \varepsilon_o = 1, \quad \varepsilon_m = 2 \quad \text{for } m > 0$$

$$\sigma = e,o \; ; \; m,n = 0,1,2, \ldots, m \leq n$$

$$\mathcal{F} = \text{unit dyadic} = \underset{\sim}{e}_x\underset{\sim}{e}_x + \underset{\sim}{e}_y\underset{\sim}{e}_y + \underset{\sim}{e}_z\underset{\sim}{e}_z \qquad \text{(A1.5)}$$

The vector functions $\underset{\sim}{P}_{mn}^{\sigma}$, $\underset{\sim}{b}_{mn}^{\sigma}$, $\underset{\sim}{c}_{mn}^{\sigma}$ are the vector spherical harmonics. Their definitions are given in [1] and are included below.

(A1.5) can now be used to expand $\underset{\sim}{u}^{(i)}$, $\underset{\sim}{u}_1^{(r)}$ and $\underset{\sim}{u}_2^{(r)}$. The incident plane P-wave has displacement given by

$$\underset{\sim}{u}^{(i)} = i \underset{\sim}{k}_{\alpha}^{(i)} \exp i \underset{\sim}{k}_{\alpha}^{(i)} \cdot \underset{\sim}{r}$$

$$= i k_{\alpha}(\sin\gamma \, \underset{\sim}{e}_x + \cos\gamma \, \underset{\sim}{e}_z) \exp i k_{\alpha}(x \sin\gamma + z \cos\gamma) \qquad \text{(A1.6)}$$

Since the longitudinal (P) displacement has a non-vanishing divergence, its expansion involves only the $\underset{\sim}{L}$ function. Thus, applying the dyadic

$$\underset{\sim}{u}^{(i)} = \sum_{\sigma,m,n} \delta_{mn} (-i) \, i \underset{\sim}{k}_{\alpha}^{(i)} \cdot \underset{\sim}{P}_{mn}^{\sigma}(u,v) \; \underset{\sim}{L}_{\sigma mn}^{1}(r) \qquad \text{(A1.7)}$$

For $\underset{\sim}{k}_{\alpha}^{(i)}$, $u = \gamma$, $v = 0$, so

$$\underset{\sim}{P}_{mn}^{e}(u,v) = \underset{\sim}{e}_r P_n^m(\cos\gamma)$$

$$\underset{\sim}{P}_{mn}^{o}(u,v) = \underset{\sim}{0} \qquad \text{(A1.8)}$$

from which we obtain the scalar potential $\Phi^{(i)}$ corresponding to $\underset{\sim}{u}^{(i)}$, using (A1.4) and (A1.7)

$$\Phi^{(i)} = \sum_{m,n} A_{mn}^{(i)} P_n^m(\mu) j_n(k_\alpha r) \cos m\phi \qquad \text{(A1.9)}$$

where

$$A_{mn}^{(i)} = \delta_{mn}^{+} P_n^m(\cos\gamma) \qquad m,n = 0,1,2,\ldots$$

$m \leq n$ in the summation.

Similarly, the reflected P-wave has displacement given by

$$\underset{\sim}{u}_1^{(r)} = iK_1 \underset{\sim}{k}_\alpha^{(r)} \exp i \underset{\sim}{k}_\alpha^{(r)} \cdot \underset{\sim}{r}$$

$$= iK_1 k_\alpha (\sin\gamma \, \underset{\sim}{e}_x - \cos\gamma \, \underset{\sim}{e}_z) \exp i k_\alpha (x \sin\gamma - z \cos\gamma) \qquad \text{(A1.10)}$$

For $\underset{\sim}{k}_\alpha^{(r)}$, $u = \pi - \gamma$, $v = 0$, so

$$\underset{\sim}{P}_{mn}^{e}(u,v) = \underset{\sim}{e}_r P_n^m(-\cos\gamma)$$

$$\underset{\sim}{P}_{mn}^{o}(u,v) = 0 \qquad \text{(A1.11)}$$

from which

$$\Phi^{(r)} = \sum_{\min} A_{mn}^{(r)} P_n^m(\mu) j_n(k_\alpha r) \cos m\phi$$

$$A_{mn}^{(r)} = \delta_{mn} P_n^m(-\cos\gamma) K_1 \qquad \text{(A1.12)}$$

Finally, the reflected SV-wave has displacement given by

$$\underset{\sim}{u}_2^{(r)} = iK_2 k_\beta (\cos\delta \, \underset{\sim}{e}_x + \sin\delta \, \underset{\sim}{e}_z) \exp i k_\beta (x \sin\delta - z \cos\delta) \qquad \text{(A1.13)}$$

where $\underset{\sim}{k}_\beta = k_\beta (\sin\delta \, \underset{\sim}{e}_x - \cos\delta \, \underset{\sim}{e}_z)$ has angles

$u = \pi - \delta$, $v = 0$.

The divergence of $\underset{\sim}{u}_2^{(r)}$ is zero and consequently it can be expanded in terms of the vector function $\underset{\sim}{M}_{o\,mn}^{e}$, $\underset{\sim}{N}_{o\,mn}^{e}$ only. Before applying the dyadic, we write

$$\underset{\sim}{c}_{mn} = \underset{\sim}{c}_{mn}^{e} + i\,\underset{\sim}{c}_{mn}^{o}$$

$$\underset{\sim}{b}_{mn} = \underset{\sim}{b}_{mn}^{e} + i\,\underset{\sim}{b}_{mn}^{o}$$

$$\underset{\sim}{c}_{mn} = (c_{mnx}, c_{mny}, c_{mnz})$$

$$\underset{\sim}{b}_{mn} = (b_{mnx}, b_{mny}, b_{mnz}) \qquad \text{(A1.14)}$$

The above terms are given in (A1.20) below.

For $\underset{\sim}{k}_\beta$, $u = \pi-\delta$, $v = 0$ and we have

$$\underset{\sim}{c}_{mn}^{e} = \underset{\sim}{b}_{mn}^{o} = 0 \qquad \text{(A1.15)}$$

Applying the dyadic, with $(u,v) = (\pi-\delta, 0)$, (A1.13) can be written as

$$\underset{\sim}{u}_2^{(r)} = \sum_{m,n} \frac{iK_2 k_\beta \delta_{mn}}{\sqrt{n(n+1)}} \left[(c_{mnx}^{o}\cos\delta + c_{mnz}^{o}\sin\delta)\underset{\sim}{M}_{omn}^{1} \right.$$

$$\left. - i(b_{mnx}^{e}\cos\delta + b_{mnz}^{e}\sin\delta)\underset{\sim}{N}_{emn}^{1} \right] \qquad \text{(A1.16)}$$

From (A1.16), $\underset{\sim}{u}_2^{(r)}$ corresponds to scalar potentials given by

$$\psi^{(r)} = \sum_{m,n} k_\beta B_{mn}^{(r)} j_n(k_\beta r) P_n^m(\mu)\ \sin m\phi$$

$$\chi^{(r)} = \sum_{m,n} C_{mn}^{(r)} j_n(k_\beta r) P_n^m(\mu)\ \cos m\phi \qquad \text{(A1.17)}$$

where for $m,n = 0,1,2, \ldots, m \le n$

$$B_{mn}^{(r)} = iK_2\delta_{mn}(c_{mnx}^{o}\cos\delta + c_{mnz}^{o}\sin\delta)/\sqrt{n(n+1)}$$

$$C_{mn}^{(r)} = K_2\delta_{mn}(b_{mnx}^{e}\cos\delta + b_{mnz}^{e}\sin\delta)/\sqrt{n(n+1)}\ . \qquad \text{(A1.18)}$$

To complete the analysis, we include below the terms $\underset{\sim}{b}_{mn}$, $\underset{\sim}{c}_{mn}$ given in reference 1. With

$$\underset{\sim}{c}_{mn} = \underset{\sim}{c}_{mn}^{e} + i\underset{\sim}{c}_{mn}^{o} = \underset{\sim}{c}_{mn}(u,v)$$

$$\underset{\sim}{b}_{mn} = \underset{\sim}{b}_{mn}^{e} + i\underset{\sim}{b}_{mn}^{o} = \underset{\sim}{b}_{mn}(u,v)$$

let

$$X_n^m(u,v) = P_n^m(\cos u)\exp i m v$$

$$\underset{\sim}{c}_{mn} = (c_{mnx}, c_{mny}, c_{mnz})$$

$$\underset{\sim}{b}_{mn} = (b_{mnx}, b_{mny}, b_{mnz}) \qquad \text{(A1.19)}$$

$$b_{mnx} = \frac{.5}{2n+1}\left\{\sqrt{\frac{n+1}{n}}\left[(1-\delta_{om})(n+m)(n+m-1)X_{n-1}^{m-1} - (1+\delta_{om})X_{n-1}^{m+1}\right]\right.$$
$$\left. + \sqrt{\frac{n}{n+1}}\left[(1-\delta_{om})(n-m+1)(n-m+2)X_{n+1}^{m-1} - (1+\delta_{om})X_{n+1}^{m+1}\right]\right\}$$

$$b_{mny} = \frac{.5}{2n+1}\left\{\sqrt{\frac{n+1}{n}}\left[(1-\delta_{om})(n+m)(n+m-1)iX_{n-1}^{m-1} + (1+\delta_{om})iX_{n-1}^{m+1}\right]\right.$$
$$\left. + \sqrt{\frac{n}{n+1}}\left[(1-\delta_{om})(n-m+1)(n-m+2)iX_{n+1}^{m-1} + (1+\delta_{om})iX_{n+1}^{m+1}\right]\right\}$$

$$b_{mnz} = \frac{1}{2n+1}\left\{\sqrt{\frac{n+1}{n}}(n+m)X_{n-1}^{m} - \sqrt{\frac{n}{n+1}}(n-m+1)X_{n+1}^{m}\right\}$$

$$c_{mnx} = \frac{.5}{\sqrt{n(n+1)}}\left[(1-\delta_{om})(n+m)(n-m+1)iX_n^{m-1} + (1+\delta_{om})iX_n^{m+1}\right]$$

$$c_{mny} = \frac{-.5}{\sqrt{n(n+1)}}\left[(1-\delta_{om})(n+m)(n-m+1)\,X_n^{m-1} - (1+\delta_{om})\,X_n^{m+1}\right]$$

$$c_{mnz} = \frac{-1}{\sqrt{n(n+1)}}\, m\, i\, X_n^m \qquad \text{(A1.20)}$$

APPENDIX II

Scattering of Spherical Waves From a Spherical Cavity

Consider a spherical cavity subjected to incident plane P-wave represented by the potential

$$\Phi^{(i)} = \exp i k_\alpha (x\sin\gamma + z\cos\gamma) \tag{A2.1}$$

From Appendix I, $\Phi^{(i)}$ can be expanded into spherical waves, given by equation (A1.9),

$$\Phi^{(i)} = \sum_{m,n} A_{mn}^{(i)} j_n(k_\alpha r) P_n^m(\mu) \cos m\phi \tag{A2.2}$$

Two types of outgoing spherical waves, longitudinal and transverse, are reflected back into the medium and they can be represented by the potentials

$$\Phi^{(s)} = \sum_{m,n} A_{mn}^{(3)} z_n^{(3)}(k_\alpha r) P_n^m(\mu) \cos m\phi$$

$$\Psi^{(s)} = \sum_{m,n} k_\beta B_{mn}^{(3)} z_n^{(3)}(k_\beta r) P_n^m(\mu) \sin m\phi$$

$$\chi^{(s)} = \sum_{m,n} C_{mn}^{(3)} z_n^{(3)}(k_\beta r) P_n^m(\mu) \cos m\phi \tag{A2.3}$$

where $m,n = 0,1,2, \ldots, m \leq n$ in the summation. $A_{mn}^{(3)}$, $B_{nm}^{(3)}$, $C_{mn}^{(3)}$ are expansion coefficients to be determined by the boundary conditions. The Hankel function $z_n^{(3)} \equiv h_n^{(1)}$ is used because $h_n^{(1)}(kr)\exp(-i\omega t)$ represents outgoing spherical waves.

The boundary conditions at $r = a$ are

$$\sigma_{rr} = \sigma_{r\theta} = \sigma_{r\phi} = 0 \qquad \text{all } \theta,\phi \tag{A2.4}$$

Applying (A2.4) to each "(m,n) component," we have, for $m,n = 0,1,2 \ldots$ $m \leq n$

$$\sigma_{rr}: \quad A_{mn}^{(i)} E_{11}^{(i)} + A_{mn}^{(3)} E_{11}^{(3)} + C_{mn}^{(3)} E_{13}^{(3)} = 0 \qquad \text{(A2.5)}$$

$$\sigma_{r\theta}: \left[A_{mn}^{(i)} E_{41}^{(1)} + A_{mn}^{(3)} E_{41}^{(3)} + C_{mn}^{(3)} E_{43}^{(3)} \right] \frac{dP_n^m}{d\theta} + \frac{mk_\beta a}{\sin\theta} B_{mn}^{(3)} E_{42}^{(3)} P_n^m = 0 \qquad \text{(A2.6)}$$

$$\sigma_{r\phi}: \quad \frac{m}{\sin\theta} \left[A_{mn}^{(i)} E_{41}^{(1)} + A_{mn}^{(3)} E_{41}^{(3)} + C_{mn}^{(3)} E_{43}^{(3)} \right] P_n^m + k_\beta a B_{mn}^{(3)} E_{42}^{(3)} \frac{dP_n^m}{d\theta} \qquad \text{(A2.7)}$$

where $E_{ij}^{(k)} = E_{ij}^{(k)}(m,n)$ is given in Appendix III.

For (A2.5), (A2,6), (A2.7) to hold for all θ,ϕ, $0 \leq \theta,\phi \leq 2\pi$, one needs

$$A_{mn}^{(3)} E_{11}^{(3)} + C_{mn}^{(3)} E_{13}^{(3)} = -A_{mn}^{(i)} E_{11}^{(1)}$$

$$A_{mn}^{(3)} E_{41}^{(3)} + C_{mn}^{(3)} E_{43}^{(3)} = -A_{mn}^{(i)} E_{41}^{(1)}$$

$$k_\beta a B_{mn}^{(3)} E_{42}^{(3)} = 0 \; . \qquad \text{(A2.8)}$$

which solves for $A_{mn}^{(3)}$, $B_{mn}^{(3)}(=0)$ and $C_{mn}^{(3)}$.

APPENDIX III

Displacement Vector and Stress Tensor

The physical components (u_r, u_θ, u_ϕ) of the displacement vector and those of the stress tensor $(\sigma_{rr}, \sigma_{\theta\theta}, \sigma_{\phi\phi}, \sigma_{r\theta}, \sigma_{r\phi}, \sigma_{\theta\phi})$ in terms of the scalar potentials (Φ,Ψ,χ) are given in Mow and Pao (reference 2). Set

$$\Phi = z_n(k_\alpha r)P_n^m(\mu) \begin{matrix}\cos\\ \sin\end{matrix} m\phi$$

$$\Psi = z_n(k_\beta r)P_n^m(\mu) \begin{matrix}\sin\\ \cos\end{matrix} m\phi$$

$$\chi = z_n(k_\beta r)P_n^m(\mu) \begin{matrix}\cos\\ \sin\end{matrix} m\phi \qquad \text{(A3.1)}$$

where $z_n \equiv z_n^{(i)}$ denotes one of the spherical Bessel functions given in equation (11), $\mu = \cos\theta$, $m,n = 0,1,2,\ldots$ and $m \le n$.

The components of the displacement vector take the form

$$u_r = \frac{1}{r}\left[d_{11}^{(i)} + \ell d_{13}^{(i)}\right] P_n^m \begin{matrix}\cos\\ \sin\end{matrix} m\phi$$

$$u_\theta = \frac{1}{r}\left[(d_{21}^{(i)} + \ell d_{23}^{(i)})\frac{dP_n^m}{d\theta} \pm \frac{mrd_{22}^{(i)}}{\sin\theta} P_n^m\right] \begin{matrix}\cos\\ \sin\end{matrix} m\phi$$

$$u_\phi = \frac{1}{r}\left[\frac{\mp m}{\sin\theta}(d_{21}^{(i)} + \ell d_{23}^{(i)})P_n^m - rd_{22}^{(i)}\frac{dP_n^m}{d\theta}\right] \begin{matrix}\sin\\ \cos\end{matrix} m\phi \qquad \text{(A3.2)}$$

where ℓ is introduced so that all terms have the same dimensions,

$$P_n^m = P_n^m(\mu) \ ,$$

$$\frac{dP_n^m(\mu)}{d\theta} = \left[n\mu P_n^m(\mu) - (n+m)P_{n-1}^m(\mu)\right]/\sin\theta \ , \qquad \text{(A3.3)}$$

and for $z_n \equiv z_n^{(i)}$

$$d_{11}^{(i)} = nz_n(k_\alpha r) - k_\alpha r z_{n+1}(k_\alpha r)$$

$$d_{12}^{(i)} = 0$$

$$d_{13}^{(i)} = n(n+1)z_n(k_\beta r)$$

$$d_{21}^{(i)} = z_n(k_\alpha r)$$

$$d_{22}^{(i)} = z_n(k_\beta r)$$

$$d_{23}^{(i)} = (n+1)z_n(k_\beta r) - k_\beta r z_{n+1}(k_\beta r) \quad . \qquad \text{(A3.4)}$$

At $\theta = \pi/2$ $(z = 0)$, $\mu = 0$ and

$$\frac{dP_n^m}{d\theta} = -(n+m)P_{n-1}^m(0)$$

and (A3.2) takes the form

$$u_r = \frac{1}{r}\left[d_{11}^{(i)} + \ell d_{13}^{(i)}\right]P_n^m(0) \begin{matrix}\cos\\ \sin\end{matrix} m\phi$$

$$u_\theta = \frac{1}{r}\left[-(d_{21}^{(i)} + \ell d_{23}^{(i)})(n+m)P_{n-1}^m(0) \pm mrd_{22}^{(i)}P_n^m(0)\right]\begin{matrix}\cos\\ \sin\end{matrix} m\phi$$

$$u_\phi = \frac{1}{r}\left[\mp m(d_{21}^{(i)} + \ell d_{23}^{(i)})P_n^m(0) + r(n+m)d_{22}^{(1)}P_{n-1}^m(0)\right]\begin{matrix}\sin\\ \cos\end{matrix} m\phi$$

(A3.5)

The components of the stress tensor take the form

σ_{rr} due to:

Φ: $\left(\frac{2\mu}{r^2}\right)\mathcal{E}_{11}^{(i)} \begin{matrix}\cos\\ \sin\end{matrix} m\phi$; $\mathcal{E}_{11}^{(i)} = E_{11}^{(i)}P_n^m$

Ψ: none ; $\mathcal{E}_{12}^{(i)} = 0$

χ: $\left(\frac{2\mu\ell}{r^2}\right)\mathcal{E}_{13}^{(i)} \begin{matrix}\cos\\ \sin\end{matrix} m\phi$; $\mathcal{E}_{13}^{(i)} = E_{13}^{(i)}P_n^m$

$$E_{11}^{(i)} = \left(n^2 - n - k_\beta^2 \frac{r^2}{2}\right) z_n(k_\alpha r) + 2k_\alpha r z_{n+1}(k_\alpha r)$$

$$E_{12}^{(i)} = 0$$

$$E_{13}^{(i)} = n(n+1)\left[(n-1)z_n(k_\beta r) - k_\beta r z_{n+1}(k_\beta r)\right] \qquad \text{(A3.6)}$$

$\sigma_{\theta\theta}$ due to

$$\Phi: \left(\frac{2\mu}{r^2}\right) \mathscr{E}_{21}^{(i)} \begin{matrix}\cos \\ \sin\end{matrix} m\phi \quad ; \quad \mathscr{E}_{21}^{(i)} = E_{21}^{(i)} P_n^m + \hat{E}_{21}^{(i)} \hat{P}_n^m$$

$$\Psi: \left(\frac{2\mu}{r}\right) \mathscr{E}_{22}^{(i)} \begin{matrix}\cos \\ \sin\end{matrix} m\phi \quad ;$$

$$\chi: \left(\frac{2\mu\ell}{r^2}\right) \mathscr{E}_{23}^{(i)} \begin{matrix}\cos \\ \sin\end{matrix} m\phi \quad ; \quad \mathscr{E}_{23}^{(i)} = E_{23}^{(i)} P_n^m + \hat{E}_{23}^{(i)} \hat{P}_n^m$$

$$E_{21}^{(i)} = (-n^2 - k_\beta^2 r^2/2 + k_\alpha^2 r^2) z_n(k_\alpha r) - k_\alpha r z_{n+1}(k_\alpha r)$$

$$\hat{E}_{21}^{(i)} = z_n(k_\alpha r)$$

$$\mathscr{E}_{22}^{(i)} = \frac{\pm m}{1-\mu^2} z_n(k_\beta r)\left[(n-1)\mu P_n^m - (n+m) P_{n-1}^m\right]$$

$$E_{23}^{(i)} = -(n^2 + n)\left[n z_n(k_\beta r) - k_\beta r z_{n+1}(k_\beta r)\right]$$

$$\hat{E}_{23}^{(i)} = (n+1) z_n(k_\beta r) - k_\beta r z_{n+1}(k_\beta r)$$

$$\hat{P}_n^m = \hat{P}_n^m(\mu) = \frac{1}{1-\mu^2}\left[(m^2 - \mu^2 n) P_n^m + (n+m)\mu P_{n-1}^m\right] \qquad \text{(A3.7)}$$

$\sigma_{\phi\phi}$ due to

$$\Phi: \left(\frac{2\mu}{r^2}\right) \mathscr{E}_{31}^{(i)} \begin{matrix}\cos \\ \sin\end{matrix} m\phi \quad ; \quad \mathscr{E}_{31}^{(i)} = E_{31}^{(i)} P_n^m - \hat{E}_{31}^{(i)} \hat{P}_n^m$$

$$\Psi: \left(\frac{2\mu}{r}\right) \mathscr{E}_{32}^{(i)} \begin{matrix}\cos\\ \sin\end{matrix} m\phi \quad ;$$

$$\chi: \left(\frac{2\mu\ell}{r^2}\right) \mathscr{E}_{33}^{(i)} \begin{matrix}\cos\\ \sin\end{matrix} m\phi \quad ; \quad \mathscr{E}_{33}^{(i)} = E_{33}^{(i)} P_n^m - \hat{E}_{33}^{(i)} \hat{P}_n^m$$

$$E_{31}^{(i)} = (n - k_\beta^2 r^2/2 + k_\alpha^2 r^2) z_n(k_\alpha r) - k_\alpha r a_{n+1}(k_\alpha r)$$

$$\hat{E}_{31}^{(i)} = z_n(k_\alpha r)$$

$$\mathscr{E}_{32}^{(i)} = \frac{\pm m}{1-\mu^2} z_n(k_\beta r)\left[-(n-1)\mu P_n^m + (n+m) P_{n-1}^m\right]$$

$$E_{33}^{(i)} = n(n+1) z_n(k_\beta r)$$

$$\hat{E}_{33}^{(i)} = (n+1) z_n(k_\beta r) - k_\beta r z_{n+1}(k_\beta r)$$

$$\hat{P}_n^m = \hat{P}_n^m(\mu) = \frac{1}{1-\mu^2}\left[(m^2 - \mu^2 n) P_n^m + (n+m)\mu P_{n-1}^m\right] \qquad \text{(A3.8)}$$

$\sigma_{r\theta}$ due to:

$$\Phi: \left(\frac{2\mu}{r^2}\right) \mathscr{E}_{41}^{(i)} \begin{matrix}\cos\\ \sin\end{matrix} m\phi \quad ; \quad \mathscr{E}_{41}^{(i)} = E_{41}^{(i)} \frac{dP_n^m}{d\theta}$$

$$\Psi: \left(\frac{2\mu}{r}\right) \mathscr{E}_{42}^{(i)} \begin{matrix}\cos\\ \sin\end{matrix} m\phi \quad ; \quad \mathscr{E}_{42}^{(i)} = \frac{\pm m}{\sin\theta} E_{42}^{(i)} P_n^m$$

$$\chi: \left(\frac{2\mu\ell}{r^2}\right) \mathscr{E}_{43}^{(i)} \begin{matrix}\cos\\ \sin\end{matrix} m\phi \quad ; \quad \mathscr{E}_{43}^{(i)} = E_{43}^{(i)} \frac{dP_n^m}{d\theta}$$

$$E_{41}^{(i)} = (n-1) z_n(k_\alpha r) - k_\alpha r z_{n+1}(k_\alpha r)$$

$$E_{42}^{(i)} = .5*\left[(n-1) z_n(k_\beta r) - k_\beta r z_{n+1}(k_\beta r)\right]$$

$$E_{43}^{(i)} = (n^2 - 1 - k_\beta{}^2 r^2/2) z_n(k_\beta r) + k_\beta r z_{n+1}(k_\beta r) \qquad \text{(A3.9)}$$

$\sigma_{r\phi}$ due to

$$\Phi: \left(\frac{2\mu}{r^2}\right) \mathscr{E}_{51}^{(i)} \begin{matrix}\sin\\ \cos\end{matrix} m\phi \quad ; \quad \mathscr{E}_{51}^{(i)} = \frac{\mp m}{\sin\theta} E_{51}^{(i)} P_n^m$$

$$\Psi: -\left(\frac{2\mu}{r}\right) \mathscr{E}_{52}^{(i)} \begin{matrix}\sin\\ \cos\end{matrix} m\phi \quad ; \quad \mathscr{E}_{52}^{(i)} = E_{52}^{(i)} \frac{dP_n^m}{d\theta}$$

$$\chi: \left(\frac{2\mu\ell}{r^2}\right) \mathscr{E}_{53}^{(i)} \begin{matrix}\sin\\ \cos\end{matrix} m\phi \quad ; \quad \mathscr{E}_{53}^{(i)} = \frac{\mp m}{\sin\theta} E_{53}^{(i)} P_n^m$$

$$E_{51}^{(i)} = E_{41}^{(i)}$$

$$E_{52}^{(i)} = E_{42}^{(i)}$$

$$E_{53}^{(i)} = E_{43}^{(i)} \qquad \text{(A3.10)}$$

$\sigma_{\theta\phi}$ due to

$$\Phi: \left(\frac{2\mu}{r^2}\right) \mathscr{E}_{61}^{(i)} \begin{matrix}\sin\\ \cos\end{matrix} m\phi$$

$$\Psi: \left(\frac{2\mu}{r}\right) \mathscr{E}_{62}^{(i)} \begin{matrix}\sin\\ \cos\end{matrix} m\phi$$

$$\chi: \left(\frac{2\mu\ell}{r^2}\right) \mathscr{E}_{63}^{(i)} \begin{matrix}\sin\\ \cos\end{matrix} m\phi$$

$$\mathscr{E}_{61}^{(i)} = \frac{\mp m}{\sin\theta} E_{61}^{(i)} \left(\frac{dP_n^m}{d\theta} - \cot\theta\, P_n^m\right)$$

$$\mathscr{E}_{62}^{(i)} = \frac{E_{62}^{(i)}}{\sin^2\theta} \left[\left(\frac{n^2-n}{2}\sin^2\theta + n-m^2\right) P_n^m - (n+m)\cos\theta\, P_{n-1}^m\right]$$

$$\mathscr{E}_{63}^{(i)} = \frac{\mp m}{\sin\theta} \; E_{63}^{(i)} \left(\frac{dP_n^m}{d\theta} - \cot\theta \; P_n^m \right)$$

$$E_{61}^{(i)} = z_n(k_\alpha r)$$

$$E_{62}^{(i)} = z_n(k_\beta r)$$

$$E_{63}^{(i)} = (n+1) z_n(k_\beta r) - k_\beta r z_{n+1}(k_\beta r) \qquad \text{(A3.11)}$$

APPENDIX IV

Series Expansion

For

$$\Phi = z_n(k_\alpha r)P_n^m(\mu) \begin{matrix}\cos\\ \sin\end{matrix} m\phi$$

$$\Psi = z_n(k_\beta r)P_n^m(\mu) \begin{matrix}\sin\\ \cos\end{matrix} m\phi$$

$$\chi = z_n(k_\beta r)P_n^m(\mu) \begin{matrix}\cos\\ \sin\end{matrix} m\phi \qquad \text{(A4.1)}$$

the components of the stresses $\sigma_{\theta\theta}$, $\sigma_{\theta r}$ and $\sigma_{\theta\phi}$ are given in Appendix III (A3.7), (A3.9), (A3.11). At $\theta = \pi/2$, the half-space plane boundary ($z = 0$), these stress components take the form

1) $\sigma_{\theta\theta}$:

$$\mathscr{E}_{21}^{(i)} = \left[(m^2 - n^2 - k_\beta^2 r^2/2 + k_\alpha^2 r^2) z_n(k_\alpha r) - k_\alpha r z_{n+1}(k_\alpha r)\right] P_n^m(0)$$

$$\mathscr{E}_{22}^{(i)} = \mp m(n+m) z_n(k_\beta r) P_{n-1}^m(0)$$

$$\mathscr{E}_{23}^{(i)} = \left[(m^2 - n^2)(n+1) z_n(k_\beta r) + (n + n^2 - m^2) k_\beta r z_{n+1}(k_\beta r)\right] P_n^m(0) \qquad \text{(A4.2)}$$

2) $\sigma_{\theta r} = \sigma_{r\theta}$:

$$\mathscr{E}_{41}^{(i)} = -(n+m)\left[(n-1) z_n(k_\alpha r) - k_\alpha r z_{n+1}(k_\alpha r)\right] P_{n-1}^m(0)$$

$$\mathscr{E}_{42}^{(i)} = \pm .5m\left[(n-1) z_n(k_\beta r) - k_\beta r z_{n+1}(k_\beta r)\right] P_n^m(0)$$

$$\mathscr{E}_{43}^{(i)} = -(n+m)\left[(n^2 - 1 - k_\beta^2 r^2/2) z_n(k_\beta r) + k_\beta r z_{n+1}(k_\beta r)\right] P_{n-1}^m(0) \qquad \text{(A4.3)}$$

3) $\sigma_{\theta\phi}$:

$$\mathscr{E}_{61}^{(i)} = \pm m(n+m) z_n(k_\alpha r) P_{n-1}^{m}(0)$$

$$\mathscr{E}_{62}^{(i)} = .5*(n^2 + n - 2m^2) z_n(k_\beta r) P_n^{m}(0)$$

$$\mathscr{E}_{63}^{(i)} = \pm m(n+m)\left[(n+1) z_n(k_\beta r) - k_\beta r z_{n+1}(k_\beta r)\right] P_{n-1}^{m}(0) \qquad \text{(A4.4)}$$

All the above terms involve spherical Bessel's functions j_n, y_n or their derivatives. They can be expanded in power series of r. From

$$j_n(r) = \sqrt{\frac{\pi}{2r}}\ J_{n+\frac{1}{2}}(r) \qquad \text{(A4.5)}$$

$$J_\nu(r) = \sum_{k=0}^{\infty} \frac{(-1)^k}{\Gamma(k+1)\Gamma(\nu+k+1)} \left(\frac{r}{2}\right)^{\nu+2k} \qquad \text{(A4.6)}$$

we have

$$j_n(r) = \sum_{k=0}^{\infty} a_{nk}\left(\frac{r}{2}\right)^{n+2k} \qquad \text{(A4.7)}$$

where

$$a_{nk} = \frac{\sqrt{\pi}(-1)^k}{2\Gamma(k+1)\Gamma(n+k+3/2)} \qquad \text{(A4.8)}$$

Similarly

$$y_n(r) = \sqrt{\frac{\pi}{2r}}\ Y_{n+\frac{1}{2}}(r) \qquad \text{(A4.9)}$$

$$= \sqrt{\frac{\pi}{2r}}\ (-1)^{n+1}\ J_{-n-\frac{1}{2}}(r)$$

or

$$y_n(r) = \sum_{k=0}^{\infty} b_{nk}\left(\frac{r}{2}\right)^{-n-1+2k} \qquad \text{(A4.10)}$$

where

$$b_{nk} = \frac{(-1)^{n+k+1}\sqrt{\pi}}{2\Gamma(k+1)\Gamma(-n+k+\frac{1}{2})} \tag{A4.11}$$

Using (A4.7), (A4.10), we can expand $\mathscr{E}_{ij} = \mathscr{E}_{ij}(m,n,r)$ given in (A4.2), (A4.3), (A4.4) in series of r. For i = 2,4,6, j = 1 and 3, we write

$$\mathscr{E}_{ij}^{(1)}(m,n,r) = \sum_k e_{ij}^{(1)}(m,n,k)\left(\frac{r}{2}\right)^{n+2k}$$

$$\mathscr{E}_{ij}^{(2)}(m,n,r) = \sum_k e_{ij}^{(2)}(m,n,k)\left(\frac{r}{2}\right)^{-n-1+2k}$$

and for j = 2, we write

$$k_\beta r\,\mathscr{E}_{12}^{(1)}(m,n,r) = \sum_k e_{12}^{(1)}(m,n,r)\left(\frac{r}{2}\right)^{n+2k+1}$$

$$k_\beta r\,\mathscr{E}_{12}^{(2)}(m,n,r) = \sum_k e_{12}^{(2)}(m,n,k)\left(\frac{r}{2}\right)^{-n+2k} \tag{A4.12}$$

where k = 0,1,2, ..., in the summation, m,n = 0,1,2, ..., $m \le n$, and

$$\sigma_{\theta\theta}:\ e_{21}^{(1)} = \left[(m^2-n^2)a_{nk} - 4(\alpha^2/2\beta^2)a_{n,k-1} - 2a_{n+1,k-1}\right]P_n^m(0)k_\alpha^{n+2k}$$

$$e_{22}^{(1)} = \mp 2m(n+m)a_{nk}P_{n-1}^m(0)k_\beta^{n+2k+1}$$

$$e_{23}^{(1)} = \left[(n+1)(m^2-n^2)a_{nk} + 2(n+n^2-m^2)a_{n+1,k-1}\right]P_n^m(0)k_\beta^{n+2k}$$

$$e_{21}^{(2)} = \left[(m^2-n^2)b_{nk} - 4(\alpha^2/2\beta^2)b_{n,k-1} - 2b_{n+1,k}\right]P_n^m(0)k_\beta^{-n-1+2k}$$

$$e_{22}^{(2)} = \mp 2m(n+m)b_{nk}P_{n-1}^m(0)k_\beta^{-n+2k}$$

$$e_{23}^{(2)} = \left[(n+1)(m^2-n^2)b_{nk} + 2(n+n^2-m^2)b_{n+1,k}\right]P_n^m(0)k_\beta^{-n-1+2k} \tag{A4.13}$$

$$\sigma_{\theta r}: \quad e_{41}^{(1)} = -(n+m)\left[(n-1)a_{nk} - 2a_{n+1,k-1}\right]P_{n-1}^{m}(0)k_{\alpha}^{n+2k}$$

$$e_{42}^{(1)} = \pm m\left[(n-1)a_{nk} - 2a_{n+1,k-1}\right]P_{n}^{m}(0)k_{\beta}^{n+2k+1}$$

$$e_{43}^{(1)} = -(n+m)\left[(n^2-1)a_{nk} - 2a_{n,k-1} + 2a_{n+1,k-1}\right]P_{n-1}^{m}(0)k_{\beta}^{n+2k}$$

$$e_{41}^{(2)} = -(n+m)\left[(n-1)b_{nk} - 2b_{n+1,k}\right]P_{n-1}^{m}(0)k_{\alpha}^{-n-1+2k}$$

$$e_{42}^{(2)} = \pm m\left[(n-1)b_{nk} - 2b_{n+1,k}\right]P_{n}^{m}(0)k_{\beta}^{-n+2k}$$

$$e_{43}^{(2)} = -(n+m)\left[(n^2-1)b_{nk} - 2b_{n,k-1} + 2b_{n+1,k}\right]P_{n-1}^{m}(0)k_{\beta}^{-n-1+2k}$$

(A4.14)

$$\sigma_{\theta\phi}: \quad e_{61}^{(1)} = \pm m(n+m)a_{nk}P_{n-1}^{m}(0)k_{\alpha}^{n+2k}$$

$$e_{62}^{(1)} = (n+n^2-2m^2)a_{nk}P_{n}^{m}(0)k_{\beta}^{n+2k+1}$$

$$e_{63}^{(1)} = \pm m(n+m)\left[(n+1)a_{nk} - 2a_{n+1,k-1}\right]P_{n-1}^{m}(0)k_{\beta}^{n+2k}$$

$$e_{61}^{(2)} = \pm m(n+m)b_{nk}P_{n-1}^{m}(0)k_{\alpha}^{-n-1+2k}$$

$$e_{62}^{(2)} = (n^2+n-2m^2)b_{nk}P_{n-1}^{m}(0)k_{\beta}^{-n+2k}$$

$$e_{63}^{(2)} = \pm m(n+m)\left[(n+1)b_{nk} - 2b_{n+1,k}\right]P_{n-1}^{m}(0)k_{\beta}^{-n-1+2k}$$

(A4.15)